

Oceanographic processes and products around the Iberian margin: a new multidisciplinary approach

F.J. Hernández-Molina⁽¹⁾, A. Wählin⁽²⁾, M. Bruno⁽³⁾, G. Ercilla⁽⁴⁾, E. Llave⁽⁵⁾, N. Serra⁽⁶⁾, G. Roson⁽⁷⁾, P. Puig⁽⁴⁾, M. Rebesco⁽⁸⁾, D. Van Rooij⁽⁹⁾, D. Roque⁽¹⁰⁾, C. González-Pola⁽¹¹⁾, F. Sánchez⁽¹²⁾, M. Gómez⁽¹³⁾, B. Preu⁽¹⁴⁾, T. Schwenk⁽¹⁵⁾, T.J.J. Hanebuth^(16,17), R.F. Sánchez Leal⁽¹⁸⁾, J. García-Lafuente⁽¹⁹⁾, R.E. Brackenridge^(20,21), C. Juan^(4,9), D. A.V. Stow⁽²⁰⁾ and J.M. Sánchez-González⁽⁷⁾

- (1) Department of Earth Sciences, Royal Holloway Univ. London, Egham, Surrey TW20 0EX, UK.
Javier.Hernandez-Molina@rhul.ac.uk
- (2) Department of Earth Sciences, University of Gothenburg, PO Box 460, SE-405 30 Göteborg, Sweden.
anna.wahlin@gu.se
- (3) CACYTMAR. Univ. Cádiz, Avda República Saharaui S/N, Puerto Real, 11510, Cádiz, Spain.
miguel.bruno@uca.es,
- (4) CSIC, ICM, Paseo Marítimo de la Barceloneta, 37-49, 08003 Barcelona, Spain.
gemma@icm.csic.es, ppuig@icm.csic.es,
- (5) Instituto Geológico y Minero de España Ríos Rosas, 23, 28003 Madrid, Spain.
e.llave@igme.es
- (6) Institut für Meereskunde, Univ. Hamburg, Bundesstr.53, 20146 Hamburg, Germany.
nuno.serra@uni-hamburg.de
- (7) Facultad de Ciencias do Mar, Univ. Vigo, 36200 Vigo, Spain.
groson@uvigo.es, jsgsanchez25@gmail.com
- (8) OGS, Istituto Nazionale di Oceanografia e di Geofisica Sperimentale,
Borgo Grotta Gigante 42 /C, 34010 Sgonico, TS, Italy.
mrebesco@ogs.trieste.it
- (9) Renard Centre of Marine Geology, Dept. of Geology and Soil Science.
Ghent University, Krijgslaan 281 S8 B-9000 Gent, Belgium.
David.VanRooij@UGent.be, cjuan@icm.csic.es
- (10) CSIC, ICMAN, Campus Universitario Río San Pedro s/n. Puerto Real, Cádiz. C.P.11510.
david.roque@icman.csic.es
- (11) Instituto Español de Oceanografía. C.O. Gijón. c/ Príncipe de Asturias 70 Bis. CP 33212, Gijón, Spain.
cesar.pola@gi.ieo.es
- (12) Instituto Español de Oceanografía. C.O. de Santander, Promontorio San Martín s/n,
Apdo. 240, 39080 Santander, Spain.
f.sanchez@st.ieo.es
- (13) Instituto Español de Oceanografía, c/ Corazón de María 8, 28002 Madrid, Spain.
maria.gomez@md.ieo.es
- (14) Chevron Upstream Europe, Chevron North Sea Limited, Seaford House, Aberdeen AB15 6XL, UK.
BPreu@chevron.com
- (15) Department of Geoscience, University of Bremen, Klagenfurter Str., D-28359 Bremen, Germany.
tschwenk@uni-bremen.de
- (16) Marine Sedimentation Systems Group, MARUM - Center for Marine Environmental Sciences,
University of Bremen, Leobener Strasse, 28359 Bremen, Germany.
- (17) School of Coastal and Marine Systems Sciences, Coastal Carolina University,
P.O. Box 261954, Conway, SC 29528, U.S.A.
thanebut@uni-bremen.de
- (18) Instituto Español de Oceanografía. C.O. de Cádiz, Muelle de Levante s/n, P.O. Box 2609, 11006 Cádiz, Spain.
rleal@cd.ieo.es
- (19) Physical Oceanography Group, University of Malaga, ETSI Telecomunicación,
Campus de Teatinos s/n 29071 Málaga, Spain.
glafuente@ctima.uma.es
- (20) Institute of Petroleum Engineering, Heriot-Watt Univ., Edinburgh EH14 4AS, Scotland, UK.
Dorrik.Stow@pet.hw.ac.uk
- (21) Shell International Exploration & Production B.V. Carel van Bylandtlaan 05.0B.03,
2596 HR, The Hague, Netherlands.
Rachel.Brackenridge@shell.com

ABSTRACT

Our understanding of the role of bottom currents and associated oceanographic processes (e.g., overflows, barotropic tidal currents) including intermittent processes (e.g., vertical eddies, deep sea storms, horizontal vortices, internal waves and tsunamis) is rapidly evolving. Many deep-water processes remain poorly understood due to limited direct observations, but may generate significant depositional and erosional features on both short- and long-term time scales. This paper describes these oceanographic processes and examines their potential role in the sedimentary features around the Iberian margin. The paper explores the implications of the processes studied, given their secondary role relative to other factors such as mass-transport and turbiditic processes. An integrated interpretation of these oceanographic processes requires an understanding of contourites, sea-floor features, their spatial and temporal evolution, and the near-bottom flows that form them. Given their complex, three-dimensional and temporally-variable nature, integration of these processes into sedimentary, oceanographic and climatological frameworks will require a multidisciplinary approach that includes Geology, Physical Oceanography, Paleoceanography and Benthic Biology. This approach will synthesize oceanographic data, seafloor morphology, sediments and seismic images to improve our knowledge of permanent and intermittent processes around Iberia, and evaluate their conceptual and regional role in the sedimentary evolution of the margin.

Key words: Iberian margin, oceanographic processes, bottom currents, sedimentary features, facies model.

Procesos oceanográficos y sus productos alrededor del margen de Iberia: una nueva aproximación multidisciplinar

RESUMEN

El conocimiento del papel de las corrientes de fondo y los procesos oceanográficos asociados (overflows, corrientes de marea barotrópicas, etc), incluyendo procesos intermitentes (eddies, tormentas profundas, ondas internas, tsunamis, etc), está evolucionando rápidamente. Muchos de estos procesos son poco conocidos, en parte debido a que las observaciones directas son limitadas, si bien pueden generar importantes rasgos deposicionales y/o erosivos a escalas temporales de corto o largo periodo. Este artículo describe dichos procesos oceanográficos y examina su influencia en la presencia de rasgos sedimentarios alrededor del margen Ibérico. El trabajo discute las implicaciones de dichos procesos y el papel secundario que juegan en relación a otros factores tales como los procesos de transporte gravitacionales en masa y los turbidíticos. Para un mejor conocimiento de la sedimentación marina profunda, y en concreto de los sistemas contorníticos, se requiere de una interpretación de estos procesos oceanográficos, cuál es su evolución espacial y temporal, cómo afectan a las corrientes de fondo y cómo se ven afectados por la topografía submarina. Sin embargo, dada su complejidad y su variable naturaleza tri-dimensional y temporal, es necesario que estos procesos se integren en un marco sedimentológico, oceanográfico y climatológico con un enfoque multidisciplinar que incluyan la Geología, la Oceanografía Física, la Paleoceanografía y la Biología bentónica. Esta integración requiere de una mayor compilación de datos oceanográficos, de un mejor conocimiento de la morfología del fondo marino, y de una mejor caracterización de los sedimentos en ambientes profundos. Todo ello permitirá mejorar nuestro conocimiento de los procesos permanentes e intermitentes alrededor de Iberia y evaluar su verdadero efecto en la evolución sedimentaria de los márgenes continentales que le rodean.

Palabras clave: Margen de Iberia, procesos oceanográficos, corrientes de fondo, rasgos sedimentarios, modelo de facies.

VERSION ABREVIADA EN CASTELLANO

Introducción y resultados

El término “corriente de fondo” es un término general que se refiere al flujo de una masa de agua profunda capaz de erosionar, transportar y depositar sedimentos a lo largo del fondo del mar (Rebesco and Camerlenghi, 2008), caracterizándose generalmente por un flujo neto persistente que circula paralelamente a la batimetría local (Fig. 1) (Stow et al., 2009). Estas corrientes pueden verse afectadas por diferentes procesos oceanográficos, que son los que se describen en este trabajo evaluándose el papel que desempeñan en la morfología y en la evolución tanto del margen Ibérico como de sus cuencas oceánicas adyacentes.

Alrededor del margen Ibérico se han identificado diferentes procesos oceanográficos asociados a las corrientes de fondo, como los overflows, procesos en relación con las interfases entre masas de agua, corrientes de marea, tormentas profundas, remolinos o eddies, flujos por circulación secundaria, cascadas de aguas densas de plataforma, ondas internas y solitones, y corrientes de tracción asociadas a maremotos, olas solitarias y ciclones (Fig. 2).

Generalmente las corrientes de fondo (bottom currents) fluyen relativamente lentas (< 3 cm/s) y tabulares, aunque local o regionalmente pueden alcanzar velocidades mayores (> 0.6 -1 m/s) debido a su interacción con las irregularidades del fondo (Stow et al., 2009; Hernández-Molina et al., 2011). Llave et al. en este volumen especial, realizan una descripción en detalle de las principales corrientes de fondo y su influencia regional alrededor de Iberia.

Los overflows constituyen procesos oceanográficos permanentes relacionados tanto por el desbordamiento de una masa de agua densa a través de una barrera topográfica desde una cuenca hacia el mar abierto (Fig. 2), como entre cuencas oceánicas profundas (Legg et al., 2009). Dicha masa de agua, en su descenso por gravedad por el talud, se ve afectada por la fricción con el fondo y el transporte en la capa límite de fondo de Ekman (Fig. 3) (Wåhlin and Walin, 2001). El ejemplo más relevante de overflow en el margen Ibérico se produce en la salida de la Masa de Agua Mediterránea (Mediterranean Outflow Water-MOW) a través del Estrecho de Gibraltar (Legg et al., 2009), que una vez sobrepasado el Estrecho genera contornitas laminares arenosas, surcos erosivos, ripples, ondas sedimentarias, así como terrazas contorníticas y canales erosivos (Fig. 4) (Nelson et al., 1993; Hernández-Molina et al., 2014). Otro posible ejemplo de overflow podría producirse por el paso de la Masa de Agua Profunda Inferior (Lower Deep Water-LDW) desde la llanura abisal de Vizcaya hacia la llanura abisal de Iberia a través del Theta Gap (Fig. 5) (Jane et al., 2012).

Algunas masas de agua que circulan alrededor del margen Ibérico tienen un notable contraste de densidad que da lugar a una marcada picnoclina (Figs. 6 y 7). Este es el caso de la picnoclina existente entre la Masa de Agua del Atlántico que fluye a través del Estrecho de Gibraltar hacia el Mediterráneo (Superficial Atlantic Water – SAW y Modified Atlantic Water-MAW; Millot, 2009, 2014) y la MOW que fluye desde el Estrecho de Gibraltar hacia en Golfo de Cádiz (Serra et al., 2010a). Los procesos oceanográficos asociados a estas interfases tienen importantes implicaciones morfológicas, pues desarrollan grandes terrazas contorníticas en el Mar de Alborán (Ercilla et al., 2002; Ercilla et al., enviado), Golfo de Cádiz (Hernández-Molina et al., 2014); margen Portugués (Fig. 7, Pinheiro et al., 2010) y en el Mar Cantábrico (Fig. 6, Maestro et al., 2013; Sánchez-González, 2013).

Las corrientes de marea (tidal currents) barotrópicas normalmente tienen asociadas alrededor de Iberia una baja velocidad (raramente > 20 cm/s), y sus mayores efectos se observan en ambientes someros de plataforma, pudiendo verse amplificados también cuando interaccionan con relieves muy pronunciados del fondo marino, como el talud continental, altos, bancos, etc (Marta-Almeida and Dubert, 2006). Existen varios ejemplos de estas corrientes en el Mar de Alborán (García-Lafuente and Cano Lucaya, 1994), así como alrededor de los cabos de Extremadura y Ortegal, y montes submarinos de Gettysburg y Ormonde, los cuales se consideran como hotspots o puntos calientes para la acción de este tipo de flujos de marea (Fig. 8, Quaresma and Pichon, 2013). Uno de los pocos ejemplos del efecto de la marea sobre el fondo marino se ha descrito en el canal contornítico de Cádiz, en el sector central del Golfo de Cádiz (Figs. 9 y 10A, Stow et al., 2013a).

Las tormentas bentónicas, abisales o profundas (deep-sea storms) representan un proceso oceanográfico muy particular, y aún muy poco conocido. En el margen de Iberia se han descrito estas tormentas en el Golfo de León debido a la convección profunda (Salat et al., 2010; Puig et al., 2012; Stabholz et al., 2013), siendo también identificadas en cañones submarinos del margen Cantábrico (Sánchez et al., 2014). La escasez de información sobre estos procesos podría enmascarar su frecuencia, ya que por ejemplo, en el Golfo de Cádiz se han obtenido registros que podrían ser asignados a estas tormentas (Fig. 10B), si bien es una pura especulación y su detección requeriría un mayor análisis y monitorización de estos eventos para poder confirmar realmente su existencia y su posible relación con periodos de overflows.

Los remolinos o eddies son fenómenos oceanográficos muy frecuentes. Los ejemplos que mejor se han estudiado alrededor de Iberia se relacionan con la dinámica y desplazamiento de la MOW (por eso a veces referidos como meddies). Estos meddies comprenden masas de agua de vorticidad potencial baja, que giran en sentido horario, y que mantienen la temperatura-tipo y salinidad de la MOW durante largos periodos de tiempo a medida que se van desplazando (Fig. 12). Se han observado meddies en la cuenca de Canarias (Armi and Zenk, 1984; Pingree and Le Cann, 1993), en la cuenca Ibérica (Zenk and Armi, 1990; Schultz-Tokos et al., 1994), en la costa sur de Portugal (Serra and Ambar, 2002), al oeste de Portugal (Fig. 7, Pinheiro et al., 2010), y a lo largo de la costa del noroeste Ibérico (Paillet et al., 2002). La vorticidad de estos eddies y su interacción con el fondo puede generar rasgos sedimentarios deposicionales y erosivos (Fig. 7), los cuales deberían considerarse en el futuro.

Los flujos por circulación secundaria constituyen un proceso producto de la fricción de una masa de agua con el fondo submarino (Figs. 2 y 3) y del efecto de Coriolis (Wåhlin and Walin, 2001; Wåhlin, 2004; Cossu and Wells, 2013). El efecto de este tipo de circulación secundaria se ha descrito al este del Golfo de Cádiz,

cerca de la salida del Estrecho de Gibraltar (Fig. 4, García-Lafuente et al., 2009; Hernández-Molina et al., 2014), donde en consecuencia se han desarrollado surcos erosivos oblicuos con respecto al flujo principal de la corriente de fondo (Hernández-Molina et al., 2014).

Las cascadas de aguas densas de plataforma (dense shelf water cascades-DSWC) son procesos oceanográficos que pueden tener bastante importancia en el desarrollo de procesos sedimentarios. En los márgenes alrededor de Iberia se han descrito mayoritariamente en el Golfo de León y alrededor del Cabo de Creus (Fig. 13). Estos eventos llegan a alcanzar velocidades superiores a los 80 cm/s (Palanques et al., 2006), pudiendo removilizar grandes cantidades de partículas en suspensión que se transportan rápidamente desde la plataforma a los cañones submarinos, originando surcos erosivos así como de depósitos de arenas masivas en las cabecera de los cañones (Canals et al., 2006; Gaudin et al., 2006; Puig et al., 2008; Palanques et al., 2012). En la base del cañón la mayor parte del agua densa saliente fluye a lo largo del margen continental como una corriente de contorno (Palanques et al., 2012).

Las ondas internas (internal waves) y solitones (solitary waves or solitons) se presentan mayoritariamente en fluidos estratificados estables (Fig. 14), cuando se alteran las interfases de densidad, generalmente como consecuencia de la interacción del flujo con la topografía, especialmente en regiones con marcadas irregularidades del fondo (Shanmugam, 2006, 2012a). En Iberia, y en concreto, en torno al Umbral de Camarinal y de Espartel, en el Estrecho de Gibraltar, se generan solitones con amplitudes de 50 a 100 m y longitudes de onda de 2 a 4 km (Armi and Farmer, 1988; Jackson, 2004) que evolucionan en trenes de ondas internas bien definidos (Vlasenko et al., 2009; Sanchez Garrido et al., 2011), y que pueden alcanzar extensiones de más de 200 km en el Mediterráneo occidental (Apel, 2000; Jackson, 2004) (Fig. 15). También se han observado solitones y ondas internas a lo largo de las plataformas continentales alrededor de Iberia (Fig. 15), así como en el talud continental del Golfo de Valencia (van Haren et al., 2013) y de Mar de Alborán (Ercilla et al., enviado; Miguel Bruno, comunicación personal). Constituyen un proceso frecuente y en la mayoría de los casos descritos se generan en el borde de la plataforma (Pingree et al., 1986; Apel, 2004; Azevedo et al., 2006; Pichon et al., 2013). En el caso de las ondas internas, éstas se amplifican y adquieren una mayor velocidad dentro de los cañones submarinos (Fig. 17, Quaresma et al., 2007; Gómez-Ballesteros et al., 2014; Sánchez et al., 2014).

Los maremotos o tsunamis tienen un importante efecto en ambientes marinos, pues generan corrientes de tracción (tsunami-related traction current) con la capacidad de transportar muy rápidamente sedimentos a ambientes profundos (Shanmugam, 2006, 2012a). En el margen Ibérico diversos terremotos han provocado una serie de tsunamis en el pasado histórico (Rodríguez-Vidal et al., 2011), destacándose el de 1755 de Lisboa (1755 AD) que aparecen en el registro geológico de Portugal hasta el Estrecho de Gibraltar (v.g. Dawson et al., 1991, Dabrio et al., 1998, 2000; Luque et al., 1999, 2001, 2004; Luque, 2002; Gracia et al., 2006; Cuven et al., 2013). Registros de edades más antiguas evidencian el desarrollo de tsunamis que han afectado el suroeste de España, Portugal, Marruecos (v. g. Reicherter, 2001; Luque et al., 2001, 2002; Luque, 2002; Ruiz et al., 2004, 2005; Scheffers and Kelletat, 2005), y el Mar de Alborán (IGN, 2009; Reicherter and Becker-Heidmann, 2009). Sin embargo existen pocos trabajos que hayan considerado sus implicaciones sedimentarias en aguas profundas. Un caso descrito es el terremoto de 1522 de Almería ($M > 6.5$), que afectó a una amplia zona del Mediterráneo occidental, provocando deslizamientos submarinos en el Golfo de Almería (Reicherter and Becker-Heidmann, 2009). Durante la Expedición IODP 339 realizada en el Golfo de Cádiz, se han identificado depósitos arenosos como tsunamitas que actualmente están siendo estudiados con más detalle (Fig. 19, Stow et al., 2013b).

Finalmente, otros procesos relacionados con corrientes de tracción por olas solitarias (ó gigantes) o por los ciclones (rogue- and cyclone-related traction currents) pueden al igual que los tsunamis desencadenar flujos de fondo submarinos e inestabilidades de taludes (Shanmugam, 2006, 2012a). Algunos de estos procesos oceanográficos han sido descritos a lo largo del margen Ibérico, si bien no se ha documentado sus efectos sobre el fondo. En teoría, la influencia de estos procesos en ambientes de aguas profundas puede ser localmente de interés.

Implicaciones morfológicas y sedimentarias

Las corrientes de fondo pueden verse afectadas por numerosos procesos permanentes e intermitentes, tales como: overflows, corrientes de marea barotrópicas y baroclínicas, eddies, tormentas profundas, ondas internas, tsunamis y ciclones. Estos procesos pueden actuar individualmente, pero lo habitual es que se combinen varios de ellos, llegando a controlar localmente la dirección y la velocidad de las corrientes de fondo. Por tanto, el conocimiento de estos procesos es importante, pues pueden generar facies sedimentarias específicas y diferentes a las ya definidas para los depósitos contorníticos (Fig. 20). En general, se ha subestimado el papel de las corrientes de fondo y procesos oceanográficos asociados en la morfología del fondo marino a lo largo del margen Ibérico. Sin embargo, las corrientes de fondo y los procesos oceanográficos asociados

controlan, en buena parte, la fisiografía submarina y la sedimentación en los márgenes continentales y cuencas ibéricas adyacentes. Por ejemplo, la profundidad a la que se disponen las interfaces entre las principales masas de agua principales y su variación vertical y espacial ejercen un control fundamental en los principales cambios morfológicos (cambios a lo largo del gradiente de la pendiente) de los taludes continentales (Figs. 6, 7 y 21).

Consideraciones finales: una nueva aproximación multidisciplinaria e investigación aplicada

Las corrientes de fondo generan importantes rasgos deposicionales y erosivos a lo largo del margen continental Ibérico a diferentes profundidades y en distintos contextos, como se ha puesto de manifiesto por diversos autores y que quedan recopilados en el presente volume especial por Llave et al. Sin embargo, en este trabajo se quiere enfatizar que la circulación de las masas de aguas está fuertemente afectada por numerosos procesos oceanográficos, que pueden ser permanentes o intermitentes (Fig. 22), y que controlan localmente su dirección y velocidad. Para entender estos procesos y su influencia real en los fondos marinos se requiere realizar una aproximación multidisciplinaria, que incluiría:

- Estudios detallados para la caracterización de los procesos oceanográficos y su interacción con los rasgos morfológicos del fondo a pequeña y gran escala.
- Entender cómo son los rasgos deposicionales, erosivos y mixtos que están presentes en los sistemas contorníticos, así como su evolución en el tiempo y su distribución en diferentes puntos del margen, y asociarles un proceso oceanográfico específico.
- Estudios de detalle sobre la fisiografía general de los márgenes continentales y su relación con la estructura de las masas de agua e interfases asociadas.
- Modelos numéricos que permitan reproducir los procesos en diferentes contextos morfológicos.
- Caracterización de las interfases entre las masas de agua no solo en la actualidad, sino también en el pasado en base a estudios de paleomorfología y paleoceanografía de antiguas picnoclinas a partir del registro sedimentario.
- Detección y caracterización de capas nefeloides intermedias y profundas.
- Comprender la dinámica de fluidos alrededor de obstáculos submarinos.
- Monitorización oceanográfica para vincular los rasgos morfológicos contorníticos a las condiciones específicas actuales del fondo (v. g. velocidad, energía)
- Relación de rasgos sedimentarios y observaciones directas mediante el ROV, con el efecto reciente de las corrientes de fondo y procesos asociados. La amplia gama de estos rasgos, tanto a pequeña como a gran escala, requiere que se estudien sus vínculos con los diferentes y específicos procesos oceanográficos.
- Análisis de evidencias sedimentarias que relacionan los rasgos deposicionales, erosivos, y mixtos modernos con las corrientes de fondo y con los procesos permanentes e intermitentes asociados.
- Establecer modelos de facies más específicos dirigidos a entender la interacción entre las corrientes de fondo y los procesos oceanográficos asociados con los procesos turbidíticos y gravitacionales de masas a lo largo del margen Ibérico. Estos modelos de facies debería de incluir las facies arenosas y su asociación a posible depósitos turbidíticos retrabajados o bien a depósitos puramente contorníticos.
- La investigación debe fomentar el análisis y evaluación de la influencia de los procesos oceanográficos en los geohábitats frágiles, relictos o activos en la actualidad, que podrían situarse en escenarios de riesgo en relación a cambios medioambientales debidos a alteraciones en la circulación de las masas de agua y/o procesos oceanográficos (permanentes e intermitentes) asociados.

Con respecto a la investigación aplicada, comprender la dinámica de la circulación de las masas de aguas y los procesos oceanográficos (permanentes e intermitentes) asociados ayudará a caracterizar mejor los productos sedimentarios resultantes, la variabilidad espacial y temporal de los depósitos gruesos y finos, los modelos sedimentarios de arquitectura que definen y por ende el potencial como reservorio de los mismos. Muchos de los procesos descritos son responsables de la formación de depósitos arenosos, los cuales representan un tipo de depósito de arenas en ambientes marinos profundos diferente de los relacionados con los procesos turbidíticos, y podría cambiar el paradigma de la explotación de hidrocarburos en aguas profundas. Estos depósitos están relacionados con algunos de los procesos descritos en este trabajo (v. g. ondas internas, mareas), y estudios recientes muestran que son potencialmente buenos reservorios. Por otra parte las contornitas fangosas pueden actuar como niveles de sello, y menos frecuentemente como rocas madre de hidrocarburos (Viana, 2008; Brackenridge et al., 2013; Shanmugan, 2012a, 2013a, b; Brackenridge et al., 2013; Stow et al., 2013b). Además, comprender la dinámica de la circulación de las masas de aguas y los procesos oceanográficos (permanentes e intermitentes) asociados contribuiría a un mayor conocimiento sobre recursos metalíferos formados sobre algunos de los rasgos contorníticos que se generan en el fondo submarino.

Introduction

Deep-marine settings have been considered until 1980s as relatively low energy and quiescent depositional environments where deep-water masses flow as relatively slow-moving tabular bodies and deposition is episodically interrupted by down-slope gravity driven processes. But, since the 1990s it has been demonstrated that deep-water masses can exhibit relatively high velocity and play a dominant depositional role in certain areas (Rebesco *et al.*, 2014). These conditions hold especially when water masses interact with local seafloor irregularities (seamounts, ridges, hills, mounds, banks, scarps, etc.). Flow through deep oceanic gateways, straits or basins can also generate high velocity and turbulent flows, which create regional-scale erosional, depositional and mixed morphological features. Understanding these seafloor features therefore requires a more detailed model of bottom-current effects.

The general term 'bottom current' refers to deep-water currents capable of eroding, transporting, and depositing sediments along the seafloor (Rebesco and Camerlenghi, 2008). Background bottom currents are the result of both ocean thermohaline circulation (THC, Fig. 1A) and ocean wind-driven circulation (Rahmstorf, 2006). They generally exhibit persistent net flow alongslope (following the local bathymetry), but can considerably vary in direction and velocity (Stow *et al.*, 2009). Overflows, tides, including internal tides and other intermittent processes such as bottom reaching (vertical) eddies, deep sea storms, (horizontal) vortices (or eddies), internal waves, solitons, tsunami related currents, rogue waves and cyclonic waves (during storms and hurricanes) can also affect bottom currents (Fig.2) (e.g., Shanmugan, 2012a, 2013a, b, 2014; Rebesco *et al.*, 2014). These processes modulate the bottom current and speed, instantaneous direction, and tend to develop local and regional hydrodynamic structures (e.g., cores, branches, filaments, eddies, vortices, local turbulence, internal waves, helicoidal flows, vertical columns, etc.). Many of these oceanographic deep-water processes are poorly understood but can generate pervasive depositional and erosional features over both short- and long- term time scales.

Contourites are defined as sediments deposited or substantially reworked by the persistent action of bottom currents (e.g., Stow *et al.*, 2002a; Rebesco, 2005, 2014). The term "contourites" was originally intended to define sediments deposited in the deep sea by contour-parallel thermohaline currents (Hollister and Heezen, 1967). Usage of the term has subsequently widened to include a larger range of sediments affect-

ed by different types of currents (Rebesco *et al.*, 2014). Bottom currents are capable of building thick, extensive accumulations of sediments referred to as "contourite drifts". The term "contourite depositional system" (CDS) refers to large contourite deposits (drifts) associated with erosional features in an environment dominated by along-slope processes due to a particular water mass (Hernández-Molina *et al.*, 2003, 2008a, 2009).

The bottom-current circulation around the Iberian continental margin is described by Llave *et al.* (this issue). This paper, however, describes other persistent or intermittent oceanographic processes associated with bottom-current circulation, and their role in determining the shape and evolution of the Iberian margin and adjacent oceanic basins. The first section offers a conceptual description of these other oceanographic processes in the study region, and we then go on to describe how to proceed with the unique research challenge of integrating these complex, three-dimensional and temporally variable oceanographic processes into sedimentary and climatological models.

Oceanographic processes

Bottom currents and thermohaline circulation

Large-scale, deep-water circulation is a critical part of the global conveyor belt that regulates the Earth's climate (Rahmstorf, 2006; Kuhlbrodt *et al.*, 2007). In regions where the deep ocean currents are close enough to the ocean bottom they may shape the deep seafloor. To a first order, dense water formation at high latitudes drives the global THC. Salinity or temperature driven density variations cause sinking of the surface water masses towards greater depths and control their subsequent transport and eventual global distribution. Deep-water formation is closely associated with convection in a few localities (Fig. 1). These mainly occur in the subpolar convergence zone of the Northern Hemisphere and the convergence zone of the Antarctic polar front in the Southern Hemisphere. The principal deep-water masses forming part of the THC include the North Atlantic Deep Water (NADW) and the Antarctic Bottom Water (AABW), which spread across the deepest marine domains as Deep Western Boundary Currents (DWBC) (Rahmstorf, 2006). Bottom circulation and distribution along the oceanic basins is conditioned by their proximity to high-latitude input sources, seafloor morphology, inter-oceanic connection via deep gateways and the Coriolis Effect (Kennet, 1982;

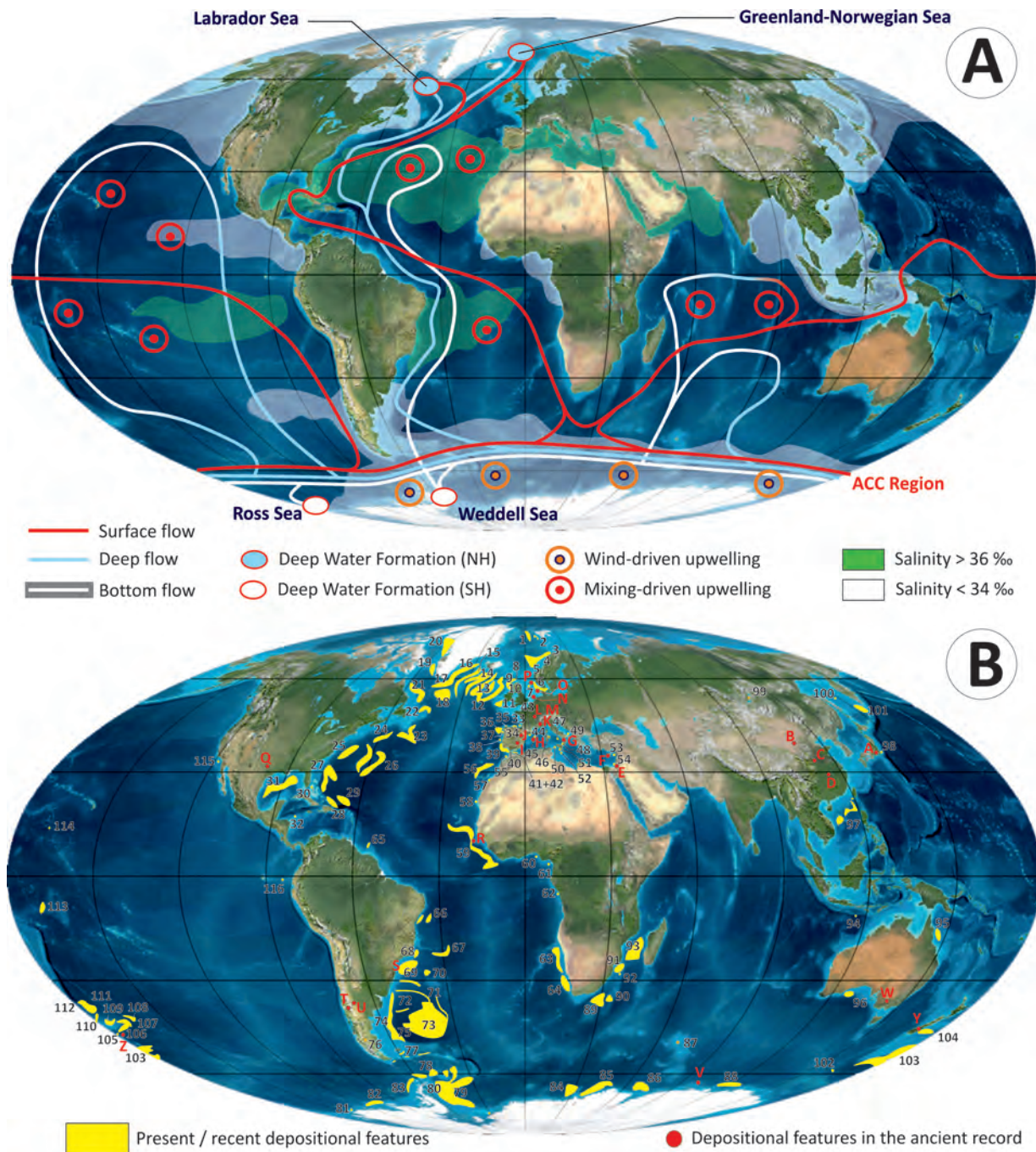


Figure 1. A) Global thermohaline circulation. In the Atlantic, warm and saline waters flow northward from the Southern Ocean into the Labrador and Nordic seas. In contrast, there is no deep-water formation in the North Pacific, and its surface waters are fresher. Deep waters formed in the Southern Ocean become denser and thus spread at deeper levels than those from the North Atlantic. Wind-driven upwelling occurs along the Antarctic Circumpolar Current (Adapted from Rahmstorf, 2006; Kuhlbrodt *et al.*, 2007); B) occurrence of the large contourite deposits in the present (recent) ocean basins (yellow areas) and in the ancient sedimentary record (red points). Compilation published in Rebesco *et al.* (2014), reproduced with permission from Elsevier. Base maps from A and B are from Ron Blakey, Colorado Plateau Geosystems at <http://cpgeosystems.com/mollglobe.html>.

Figura 1. A) Circulación global termohalina. En el Atlántico, las aguas cálidas y salinas circulan desde el Océano meridional hacia los Mares del Labrador y Nórdico. Por el contrario, no existe formación de agua profunda en el Pacífico Norte, y sus aguas superficiales son por tanto más dulces. Las aguas profundas formadas en el Océano meridional son más densas y se expanden en niveles más profundos que aquellas del Atlántico Norte. Se producen afloramientos por el viento a lo largo de la Corriente Circumpolar Antártica (adaptado de Rahmstorf, 2006; Kuhlbrodt *et al.*, 2007); B) Localización de grandes depósitos contorníticos en la actualidad (recientes) en las cuencas oceánicas (áreas en amarillo) y en el registro fósil (puntos rojos). Recopilación en Rebesco *et al.* (2004) y publicada con el permiso de Elsevier. Mapas base de A y B tomados del Ron Blakey, Colorado Plateau Geosystems en <http://cpgeosystems.com/mollglobe.html>

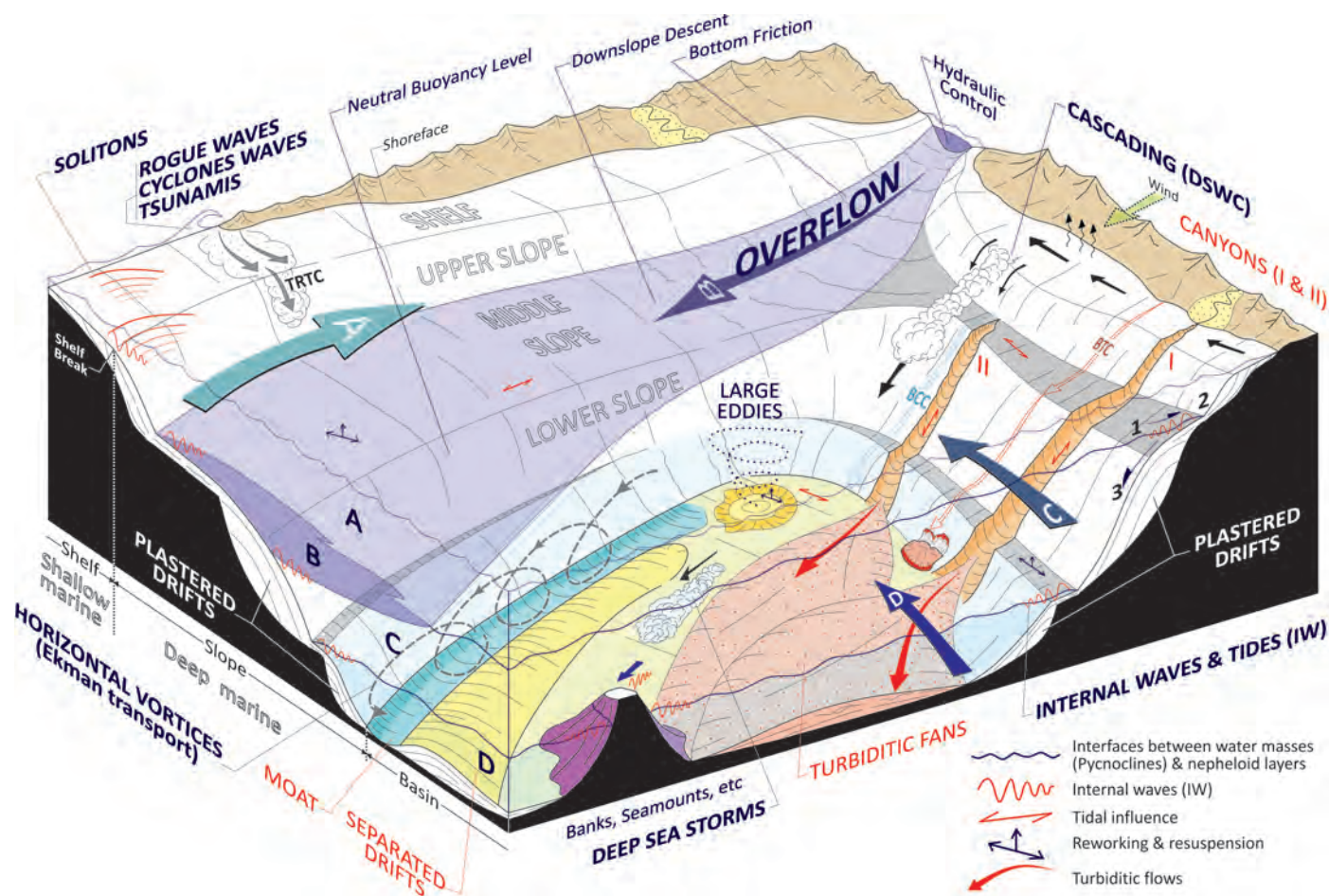


Figure 2. 3D sketch depicting the possible oceanographic processes in deep-water environments. In addition to density currents and overflows, the velocity at the seafloor can also be affected by barotropic currents or intermittent processes such as cascading, giant eddies, deep sea storms, vortices, internal waves, internal tides, tsunamis, cyclone waves and rogue waves (From Rebesco *et al.*, 2014, with permission from Elsevier).

Figura 2. Esquema en 3D donde se indican los posibles procesos oceanográficos en ambientes de aguas profundas. La velocidad en el fondo marino puede verse afectada además de por las corrientes de densidad y desbordamientos, por corrientes barotrópicas o procesos intermitentes como cascadas densas de plataforma, remolinos gigantes, tormentas profundas, vórtices, ondas internas, mareas internas, tsunamis, ondas ciclones y olas aisladas (de Rebesco *et al.*, 2014, con permiso de Elsevier).

Faugères *et al.*, 1993; Rahmstorf, 2006). Other bottom currents, such the extension of the wind-generated currents, are not linked to THC. These latter currents include the Gulf of Mexico current system (e.g., Loop Current; Wunsch, 2002) and the Antarctic Circumpolar Current (Orsi *et al.*, 1995).

Bottom-water masses generally move relatively slowly as laminar flows over their global course (< 3 cm/s). Regional and local bottom-current velocities exhibit local heterogeneity due to varying seafloor stress and other current instabilities, such as mesoscale variability. Western stretches of ocean basins and topographic obstacles along the seafloor facilitate higher velocities (> 0.6-1 m/s) (Stow *et al.*,

2009; Hernández-Molina *et al.*, 2011). Bottom-water behaviour and velocity partially affect the seafloor through lateral transport of suspended particulate matter in the water column. This material is up to 10 times higher in concentration in the deep nepheloid layer (at 50 – 200 m above the seafloor) of the Deep Western Boundary Currents compared to other oceanic areas (Rebesco *et al.*, 2014). A sufficiently active bottom current acting for a prolonged period of time will thus profoundly affect the seafloor by winnowing fine-grained sediments and generating large-scale erosion, depositional and mixed features (Stow *et al.*, 2002b; Rebesco and Camerlenghi, 2008; Rebesco *et al.*, 2014). Bottom currents represent long-

term hydrologic conditions on geological time scales. The establishment of the main CDSs around the world in fact coincides with the Eocene / Oligocene boundary (~32 Ma), and was more recently reactivated by THC during the Middle Miocene (Hernández-Molina *et al.*, 2008a).

The topic of bottom-current processes around Iberia is addressed by Llave *et al.* in this issue. Along the Iberian margin, several important bottom currents shape the continental margins and abyssal plains (e.g., Iorga and Lozier, 1999; Millot, 1999, 2009; Serra *et al.*, 2010a). These currents derive primarily from the Western Mediterranean Deep Water (WMDW) and the Levantine Intermediate Water (LIW) in the Alboran Sea, as well as the Mediterranean Overflow Water (MOW) and the Lower Deep Water (LDW) in the Atlantic (see the water-mass compilation in Hernández-Molina *et al.*, 2011 and Llave *et al.*, this issue). Well-developed CDSs around Iberia have not been systematically interpreted according to bottom-current models and thus are not well understood.

Overflows

Overflows constitute permanent oceanographic processes related to: 1) flow over a topographic barrier from a regional basin into the open ocean (Fig. 2) and 2) open-ocean flow into an isolated regional basin. The Denmark Strait Overflow Water (DSOW); Iceland-Scotland Overflow Water (ISOW) and MOW (Price and Baringer, 1994; Legg *et al.*, 2009, Fig. 3A) are good examples of the first type of overflow. The second type of overflow occurs in association with deep gateways such as the Bruce Passage between the Weddell Sea and Scotia Sea (Legg *et al.*, 2009; Lobo *et al.*, 2011, Fig. 3A) and the overflow of AABW from the Brazil Basin into the North Atlantic Basin across the Atlantic ridge or in the Gulf of Mexico (Legg *et al.*, 2009). In the aforementioned cases, a dense gravity current, carrying a particular water mass, descends the regional slope to a greater depth until it reaches density equilibrium. Entrainment of surrounding water, bottom friction and inertial accelerations modify the bottom current along the slope (Fig. 3B). Bottom friction and the Earth's rotation induce the Ekman bottom boundary layer (e.g., Pedlosky, 1996; Wåhlin and Walin, 2001), which produces a net transport to the left in the Northern Hemisphere. Although the frictional transport is confined to a thin layer near the bottom (the Ekman boundary layer), it affects the whole water column asymptotically. The dense water adjusts to the divergence of the frictional transport, which acts as a hori-

zontal diffusive process, minimizing the curvature of the dense interface. The lower (seaward) edge moves downhill (Figure 3C) as the Ekman layer expels the Ekman transport from its interior (e.g., Wåhlin and Walin, 2001). At the upper (landward) edge, the dense interface then becomes almost horizontal, with diminished geostrophic velocity and frictional transport (e.g., Wåhlin and Walin, 2001). The combined frictional effect over the entire outflow causes it to gradually widen (Fig. 3C), keeping the upper horizontal boundary at a nearly constant depth (e.g., Borenäs and Wåhlin, 2000). If these processes occur over a laterally varying bottom slope, they act to split the flow into two or more cores and branches, as suggested for example, in an interpretation of the Mediterranean Outflow (Borenäs *et al.*, 2002; Serra *et al.*, 2010a, b). As dense water passes from its formation site into the open ocean as an overflow, it undergoes mixing with the overlying water column. This process determines the eventual properties and volume transport of the resultant bottom currents, and triggers eddy formation (Legg *et al.*, 2009).

The main overflow example in the Iberian margin stems from MOW dynamics during the late Miocene opening of the Gibraltar gateway (Duggen *et al.*, 2003; Bache *et al.*, 2012; Roveri *et al.*, 2014). The Strait of Gibraltar, which consists of a 60 km long sill and narrows gateway (Armi and Farmer, 1986), plays a key role in the water exchange between the Mediterranean Sea and the Atlantic Ocean. The excess evaporation over precipitation (0.5 to 0.8 m/yr) dramatically enhances the salinity and density of the Mediterranean, relative to waters of the adjacent Atlantic Ocean (Millot *et al.*, 2006). Mediterranean salinity tongues develop in the Atlantic Ocean from the overflow (0.68 Sv) of dense, warm, (13°C) highly saline (37) water (Bryden *et al.*, 1994; Candela, 2001; Serra *et al.*, 2010a). Mediterranean Levantine Intermediate Water (LIW) and Western Mediterranean Deep Water (WMDW) mix when they flow out through the Strait and originate the MOW that is around 2 times saltier than any other Atlantic water mass. The overflow spills over the Strait of Gibraltar sills and cascades from a depth of 300 m at the edge of the strait down the continental slope of the eastern Gulf of Cadiz. As it does so, it entrains the overlying, less dense North Atlantic Central Water (NACW) (Johnson and Stevens, 2000). Overflows typically occur at velocities of 50 to 100 cm/s (Legg *et al.*, 2009), but in the case of MOW, the current velocity decreases from around 200 cm/s in the neighbourhood of the Camarinal sill and its western approaches (Sánchez Román *et al.*, 2009; Gasser *et al.*, 2011), down to 60 - 100 cm/s further to the northwest. From the first 100

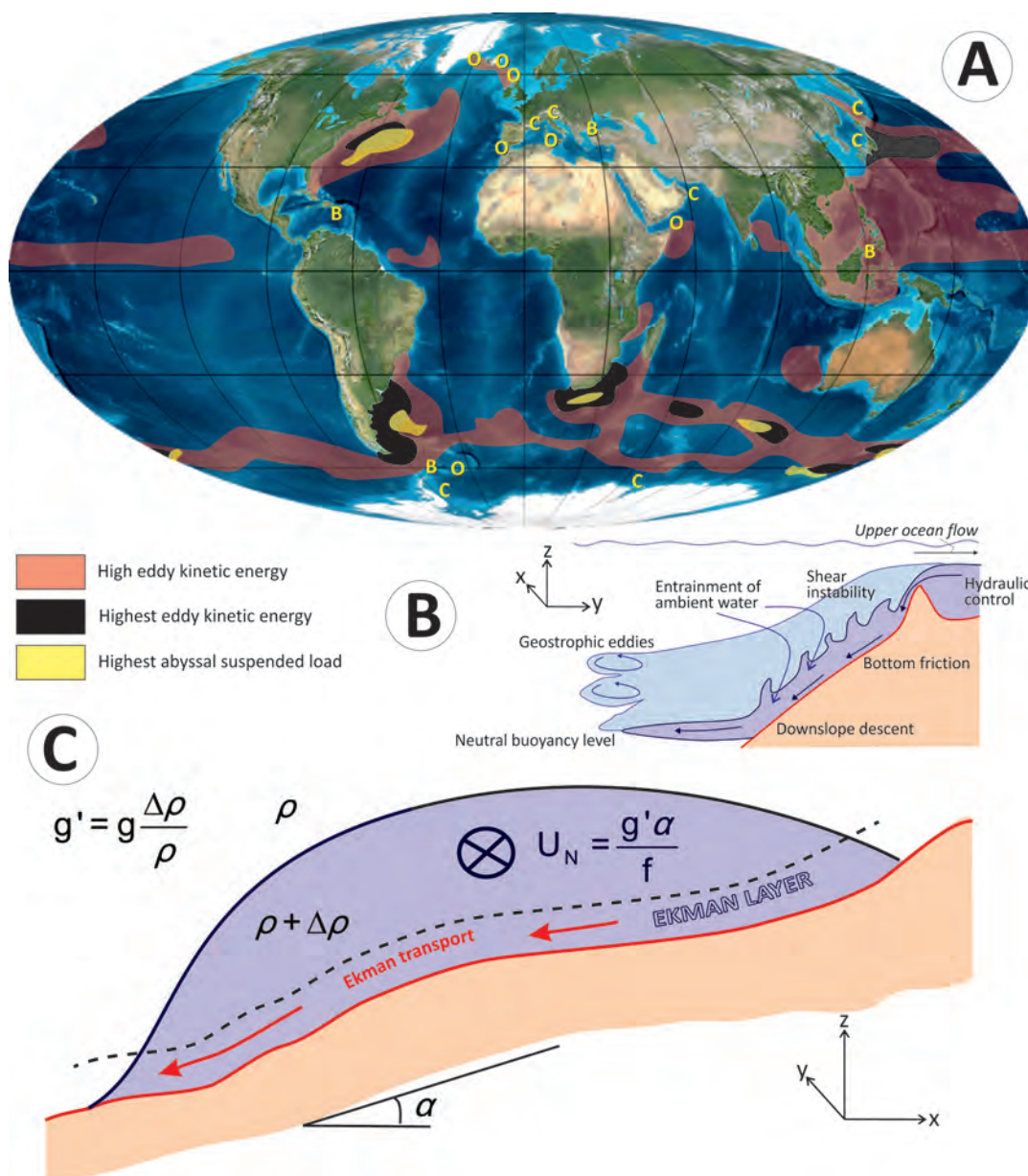


Figure 3. A) Map showing the relation between kinetic energy and suspended load, indicating the areas with higher suspended load in deep basins. The position of main gravity currents by type is also indicated: O= overflow over a topographic barrier from a regional basin into the open ocean; B= open-ocean overflow into an isolated regional basin; C= cascade of dense water from a continental shelf. Not shown are numerous overflows across multiple sills of the mid-ocean ridge system, within the series of basins of the western South Pacific; and the cascades of shelf water over the slope of the Arctic Sea. Base map from Ron Blakey, Colorado Plateau Geosystems at <http://cpgeosystems.com/mollglobe.html>. B) Physical processes acting in overflows. C) Sketch of a dense overflow showing the coordinate system and some of the notations used: ambient density ρ , plume density $\rho + \Delta \rho$, reduced gravity g' , bottom slope α , Coriolis parameter f and Nof velocity U_N . Also indicated are the Ekman layer and the benthic Ekman transport. Figure from Rebescio *et al.*, (2014) with permission from Elsevier.

Figura 3. A) El mapa muestra la relación entre la energía cinética y la carga suspendida, indicando las zonas con mayor carga suspendida en cuencas profundas. También se indica la posición de las corrientes principales de gravedad por tipos: O= overflows a través de una barrera topográfica de una cuenca regional hacia el océano abierto; B= overflows desde alta mar hacia una cuenca regional aislada; C= overflows desde una plataforma continental. Aunque no se muestran en la figura, hay numerosos overflows, a través de múltiples umbrales del sistema de dorsales oceánicas, dentro de las cuencas del oeste del Pacífico Sur; y las cascadas de agua de la plataforma sobre la vertiente del Mar Ártico. Mapa base de Ron Blakey, Colorado Plateau Geosystems en <http://cpgeosystems.com/mollglobe.html>. b) Procesos físicos que actúan en los overflows. c) Esquema de un overflow denso que muestra el sistema de coordenadas y algunas de las notaciones usadas: densidad ambiente ρ , densidad de la pluma $\rho + \Delta \rho$, gravedad reducida g' , pendiente del fondo α , parámetro de Coriolis f y velocidad Nof U_N . Se indican además la capa de Ekman y el transporte bentónico Ekman. Figura de Rebescio *et al.*, (2014), reproducida con permiso de Elsevier.

km of the overflow path, volume transport increases by a factor of three to four (Serra *et al.*, 2010a; Rogerson *et al.*, 2012). As it descends, the overflow veers north and follows the Iberian continental margin, approaching its neutral buoyancy as it nears 8°W at about 1,000 m depth (Ochoa and Bray, 1991; Baringer and Price, 1997, 1999; Käse and Zenk, 1996; Ambar *et al.*, 2002, 2008; Bower *et al.*, 2002; Serra *et al.*, 2005, 2010a; García-Lafuente *et al.*, 2009).

In the Gulf of Cadiz, friction in the bottom Ekman boundary layer and entrainment in its upper part affect the MOW plume (Baringer and Price, 1997;

Gasser *et al.*, 2011). The vertical distribution of the along-stream velocity comprises two regions separated by a velocity maximum (called the plume nose). These consist of an upper (interfacial) layer characterised by sharp velocity and salinity gradients, and a bottom layer, which exhibits constant salinity and a sharp decrease in velocity (Johnson *et al.*, 1994a,b). Secondary across-stream circulation spreads water from the upper layer upslope and dense water from the bottom layer downslope. In the eastern Gulf of Cadiz, near the Strait of Gibraltar, this overflow is associated with sandy-sheeted drifts, scours, ripples,

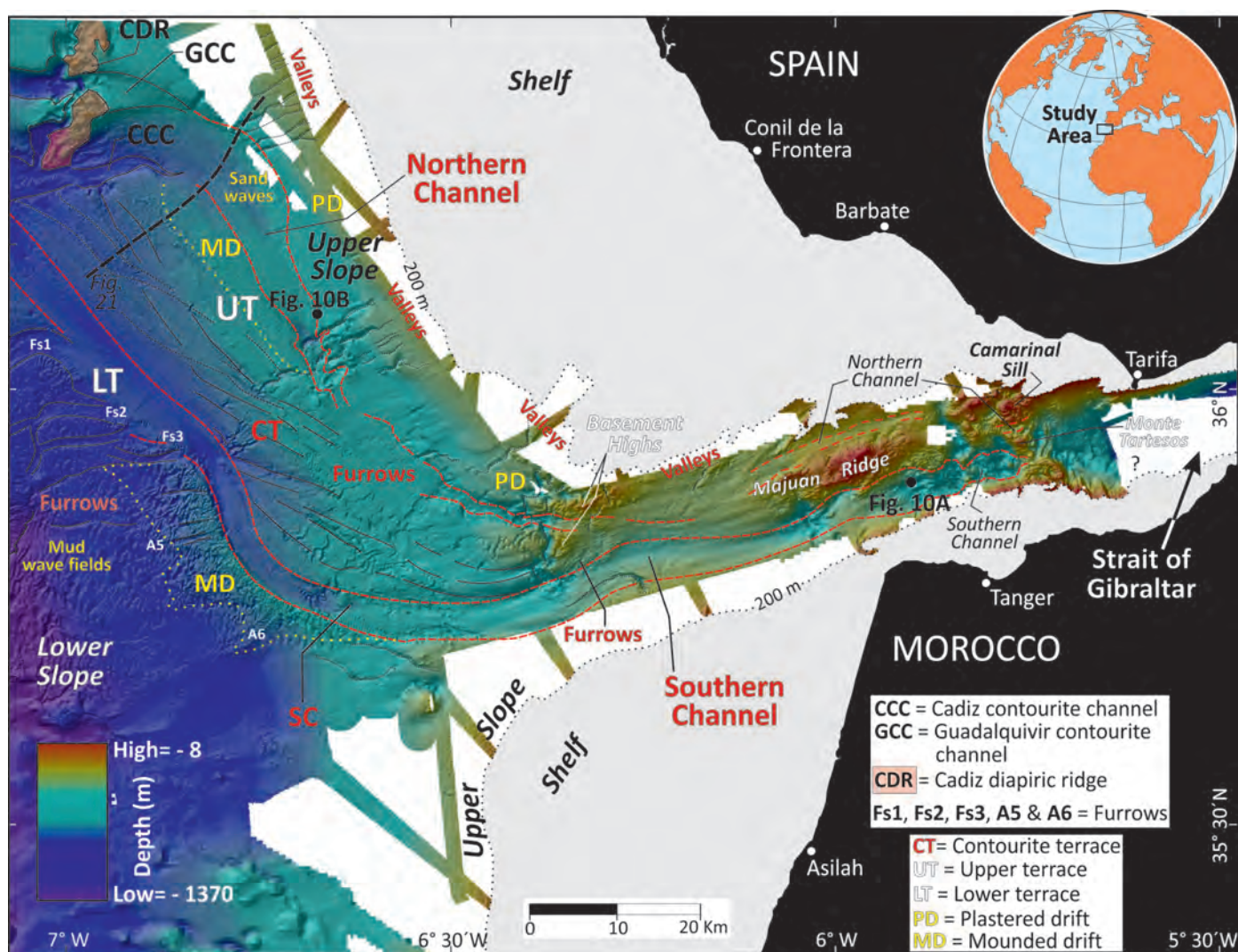


Figure 4. Swath bathymetry at the exit of the Strait of Gibraltar. Main depositional and erosive features are shown (figure from Hernández-Molina *et al.*, 2014 with permission from GSA). Note that furrows are oblique to the main channels due to the secondary circulation related to the benthic Ekman transport.

Figura 4. Batimetría multihaz en la salida del Estrecho de Gibraltar. Se muestran los principales rasgos deposicionales y erosivos (adaptada de Hernández-Molina *et al.*, 2014, con permiso de GSA). Se puede observar que los furrows son oblicuos a los canales principales como consecuencia del flujo secundario asociado al transporte bentónico Ekman.

sand ribbons and sediment waves (Nelson *et al.*, 1993), and generates large terraces and erosive channels (Fig. 4) (Hernández-Molina *et al.*, 2014). The secondary circulation here is especially relevant to the erosion, resuspension and deposition of sediment, as well as to the formation of large contourite features (Hernández-Molina *et al.*, 2014).

Other examples of open-ocean overflow may occur between oceanic basins with different depths (Legg *et al.*, 2009). A possible case to be explored along the Iberian margin may theoretically develop through the Theta Gap, a passage formed between the La Coruña and Finisterre structural highs (Fig. 5), and narrows to a width of approximately 5 km between the Biscay abyssal plain (average water depth of 5,100 m) and the Iberian abyssal plain (about 5,300 m deep), or other deep channels between the

abyssal plains. Heezen *et al.* (1959) first described the Theta Gap connection as “a constricted passage connecting two abyssal plains which, in the vicinity of the gap, lie at different levels”. The Biscay abyssal plain regionally slopes in a southward direction, with its deepest section in the southwest corner, where the slope connects to the Theta gap. Active erosion occurs about 15 km upslope of the narrowing between the structural highs (Laughton, 1960, 1968), and creates initial incisions of up to 300 m and later incisions of about 100 m at points further along the course of the current. The LDW water mass, which makes up this overflow (>3450 m water depth), penetrates into the North Atlantic through the Discovery Gap on the western flank of the Madeira–Tore Rise (Haynes and Barton, 1990; McCartney, 1992; Van Aken, 2000), and veers northward along the Galicia

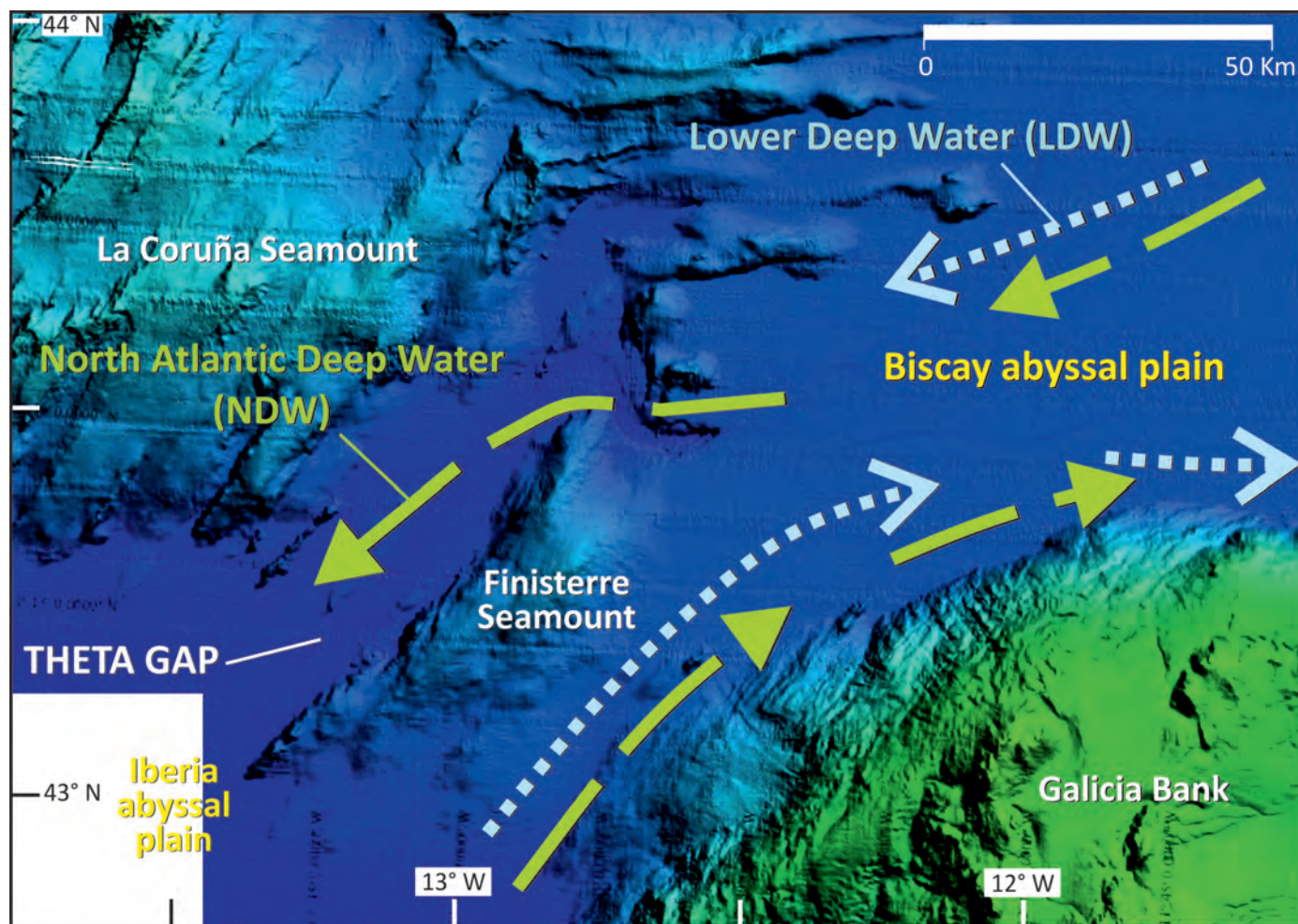


Figure 5. Main morphologic features around the Theta Gap showing the regional water-mass circulation.

Figura 5. Principales rasgos morfológicos alrededor del Theta Gap, donde se muestra la circulación regional de las masas de agua.

margin as a near-bottom flow (Paillet and Mercier, 1997; Van Aken, 2000). A cyclonic recirculation cell occurring above the Biscay Abyssal plain deflects the current poleward however, with a velocity near the continental margin of $1.2 (\pm 1.0)$ cm/s (Dickson *et al.*, 1985; Paillet and Mercier, 1997) (Fig. 5).

Processes at the interface between water masses

A pycnocline represents a layer with maximum gradient of density, which can be sharp and well defined, or diffuse with a gradual transition from one water mass to the other (Fig. 2). Turbulent mixing of water masses caused by tides (or other processes) can disrupt the pycnocline, whereas stratifying processes (e.g., regional positive buoyancy flux at the surface) maintain it. The relative balance between these two

factors defines the structure of the pycnocline in different regions and at different times of the year. The interface often tilts in one dominant direction (e.g., Reid *et al.*, 1977) but can be locally and temporarily displaced by eddies (e.g., Piola and Matano, 2001; Arhan *et al.*, 2002, 2003) and internal waves. Energetic current patterns associated with these waves and eddies (Reid *et al.*, 1977) strongly affect the seafloor (e.g., Hernández-Molina *et al.*, 2009, 2011; Preu *et al.*, 2013) through erosion and re-suspension (Dickson and McCave, 1986; Cacchione *et al.*, 2002; Puig *et al.*, 2004; Shanmugan, 2013a, 2014).

Some water masses circulating around the Iberian margin have remarkable density contrasts (Figs. 6 and 7). The exchange flow through the Strait of Gibraltar exhibits these contrasts for example, as do the base and top boundaries of the MOW (Serra *et al.*, 2010a), which was enhanced during cold (e.g.; glacial)

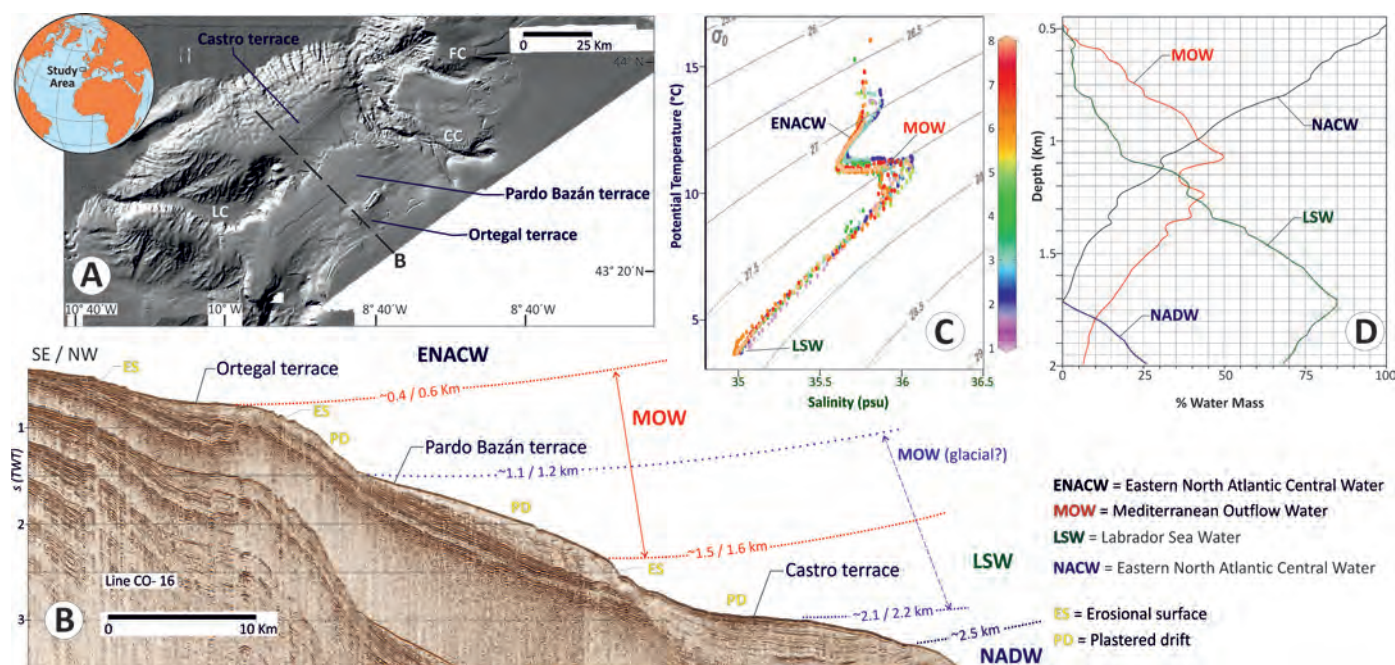


Figure 6. Example of three contourite terraces (Ortegal, Pardo Bazán and Castro) along the continental slope northwest of Galicia and its relation with the range of depth of the interfaces between water masses. A) Multibeam bathymetry indicating the position of the terraces at water depths around 0.2-0.4 km; 0.9-2 km and 2.2-2.4 km (adapted from Maestro *et al.*, 2012); B) Seismic profile (CO-16) acquired during the CONTOURIBER-2 cruise crossing the terraces (line position in A). Interfaces between regional water masses at present time is included, with the theoretical position of MOW during glacial stages (in blue); C) T/S diagram corresponding to eight profiles from ARGOS buoy (6900469, PROVOR Profiling Float CTS3- OVIDE Project) between the 9.11.2012 to 18.01.2013 (from Sánchez-González, 2013); D) Water-mass percentage in the adjacent area to the contourite terraces (from Sánchez-González, 2013).

Figura 6. Ejemplo de tres terrazas contorníticas (Ortegal, Pardo Bazán y Castro) a lo largo del talud continental al noroeste de Galicia y su relación con el rango de profundidad de las interfases entre las masas de agua. A) Batimetría multihaz que indica la localización de las terrazas a 0.2-0.4 km; 0.9-2 Km y 2.2-2.4 km (adaptado de Maestro *et al.*, 2012); B) Perfil sísmico (CO-16) adquirido durante la campaña Contouriber-2 que cruza las terrazas (posición de línea en A). Se incluyen las interfases entre las masas de agua regionales en el momento actual, con la posición teórica de la MOW durante las fases glaciales (en azul); C) Diagrama T/S correspondiente a ocho perfiles de la boya ARGOS (6900469, PROVOR Profiling Float CTS3- OVIDE Proyecto) entre el 09/11/2012 al 18/01/2013 (de Sánchez-González, 2013); D) Porcentaje de las masas de agua en el área adyacente a las terrazas contorníticas (de Sánchez-González, 2013).

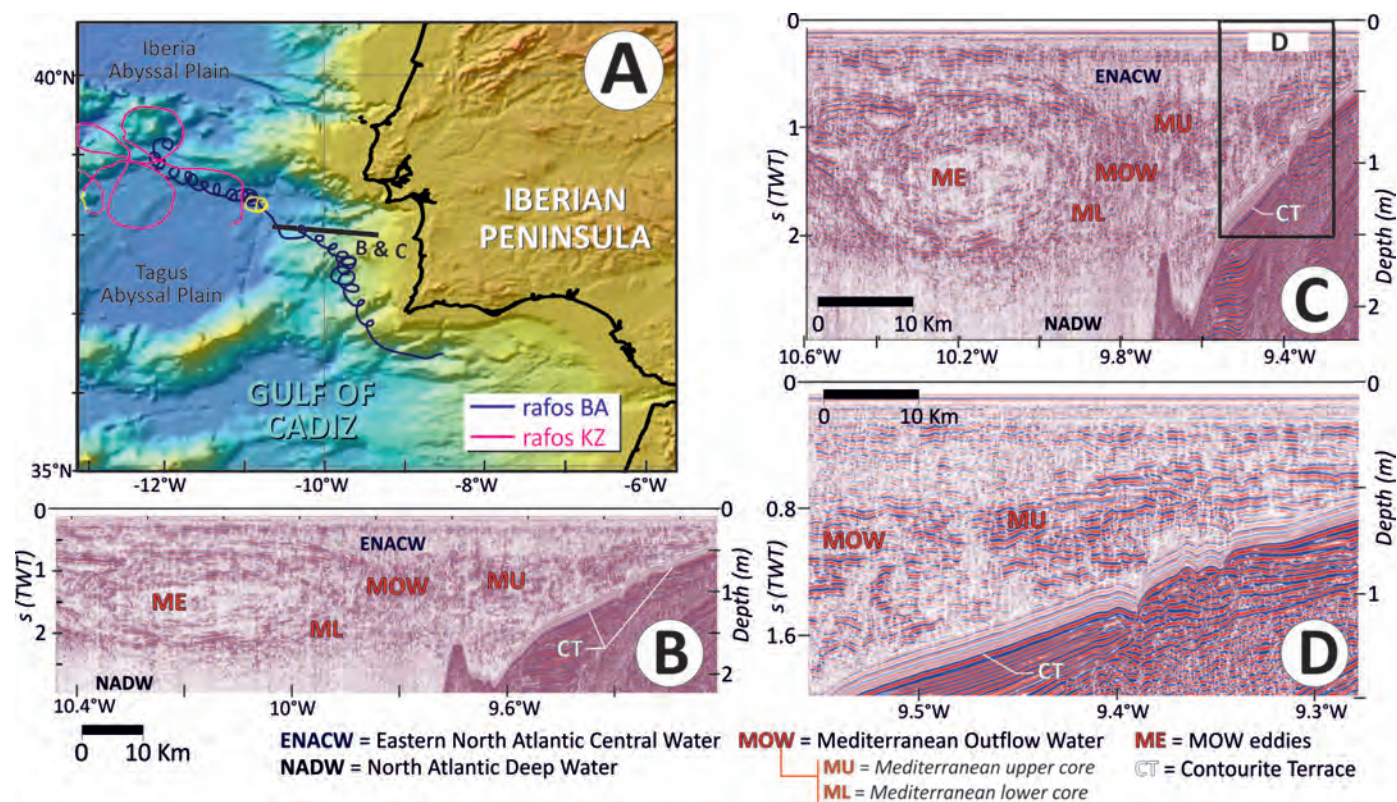


Figure 7. A) Bathymetric map of the western Iberian margin, showing the trajectories of the RAFOS floats that were caught by meddy-9 (blue line) and the cyclone C (magenta line) reported (from Pinheiro *et al.*, 2010); the yellow fractions of these trajectories correspond to the period between the 28 August and 3 September 1993, during which the seismic profile in B and C was acquired. B and C) complete migrated seismic section showing the eddies (meddies) related to the Mediterranean Outflow Water (MOW) and their interaction with the sea-floor (Pinheiro *et al.*, 2010), including the water masses and the interaction of MOW with a contourite terrace in the middle slope. The segment to the east of the line was acquired from W to E, from the 2 to 3 September 1993. Approximate depth based on 1500 m/s sound speed, and longitude axis are indicated; C) detail of a migrated section with interpreted upper (MU) and lower (ML) MOW (Pinheiro *et al.*, 2010); and D) detail of a migrated section with the interpreted upper MU (Pinheiro *et al.*, 2010). High amplitude reflections within the profiles, especially to the upper and lower boundaries of MOW and meddies are indicative of density contrast surfaces in the water column.

Figura 7. A) Mapa batimétrico del margen occidental Ibérico, que muestra las trayectorias de los flotadores RAFOS que se tomaron por Meddy-9 (línea azul) y el ciclón C (línea magenta) (de Pinheiro *et al.*, 2010); las fracciones amarillas de estas trayectorias corresponden al periodo entre el 28 de Agosto y el 3 de Septiembre de 1993, durante el cual se adquirió el perfil sísmico en B y C. B y C) Sección sísmica migrada que muestra los remolinos (meddies) relacionados con la Masa de Agua de Salida del Mediterráneo (MOW) y su interacción con el fondo marino (Pinheiro *et al.*, 2010), incluyendo las masas de agua y la interacción de la MOW con un terraza contornítica del talud medio. El segmento al Este de la línea se adquirió de O a E, del 2 al 3 de Septiembre. Se indica la profundidad aproximada, basada en una velocidad del sonido de 1500 ms⁻¹, y el eje de longitud; C) Detalle de una sección migrada con la interpretación del núcleo superior (MU) e inferior (ML) de la MOW (Pinheiro *et al.*, 2010); y D) detalle de una sección migrada con la interpretación del núcleo superior MU de la MOW (Pinheiro *et al.*, 2010). Las reflexiones de mayor amplitud que se pueden observar en los perfiles, especialmente a la base y el techo de la MOW y asociadas a los meddies, son indicativas de la existencia de superficies con un contraste de densidad en la columna de agua.

periods (Schönfeld *et al.*, 2003; Voelker *et al.*, 2006; Toucanne *et al.*, 2007; Rogerson *et al.*, 2012). The associated currents indicate a relationship between the position of the interface and the development of large contourite terraces (Hernández-Molina *et al.*, 2009, 2011; Preu *et al.*, 2013; Rebesco *et al.*, 2014). Several examples of this relationship have been described along the Iberian margin in the Alboran Sea (Ercilla *et al.*, 2002; Ercilla *et al.*, submitted), the Gulf of Cadiz (Hernández-Molina *et al.*, 2014); the

Portuguese Margin (Fig. 7, Pinheiro *et al.*, 2010); and the Cantabrian Sea (Fig. 6, Maestro *et al.*, 2013; Sánchez-González, 2013).

Deep-water tidal currents

Surface tides are mostly driven by the response of the ocean to the gravitational fields of the Sun and the Moon. Surface tides are considered barotropic tides

because their associated currents are mainly depth-independent (Fig. 2). Tidal signals consist of the superposition of several harmonics (tidal constituents) with the principle lunar semi-diurnal frequency (M_2 ; 12.42 h) exerting the strongest global effects in agreement with the tide-generating potential theory (Lakshmi *et al.*, 2000). Tidal energy may be transferred to baroclinic modes in stratified fluids, thus generating baroclinic tides (Fig. 2). Baroclinic tides can dissipate tidal energy by transferring motion along distant features. Both barotropic and baroclinic tides influence the bottom-water circulation in deep-water environments (Dykstra, 2012). Tidal currents change direction periodically with time, describing an elliptical hodograph usually aligned along bathymetric contours in the ocean interior. Tidal energy tends to dissipate, and hence, to exert a stronger effect on continental slopes within submarine canyons and adjacent areas (e.g., Shepard, 1976; Shepard *et al.*, 1979; Viana *et al.*, 1998; Kunze *et al.*, 2002; Garrett, 2003; Shanmugam, 2012a, 2013b; Gómez-Ballesteros *et al.*, 2014; Gong *et al.*, 2013, in press) and within certain contourite channels (Stow *et al.*, 2013a). Shanmugam (2012a) has proposed that barotropic tidal currents affect land- or shelf-incising canyons connected to estuaries or rivers. Baroclinic tide currents affect slope-incising canyons but do not clearly connect to major rivers or estuary systems. Inversion of bottom current directions due to tidal influence occurs outside these canyons (Kennett, 1982; Stow *et al.*, 2013a). Deep-marine tidal bottom-current velocities range from 25-50 cm/s but can reach 70-75 cm/s, and exhibit periods of up to 24 hours (Shanmugam, 2012a).

According to both *in situ* measurements (tidal gauges) and numerical models, the most important harmonic affecting the Atlantic Iberian margin is M_2 (sea-level amplitudes between 100-180 cm, Fig. 8), followed by S_2 (12.00 h, 30-50 cm) (Alvarez-Fanjul *et al.*, 1997). A typical spring/neap tidal modulation of 14.8 days (the fortnightly tidal cycle) thus affects Iberian coastal areas. The regional surface tide dynamics around the Atlantic Iberian Peninsula is part of the amphidromic system that characterises the semi-diurnal tidal waves in the North Atlantic (Cartwright *et al.*, 1980), where a barotropic Kelvin wave propagates northward along the western Iberian coast with a phase speed close to 900 km/h. The wave diffracts eastward in the Cantabrian Sea and its amplitude increases steadily shoreward. Kelvin wave dynamics predict counter clockwise tidal ellipses aligned parallelly to the coast. This simple model adequately approximates observed propagation directions (e.g., the largest phase lags in the

Cantabrian Sea, Alvarez-Fanjul *et al.*, 1997), observed and simulated wave amplitudes, which maximize along the northern coast, and open ocean dynamics. The model, however, does not adequately describe tidal current variation in the shelf/slope region where baroclinic tides start playing a significant role and the cross-shore movement becomes increasingly important. Marta-Almeida and Dubert (2006) concluded that bathymetric irregularities exert a major influence on the velocity field where steepened areas of the slope amplify tidal currents, orthogonally polarising tidal ellipses along bathymetric contours. Bottom features can therefore theoretically change the S-N orientation of tidal currents. Quaresma and Pichon (2013) have recently shown that the cross-shelf velocity component over the slope and shelf can supersede the along-shelf velocity component, giving rise to a clockwise rotation of tidal currents. The ellipse eccentricity decreases as a function of the slope gradient of the sea-floor. Along the Mediterranean area of the Iberian margin, tidal currents only exert significant effects in the Alboran Sea (García-Lafuente and Cano Lucaya, 1994), where phases increase eastward. The velocities of semi-diurnal components decrease from a few 10^{-2} m/s to 10^{-3} m/s in the Algero-Provençal Basin (Alberola *et al.*, 1995).

Both M_2 and S_2 amplitudes increase from the Gulf of Cadiz to the Bay of Biscay, and exert the dominant influence on tidal wave amplitude and current velocity throughout the shelf (Battisti and Clarke, 1982). Across-shelf, the tidal amplitude decreases offshore with an average gradient of ~ 0.027 cm/km. The maximum speeds of around 50 cm/s and 20 cm/s (in a clockwise direction) for the M_2 and S_2 ellipses (respectively) occur on the French shelf. The Bay of Biscay confines the tidal wave and forces the generation of noticeable baroclinic tides that amplify the semi-diurnal constituents as the barotropic tidal wave impinges the French Armorican shelf. Velocities are much less around Iberia, with maximum of 5 and 2 cm/s for the respective M_2 and S_2 ellipses (Quaresma and Pichon, 2013), and exhibit strong along-shore spatial variability. The O_1 and K_1 diurnal constituents are also present (8 and 6 cm amplitude, respectively), and cause the observed diurnal inequality of the tide.

Although the observed tidal currents are slight (rarely above 20 cm/s) around Iberia, they are the primary driving force behind strong, high-frequency baroclinic activity, which does not affect other coastal regions. The combination of regional, barotropic tidal velocities and steep bathymetry amplifies this effect into "hotspots", which occur along the Atlantic margin of Iberia (Quaresma and Pichon, 2013, Fig. 8C). These hotspot areas include the Extremadura and

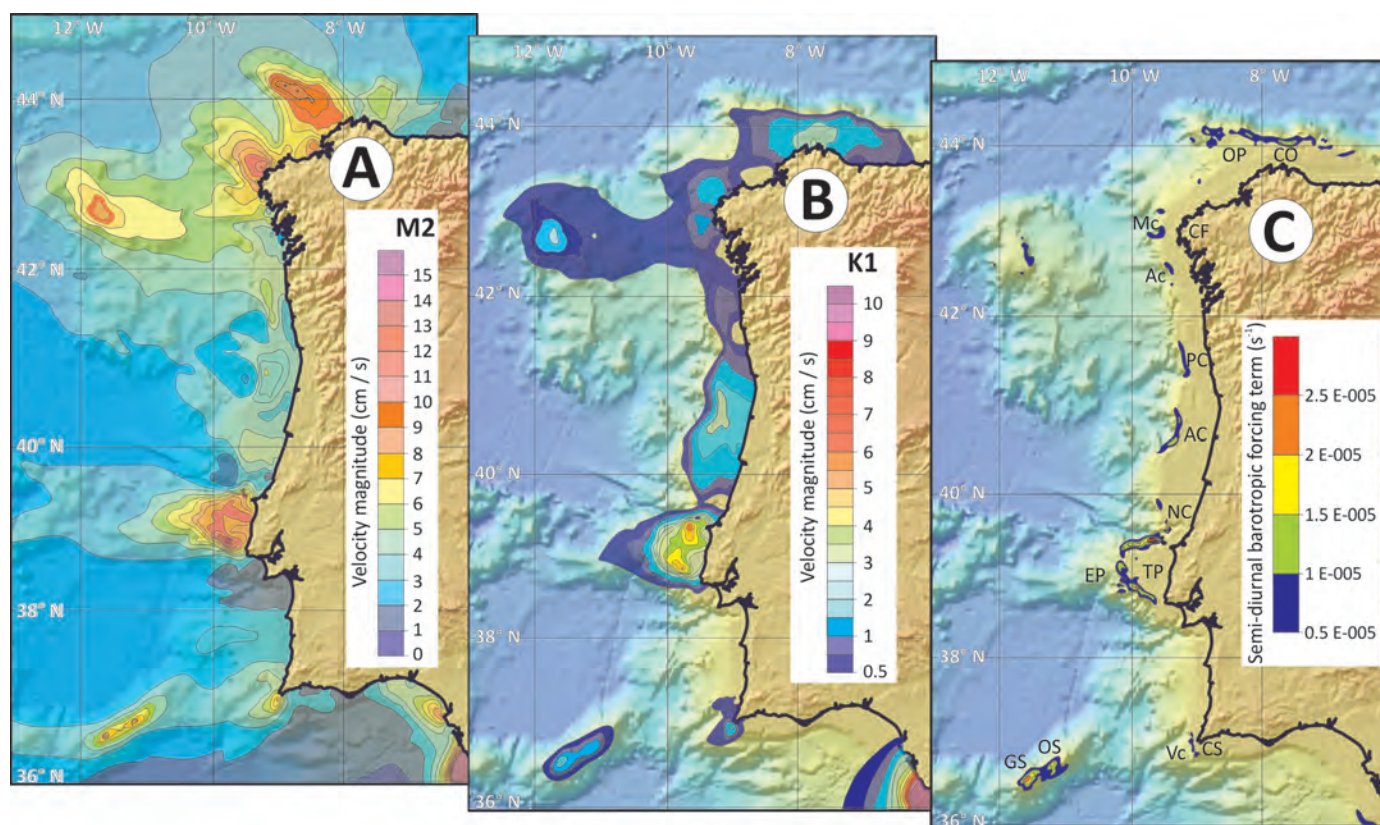


Figure 8. Maps showing: A) the M2 barotropic current velocity map. The maximum M2 velocities (cm/s) are illustrated by the tidal ellipse semi-major axis magnitude; B) K1 barotropic current velocity phase map. This corresponds to the phase lag of the maximum current behind the maximum tidal potential of M2 (degrees referenced to GMT); C) semi-diurnal barotropic forcing term map ($1/s$). Internal tide generation “hotspots” are pointed out by the following symbols: AC= Arosa Canyon; AV= Aveiro Canyon; CB= Conil-Barbate; CF= Cape of Finisterre; CS= Cape of Sagres; CO= Cape of Ortegal; EC= Estremadura promontory; GB= Galician Bank; GS= Gettysburg seamount; MC= Murgia Canyon; NC= Nazaré Canyon; OP= Ortegal promontory; OS= Ormonde seamount; PC= Porto Canyon; TP= Tagus Plateau; VC= S. Vicente Canyon (from Quaresma and Pichon 2013).

Figura 8. Esquema donde se muestra: A) Mapa de la velocidad de la corriente barotrópica M2. Las velocidades máximas de M2 ($cm\ s^{-1}$) se ilustran por la elipse de mareas del eje de magnitud semi-mayor; B) Mapa que indica la velocidad de la fase de la corriente de marea barotrópica K1. Este valor corresponde al retardo de la fase de la corriente máxima detrás del máximo potencial de marea de M2 (grados referenciados en GMT) y C) Mapa del periodo semi-diurno forzoso barotrópico (s^{-1}). Generación de “hotspots” o puntos calientes de mareas internas (baroclínicas). Ac = Cañón de Arosa; AV = Cañón de Aveiro; CB = Conil-Barbate; CF = Cabo de Finisterre; CS = Cabo de Sagres; CO = Cabo de Ortegal; EC = Promontorio de Extremadura; GB = Banco de Galicia; GS = Montaña submarina Gettysburg; MC = Cañón de Murgia; NC = Cañón de Nazaré; OP = Promontorio de Ortegal; OS = Montaña submarina Ormonde; PC = Cañón de Porto; TP = Meseta del Tajo; Vc = Cañón de S. Vicente (de Quaresma y Pichon 2013).

Ortegal Spurs as well as the Gettysburg and Ormonde seamounts. The Cadiz Contourite Channel, in the central sector of the Gulf of Cadiz, offers one of the best examples of sandy bedforms caused directly by the dynamic interaction of tidal currents and seafloor (Stow *et al.*, 2013a, Fig. 9). The narrowness of this channel (2-12 km) amplifies bottom tidal currents due to a funnelling effect. Current meter data from this area show a strongly directional, westerly MOW moving at speeds of 1 m/s at the instrument height of 78 m with a clear periodicity in its velocity, suggestive of a semi-diurnal tidal signal and of a spring/neap cycle (Fig. 10A).

Deep-sea storms

Benthic storms (also known as deep-sea storms or abyssal storms) refer to intermittent, strong, bottom-intensified currents affecting the seafloor (Fig. 2). The HEBBLE (High Energy Benthic Boundary Layer Experiment; Hollister *et al.*, 1980) first documented the existence of benthic storms while investigating the response of the cohesive seafloor to high-stress events. During these storms, bottom-current velocity can increase by a factor of 2-5 times (average 15-20 cm/s with peaks of over 43 cm/s) over a period of a few days (2 to 25 days) to several weeks. Benthic

storms occur at a frequency of about 8 to 10 events per year (Holger, 1987). Benthic storm-related flows can rework up to several millimetres of seafloor sediment per event. Entrainment of the bottom nepheloid layer or bottom boundary layer by turbulent and diffusive mixing favours rapid resuspension of particulate matter (Gardner and Sullivan, 1981; Hollister and McCave, 1984; Nowell and Hollister, 1985; Gross and Williams, 1991). During the occurrence of these storms, the benthic boundary layer (BBL) increases in thickness from a few metres up to 70 m, and in turbidity up to values of 5 g/l (Tucholke, 2002). Other mechanisms for benthic storms hypothesize sediment plumes descending from continental slopes and rapid input of organic-rich phytodetritus from plankton blooms in surface waters (Richardson *et al.*, 1993; Puig *et al.*, 2013). In this latter case, the organic-rich detritus draping the seafloor is easier to flocculate and maintain in suspension. Detailed studies of suspended particulate matter throughout the BBL indicate that sediment concentration depends on the interplay of several factors, including initial concentration in suspension, turbulence, height of entrainment, velocity field, transport distance and settling velocity of the particles. Gross and Williams (1991) emphasized three physical processes which characterize deep-sea storm events. These include turbulence in the boundary layer, sediment at the sediment-water interface and suspended sediment winnowed by the flow. Any one of these three lines of evidence defines a storm event (Gross and Williams, 1991).

Benthic storms play an important role in the erosion, transport and redistribution of bottom sediments (Hollister *et al.*, 1980; Nowell and Hollister, 1985; Hollister, 1993). Once disturbed by the erosional effects of increased bottom shear, sediments may be transported by bottom currents and deposited in quiet regions downstream (Gardner and Sullivan, 1981; Kennett, 1982; Hollister and McCave, 1984; Flood and Shor, 1988; Bearmon, 1989; Von Lom-Keil *et al.*, 2002). These currents may travel over long distances, constrained by the Coriolis force and semi-diurnal tides parameters. Seafloor morphology from large, kilometre-scale features (e.g., seamounts) to smaller, metre-scale features (e.g., sediment waves) can affect this transport (Rebesco and Camerlenghi, 2008).

The occurrence of benthic storms relates in part to the formation of large eddies within the water column due to the interaction between major wind-driven surface currents and the bottom component of THC. Areas of the ocean with a highly variable sea surface show more frequent benthic storm activity

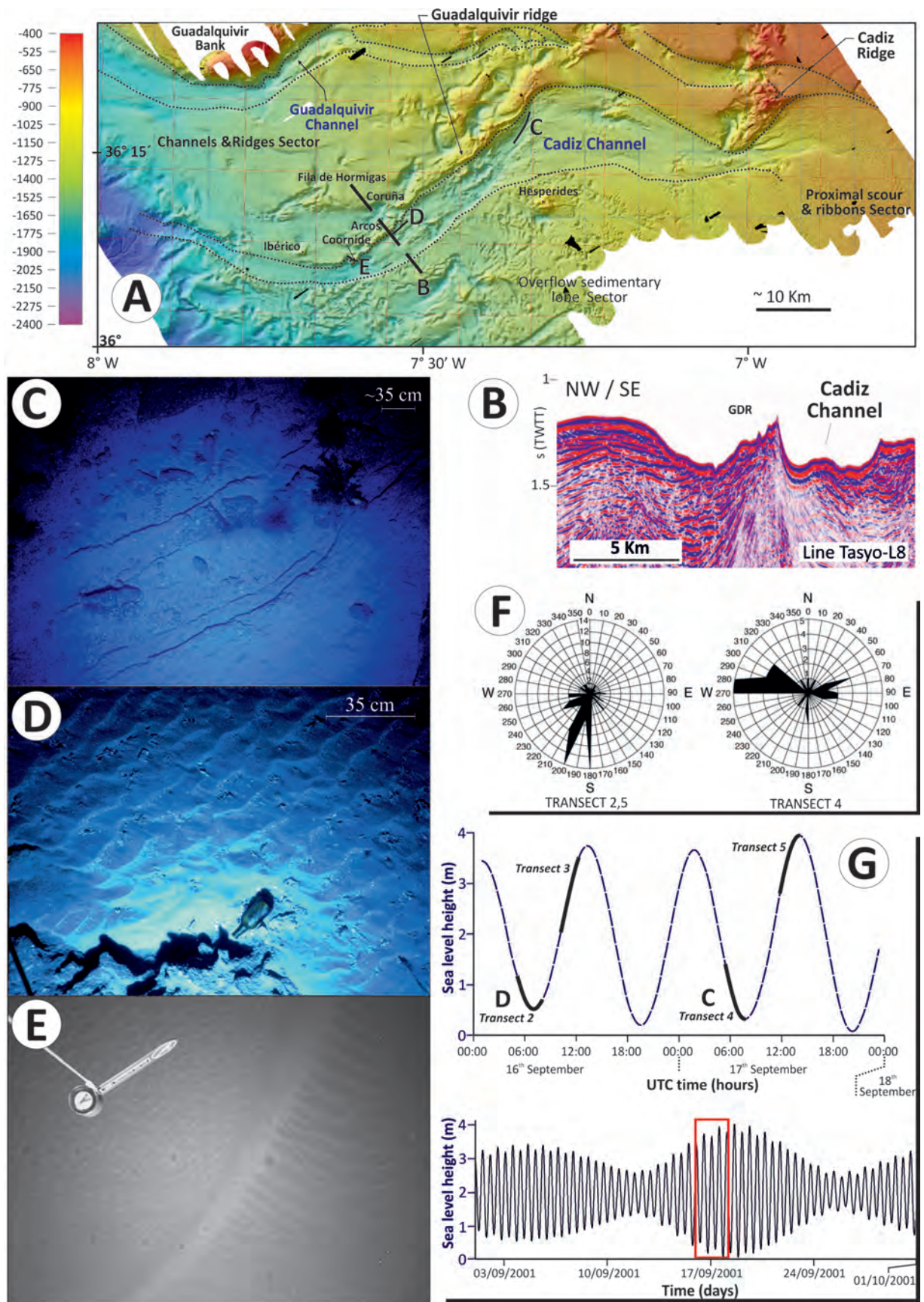
(Richardson *et al.*, 1993; Faugères and Mulder, 2011). The kinetic energy of these eddies can extend to depths of > 3000 m and thus change the direction of bottom currents. Benthic storms also occur in the presence of strong, permanent bottom currents, and in areas where seafloor sediments are easily flocculated into suspension (Richardson *et al.*, 1993). Due to the limited information concerning benthic storms, however, uncertainties persist in regards to their initiation and driving mechanism.

As major sediment entrainment processes, benthic storms play an important role in contourite development. Benthic storms also disturb benthic communities (Gross and Williams, 1991). Regions subjected to intense deep-sea storms show significant erosion of the continental slope and evidence of large submarine slides (Pickering *et al.*, 1989; Gao *et al.*, 1998; Einsele, 2000).

Only a few examples of deep-sea storms have been documented around Iberia linked to the formation of surface dense waters in the Gulf of Lions and the subsequent deep cascading and open-sea convection process (Font *et al.*, 2007; Palanques *et al.*, 2009; Durrieu de Madron *et al.*, 2013). Some of these events, such as the one observed in the winter of 2009 (Fig. 11), may be exclusively due to deep convection without the accompanying cascading process (Salat *et al.*, 2010; Puig *et al.*, 2012; Stabholz *et al.*, 2013). In the Cantabrian margin, three independent events have been identified at La Gavierra Canyon (Sanchez *et al.*, 2014). The scarcity of information on this type of phenomena may mask their frequency. For example, a current meter moored at around 554 m water depth in the Gulf of Cádiz may have recorded possible benthic storms (Fig. 10B), but further analysis of these time series-observations is required to confirm such an interpretation.

Eddies

Instabilities in bottom currents often generate vortices (Serra *et al.*, 2010a) and contribute to long-distance sediment transport and the formation of nepheloid layers (Fig. 2). Eddies occur when a water mass interleaves into a stratified environment, or when current flows meet a seafloor irregularity such as a canyon, seamount or cape (Roden, 1987; Rogers, 1994; Arhan *et al.*, 2002; Serra *et al.*, 2010a). Along some regions of the seafloor, eddy activity spans hundreds of kilometres, as for example, in the Argentine Basin (Cheney *et al.* 1983; Flood and Shor, 1988; Arhan *et al.*, 2002; Hernández-Molina *et al.*, 2009), the Weddell and Scotia Seas (Hernández-Molina *et al.*,



2008a), the Mozambique slope (Preu *et al.*, 2011), the Gulf of Cadiz and the margins off western Portugal (Serra *et al.*, 2010a).

The best-studied example of eddies around Iberia relate to the MOW (sometimes referred to as meddies). Meddies are low-potential vorticity bodies that rotate clockwise and maintain MOW-type temperature and salinity conditions in their cores for long periods of time (the order of years). These coherent vortices translate at average speeds of 2-4 cm/s and have typical azimuthal velocities of 30 cm/s (Fig.12B). The radial structure of their core velocity resembles solid body rotation (Schultz-Tokos and Rossby, 1991). Meddies have been observed in the Canary Basin (e.g., Armi and Zenk, 1984; Richardson *et al.*, 1989; Pingree and Le Cann, 1993), in the Iberian Basin (Kase *et al.*, 1989; Zenk and Armi, 1990; Schultz-Tokos *et al.*, 1994), off the southern coast of Portugal (Prater and Sanford, 1994; Bower *et al.*, 1997; Serra and Ambar, 2002), off western Portugal (Pinheiro *et al.*, 2010, Figure 7), and along the north-western Iberian coast (Paillet *et al.*, 2002). Bower *et al.* (1997) identified the Cape St.Vincent Spur and the Extremadura Promontory as points of origin for meddies. The region adjacent to Cape Finisterre (Paillet *et al.*, 2002), the region of the Portimao Canyon (Serra and Ambar, 2002) and the Gorringe Bank (Serra and Ambar, 2002) are also recognized sites of meddy formation.

The proposed mechanisms for generating these meddies include boundary layer separation of the

MOW undercurrent (Bower *et al.*, 1997), baroclinic and/or barotropic instability of the MOW undercurrent (Kase *et al.*, 1989; Cherubin *et al.*, 2000), flow intermittency (Nof, 1991) and topographic effects due to capes (Pichevin and Nof, 1996; Sadoux *et al.*, 2000; Serra *et al.*, 2005) or canyons (Cherubin *et al.*, 2000; Serra *et al.*, 2005). Three factors contribute to the meddy displacements. These include advection by mean flow (Hogg and Stommel, 1990; Dewar and Meng, 1995), the beta-effect or meridional variation of the planetary vorticity (Nof, 1982b) and interactions between different eddies (Kase and Zenk, 1996; Serra *et al.*, 2002). This latter mechanism can involve the coupling of cyclones and meddies (Richardson *et al.*, 2000; Carton *et al.*, 2002; Serra *et al.*, 2002). Near their generation sites, meddies may re-suspend sediment and carry it into the open ocean.

Secondary circulation

Dense water masses usually have main current cores that run parallel to isobaths (Figs. 2 and 12A). The velocity of these cores manifests in contourite erosional features such as moats and channels (e.g., McCave and Tucholke, 1986; Faugères *et al.*, 1993, 1999; Rebesco and Stow, 2001; Stow *et al.*, 2002a, 2009; Rebesco and Camerlenghi, 2008; Faugères and Mulder, 2011). They are often associated with deposition in downslope areas, and erosion in upslope areas. The structure of these features may result from

Figure 9. Examples from sandy deposits within the Cadiz Contourite Channel affected by bottom current and barotropic and internal tides (probably generated at the continental slope), which reinforce the normal MOW flow (from Stow *et al.*, 2013a). A) Cadiz Contourite Channel image derived from swath bathymetric data, showing the location of bottom photograph transects (black) taken with a BENTHOS-372 camera; B) airgun deep monochannel seismic profile across the Cadiz Contourite Channel (location in A); C, D and E) bottom photographs along the Cadiz Contourite Channel: deep linear scours (or small furrows) on the sea bottom with very rare starved ripples of coarse sediments (C); straight to rhomboidal asymmetrical starved ripples; linear to sinuous asymmetrical ripples (D); sinuous to crescent sand waves, observed in a secondary channel (E). Stoss side with small regular asymmetrical ripples, lee side with linear erosional chutes, and a sand wave trough region with a more irregular ripple pattern. Both ripple and dune orientation indicates a flow towards the west, whereas the current vane shows a more southward flow direction at the time of the photo. Compass diameter 7cm; current vane 25 cm; F) Bottom current directions as inferred from bedform measurement for transects 2 and 5 (left) and bottom current directions during the running of transect 4 as inferred from current vane orientation (right); G) tidal data for 16th and 17th September 2001 (Port of Cadiz), together with an indication of the duration of each photographic transect (up), and tidal amplitude through the month of September 2001 (down).

Figura 9. Ejemplos de depósitos de arena dentro del Canal Contornítico de Cádiz afectados por las corrientes de fondo y las mareas barotrópicas e internas (probablemente generadas en el talud continental), las cuales refuerzan el flujo normal de la MOW (de Stow *et al.*, 2013a). A) Imagen del Canal Contornítico de Cádiz obtenida de los datos batimétricos de multihaz, mostrándose la ubicación de los transectos de las fotografías tomadas del fondo (negro) con una cámara BENTHOS-372; B) Perfil sísmico monocanal tomado con Cañones de Aire que cruza el Canal Contornítico de Cádiz (ubicación en A); C, D y E) Fotografías de fondo a lo largo del Canal Contornítico de Cádiz: surcos lineales profundos (o pequeños furrows) en el fondo del mar con algunos ripples de sedimentos gruesos (C); ripples asimétricos que pasan de rectos a romboidales; ondas asimétricas que pasan de lineales a sinuosas (D); ripples que pasan de sinuosas a media luna, en un canal secundario (E). A barlovento de ondas de arenas se observan pequeños ripples regulares asimétricas, y a sotavento, rasgos erosivos lineales. En el seno de las ondas de arena los ripples presentan un patrón más irregular. Tanto la orientación de los ripples como de las dunas indican que el flujo circula hacia el oeste, mientras que la veleta de corriente muestra la dirección del flujo más al sur en el momento de la foto. El diámetro de la brújula es de 7cm; la veleta de corriente tiene 25cm; F) Direcciones de la corriente de fondo inferidas por medición de formas de fondo en los transectos 2 y 5 (izquierda) y las direcciones de las corrientes de fondo durante la ejecución del transecto 4 (derecha); G) Datos de marea para el 16 y 17 de Septiembre de 2001 (Puerto de Cádiz), junto con una indicación de la duración de cada transecto fotográfico (arriba), y la amplitud de las mareas del mes de septiembre de 2001 (abajo).

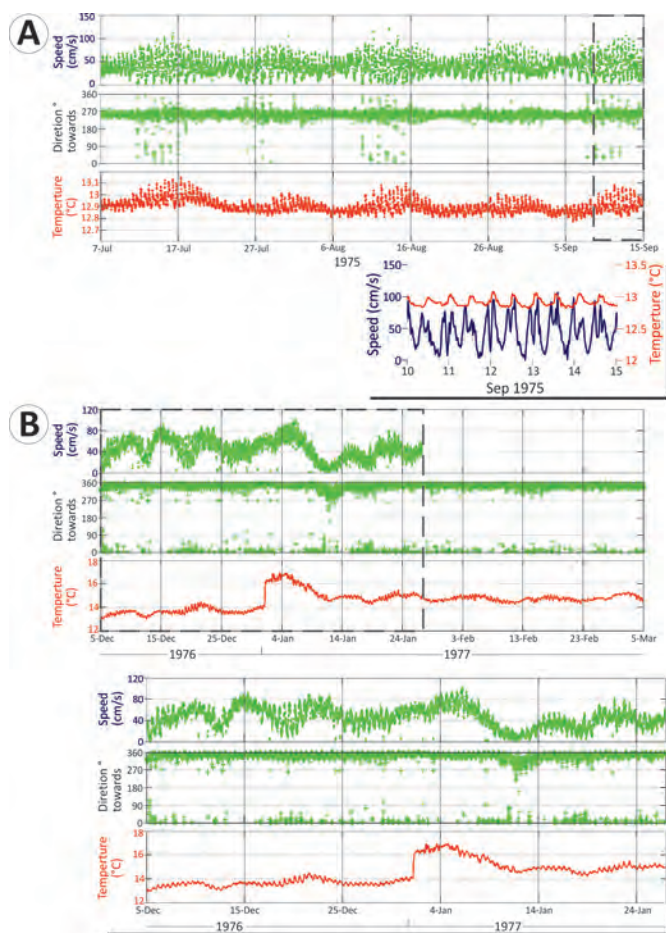


Figure 10. Time series observations of the near-bottom current (78 m above the seafloor) at the exit of the Strait of Gibraltar (A) for 79 days at 472 m water depth and at the eastern Gulf of Cadiz (B) for 97 days at 554 m water depth (see location in Fig.4), showing a strongly directional MOW towards the WSW (A) and NNW (B) with speeds up to 1 m/s. A detail in (A) illustrates the relation between the current speeds and temperature from 10-14 September 1975. Inset in B depicts a semi-diurnal tidal periodicity where a spring-neap tidal cycle is clearly observed, which also modulates the near-bottom temperature. The jump in the temperature record in B is presumably due to the mooring turn-around operation and the sampling of a slightly different water parcel after its redeployment. Published with permission from British Oceanographic Data Center (BODC) and National Oceanographic Centre, Southampton (NOCS).

Figura 10. Observaciones de series temporales para la corriente cerca del fondo (78 metros por encima del fondo marino) a la salida del Estrecho de Gibraltar durante 79 días a 472 m de profundidad (A) y durante 97 días a 554 m de profundidad donde se muestra una MOW hacia el OSO (A) y NNO (B) con una velocidad de hasta 1 m/s (ver ubicación en la Fig. 4). Se ilustra en A un detalle de la relación entre las velocidades y temperatura de la corriente desde el 10 al 14 de septiembre del 1975. El recuadro en B representa una clara periodicidad semi-diurna de marea con un ciclo de marea que también modula la temperatura cerca del fondo. El salto en la temperatura registrada en B es presumiblemente debido a la operación de mantenimiento del anclaje y del muestreo de una parcela de agua ligeramente diferente después de ser redondeado. Publicado con permiso del British Oceanographic Data Center (BODC) y el National Oceanographic Centre, de Southampton (NOCS).

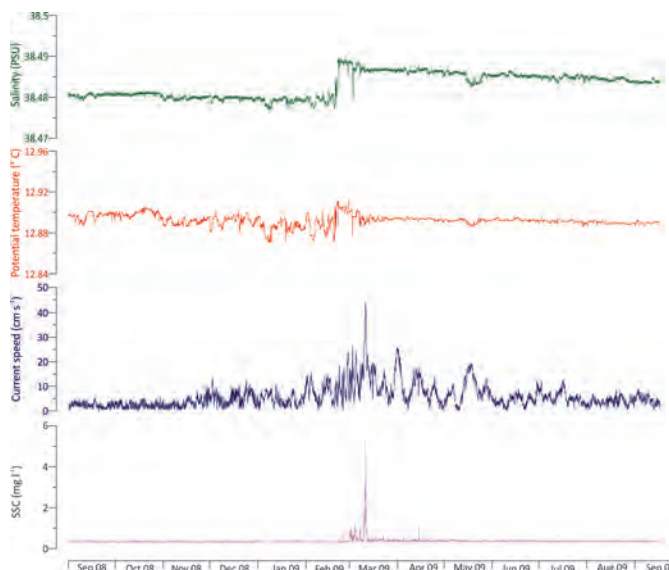


Figure 11. Time series observations of near-bottom salinity, potential temperature, current speed and suspended sediment concentration (SSC) recorded at the Catalan continental rise (1890 m in depth), illustrating an example of a benthic storm occurring in the northwestern Mediterranean basin after the winter 2009 deep, dense water-formation event. Note the sharp increase of salinity and temperature associated to the arrival of the dense waters to the basin and the subsequent increase of near-bottom velocities with a peak >40 cm/s that caused resuspension of bottom sediments (modified from Puig *et al.*, 2012).

Figura 11. Series temporales de salinidad, temperatura potencial, velocidad de la corriente y concentración de sedimento en suspensión (SSC) medidas cerca del fondo en el ascenso continental Catalán a 1890 m de profundidad, donde se ilustra un ejemplo de una tormenta bentónica generada por la convección profunda de aguas densas de superficie durante el invierno de 2009. Se puede observar el aumento brusco de la salinidad y temperatura asociado a la llegada de aguas densas al fondo de la cuenca y el incremento posterior de la velocidad de la corriente con un aumento de más de 40 cm/s que provocó la resuspensión de sedimento (modificado de Puig *et al.*, 2012).

helicoidal flow paths, or a clockwise secondary circulation of the bottom current around the core of the current. These structures are referred to as 'horizontal eddies' in geophysical literature (Davies and Laughton, 1972; Roberts *et al.*, 1974; Roden, 1987; Rogers, 1994; McCave and Carter, 1997; Hernández-Molina *et al.*, 2008a, b; Zenk, 2008). Although seafloor features along the Iberian margin suggest helicoidal flow, this interpretation requires further analysis of currents and seafloor morphology (Rebesco *et al.*, 2014). These features probably result from the Coriolis effect directing the vortex against the adjacent slope, eroding the right side of the channel and depositing sediment on the left side where the current velocity is lower (Faugères *et al.*, 1999; Llave *et al.*, 2007). The combined effect of bottom friction and

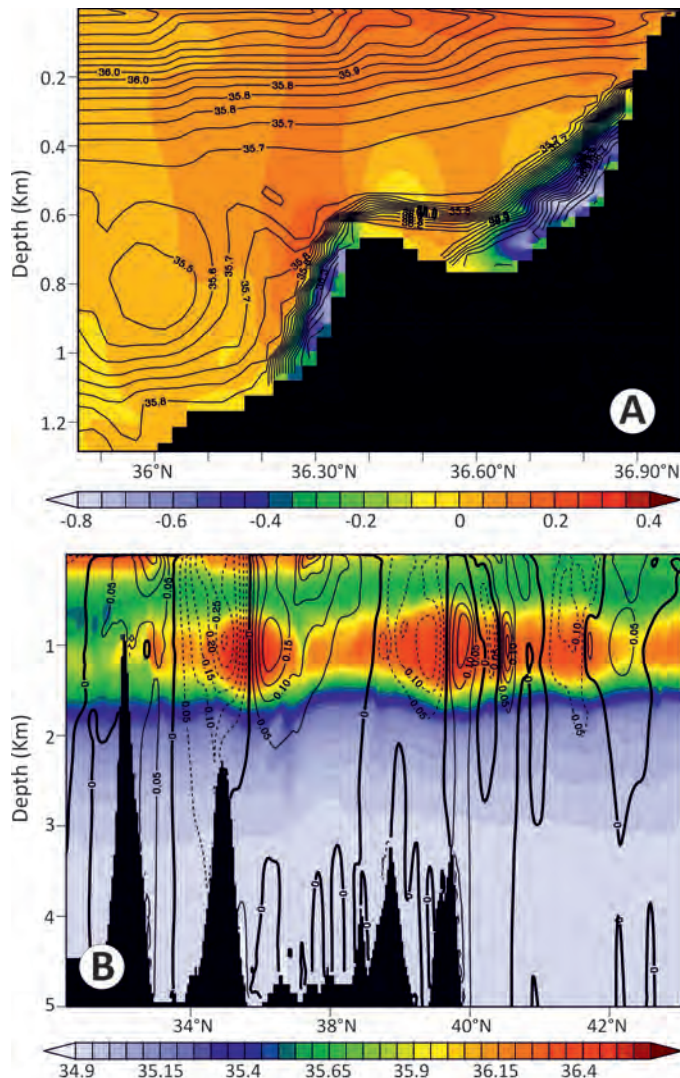


Figure 12. A) A snapshot of simulated zonal component of velocity and salinity at 7.5°W showing the MOW undercurrents flowing westwards in the Gulf of Cadiz; B) snapshot of simulated salinity and zonal component of velocity at 13°W, showing the large vertical extension of the velocity signal associated with the MOW eddies (meddies) downstream of the Portimao Canyon (from Serra *et al.*, 2010a).

Figura 12. A) Gráfico del componente zonal simulado de la velocidad y la salinidad a 7.5°W mostrando las corrientes subterráneas de la MOW que fluyen hacia el oeste en el Golfo de Cádiz; B) Gráfico de la salinidad simulada y el componente zonal de la velocidad a 13°W, que muestra la gran extensión vertical de la señal de velocidad asociada con los remolinos de la MOW aguas abajo del Cañón de Portimao (de Serra *et al.*, 2010a).

the Coriolis effect in the Ekman layer usually results in a clockwise secondary circulation in bottom currents as illustrated in Figure 3 (Wåhlin and Walin, 2001; Wåhlin, 2004; Muench *et al.*, 2009; Cossu *et al.*, 2010; Cossu and Wells, 2013).

This type of secondary circulation may occur in the eastern Gulf of Cádiz, near the exit of the Strait of Gibraltar (Fig. 4, Serra, 2004; Garcia *et al.*, 2009; Hernández-Molina *et al.*, 2014). The identification of secondary circulation further suggests its role in generating furrows observed to run obliquely relative to the main bodies of the prevailing bottom currents (Hernández-Molina *et al.*, 2014).

Dense shelf water cascades

Dense shelf-water cascades (DSWC; Fig. 2) describe the flow of dense water generated in shelf areas down the continental slope (Simpson, 1982; Killworth, 1983; Ivanov *et al.*, 2004). DSWCs are near-bottom gravity flows that develop when cooling, evaporation, freezing and/or salinization in the surface layer formed over the continental shelf causes density-driven flow over the shelf edge. The dense water plume cascades both along and across the slope area according to density, gravity effects, the Coriolis Effect, friction and mixing. Once the density of the water plume matches the density of the surrounding waters the DSWC reaches gravitational equilibrium and becomes an intermediate-depth, neutrally buoyant intrusion (Shapiro and Hill, 1997; Shapiro *et al.*, 2003). Submarine canyons incised into the shelf edge can offer preferential pathways for DSWCs (Canals *et al.*, 2006, 2009; Allen and Durrieu de Madron, 2009). This intermittent process affects biogeochemical cycles by re-suspending sediment and transporting significant volumes of minerals and organic matter (Fohrmann *et al.*, 1998; Hill *et al.*, 1998; Puig *et al.*, 2013).

The Gulf of Lions, located in the northeastern sector of the Iberian Peninsula experiences annual DSWCs (Millot *et al.*, 1990; Durrieu de Madron *et al.*, 2005; Puig *et al.*, 2013). Winter cooling and evaporation, induced by persistent, cold, dry northerly winds (the Tramontane and Mistral winds) cause increased density and mixing of coastal waters. This occurs in spite of buoyancy effects from freshwater input of the Rhone River. The prevailing westerly coastal circulation, the narrowing shelf and the topographic constraint of the Cap de Creus peninsula, all facilitate DSWCs and sediment transport. These currents develop in the Gulf's southwestern sector, primarily moving through the Lacaze-Duthiers and Cap de Creus submarine canyons, where cascading flows can reach velocities >80 cm/s (Palanques *et al.*, 2006). DSWC events occur from January to April/May lasting several days, and often begin and/or are enhanced during storms, which cause increases in

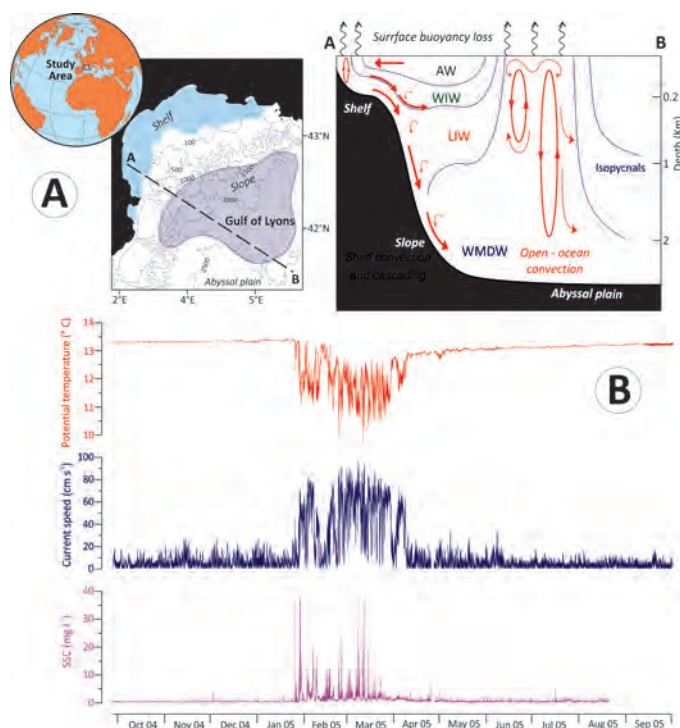


Figure 13. A) Map of the Gulf of Lions area showing the regions of dense water formation and distribution (adapted from Puig *et al.*, 2013). B) A dense shelf water cascading (DSWC) event in the Gulf of Lions' shelf illustrated by a time series of near-bottom potential temperature, current speed and suspended sediment concentration (SSC) recorded at 500 m depth (5 m above bottom) in the axis of the Cap de Creus Canyon during the winter of 2004-05. Adapted from Puig *et al.* (2008). Legend for water masses by alphabetic order: AW= Atlantic Water; LIW= Levantine Intermediate Water; WIW= Western Mediterranean Intermediate Water; WMDW= Western Mediterranean Deep Water.

Figura 13. A) Mapa de la zona del Golfo de León donde se muestran las regiones de formación de agua densa y su distribución (adaptado de Puig *et al.*, 2013); B) Cascadas de agua densa de plataforma (Dense shelf water cascading-DSWC) que se producen en la plataforma del Golfo de León, ilustradas por una serie temporal de la temperatura potencial cerca de fondo, velocidad de la corriente y la concentración de sedimentos en suspensión (SSC) registrados a 500 m de profundidad (5 m por encima del fondo) en el eje del Cañón del Cap de Creus durante el invierno 2004-05. Adaptado de Puig *et al.* (2008). Leyenda de las masas de agua, por orden alfabético y con el nombre original en inglés: AW= Atlantic Water; LIW= Levantine Intermediate Water; WIW= Western Mediterranean Intermediate Water; WMDW= Western Mediterranean Deep Water.

the suspended sediment concentration and generally amplify down-canyon sediment fluxes (Palanques *et al.*, 2008). In very dry, windy and cold periods, such as the 1998-99, 2004-05 and 2005-06 winters, the Gulf developed unusually intensive DSWCs that lasted for several weeks (Fig.13). During these major events, large quantities of water and suspended particles are rapidly advected over depths of hundreds of metres

along submarine canyons, causing erosion of the seafloor and generating sedimentary furrows (Palanques *et al.*, 2006, 2009, 2012; Canals *et al.*, 2006; Puig *et al.*, 2008). The most persistent and penetrative cascading pulses generally follow a multi-step sediment transport mechanism. Sediment is initially transported from the shelf to the upper canyon region. The subsequent cascading pulses re-suspend and redistribute the sediment down-slope, generating massive sand beds at the canyon head region (Gaudin *et al.*, 2006). At depths of 1 500 m, where the Cap de Creus submarine canyon widens, most of the dense water and suspended sediment leaves the canyon and flows along the northern Catalan continental margin as a contour current (Palanques *et al.*, 2012). Continuous monitoring of cascading events in the Cap de Creus canyon has recognized a large degree of inter-annual variability in DSWCs, as well as their complex interactions with concurrent storms and down-welling transport (Ribó *et al.*, 2011; Martín *et al.*, 2013; Rumín-Caparrós *et al.*, 2013).

Internal waves and solitons

Internal waves typically have much lower frequencies (periods from several tens of minutes to days) and higher amplitudes (up to hundreds of metres) than surface waves (Fig. 2). Internal waves can also propagate vertically through the water column transferring energy in either direction between shallower and deeper levels (Shanmugan, 2012b, 2013a, 2014, Fig.14). These phenomena occur throughout the oceans, as evident in temperature, salinity and current measurements (Kantha and Clayson, 2000). They appear as surface roughness produced by interference between the current velocity and the upper layer background dynamics (Bruno *et al.*, 2006).

Internal waves occur in stable, stratified fluids due to the restoring action of the buoyancy forces on water parcels displaced from their equilibrium position (Fig.14). Interfacial waves on the density interfaces offer a good example of internal waves (Gill, 1982). When the density interface is disturbed, waves radiate horizontally along the interface if the vertical density gradient is high enough (Shanmugan, 2012a, 2013a, b). In continuously stratified waters internal waves travel along paths (wave characteristics) that run obliquely to the horizontal plane. The exact angle is a function of the frequency of the internal wave, the buoyancy or Brunt Väisälä frequency N and the Coriolis parameter f (Gill, 1982). Perturbation of a region with high N values, such as steepened segments of the pycnocline, tend to travel rather hori-

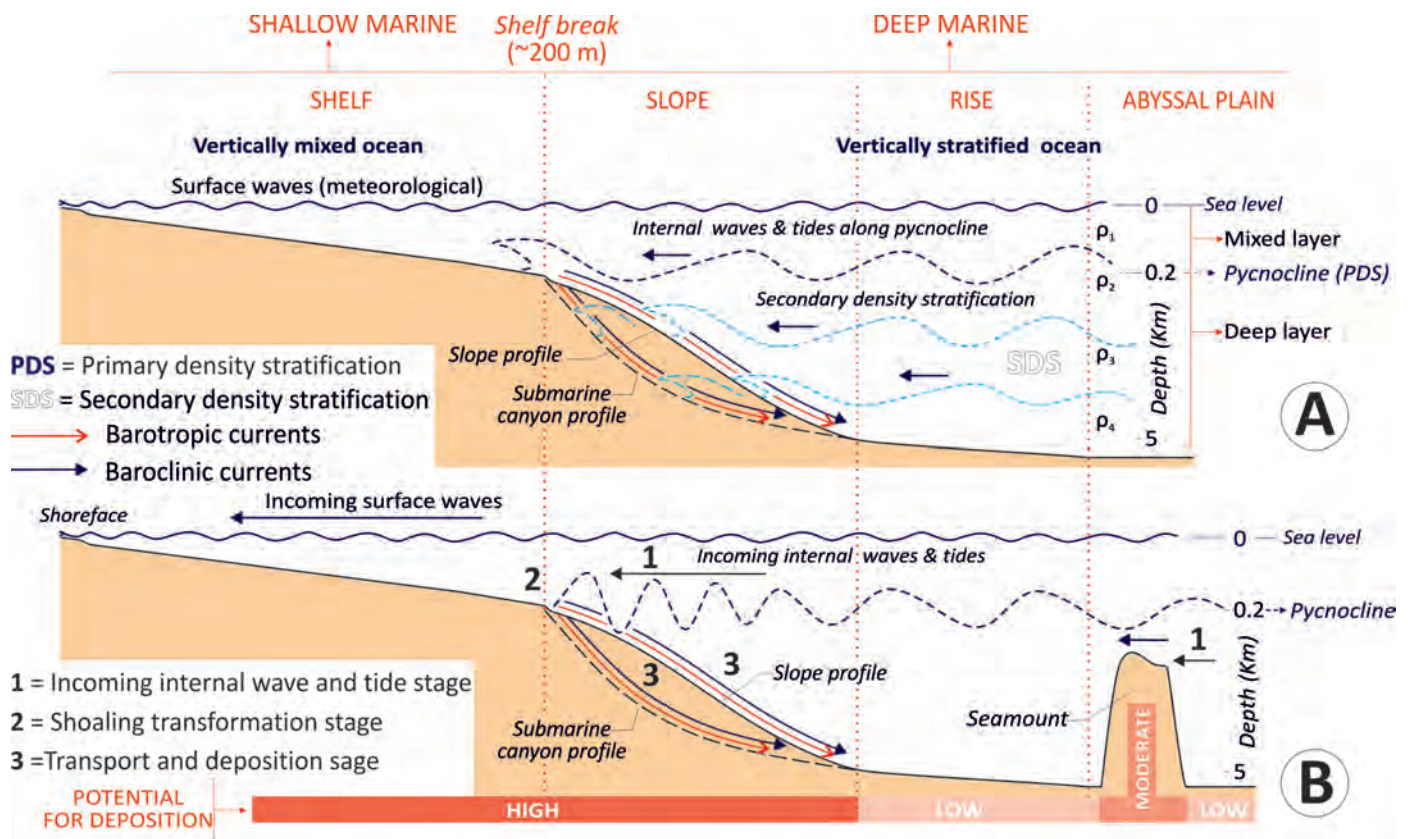


Figure 14. A) Schematic diagram showing the position of the pycnocline (i.e., primary density stratification), where the density gradient is the sharpest, between mixed (upper) and deep (lower) ocean layers of different densities (adapted from Shanmugan, 2013b). Internal waves and tides propagate along the boundaries of both primary and secondary density stratifications. Internal waves and astronomical internal tides propagate along the boundaries of density stratification in deep-marine environments. Barotropic currents (red arrow) are generated by surface waves and tides, whereas baroclinic currents (dark blue arrow) are generated by internal waves and tides; **B)** conceptual oceanographic and sedimentologic framework showing deposition from baroclinic currents on continental slopes, in submarine canyons, and on guyots. On continental slopes and in submarine canyons, deposition occurs in three progressive stages: (1) incoming internal wave and tide stage, (2) shoaling transformation stage, and (3) sediment transport and deposition stage. Continental slopes and submarine canyons are considered to be environments with high potential for deposition from baroclinic currents. In the open ocean, baroclinic currents can rework sediments on flat tops of towering guyot terraces, without the need for the three stages required for the deposition on continental slopes (From Shanmugan, 2012, 2013b).

Figura 14. A) Diagrama esquemático que muestra la posición de la picnoclina (es decir, la estratificación primaria por densidad), donde el gradiente de densidad es más abrupto, entre capas oceánicas de mezcla (superiores) y profundas (capas inferiores) con diferentes densidades (adaptado de Shanmugan, 2013b). Las ondas internas y las mareas internas astronómicas se propagan a lo largo de las interfaces de densidad en los ambientes marinos profundos. Las corrientes barotrópicas (flecha roja) se generan por las ondas superficiales y las mareas, mientras que las corrientes baroclínicas (flecha azul oscuro) se desarrollan por las ondas internas y mareas internas; **B)** Marco conceptual oceanográfico y sedimentológico que muestra el depósito por corrientes baroclínicas sobre taludes continentales, en los cañones submarinos, y en montes submarinos o guyots. En los taludes continentales y en los cañones submarinos el depósito se genera en tres etapas progresivas: (1) etapa entrante de la onda interna y marea interna, (2) etapa de transformación y somerización al chocar con el fondo, y (3) etapa de transporte y depósito de sedimentos. Los taludes continentales y cañones submarinos se consideran como ambientes con alto potencial para el depósito a partir de corrientes baroclínicas. En el océano abierto, las corrientes baroclínicas pueden re trabajar los sedimentos en las cimas planas de imponentes terrazas guyot, sin la necesidad de que se den las tres fases requeridas para el depósito en zonas de talud continental (de Shanmugan, 2012, 2013b).

zonally along the pycnocline (Shanmugan, 2012a, 2013a,b), whereas if the vertical density gradient is more uniform the internal perturbation may radiate at an angle relative to the vertical (Baines, 1982). The frequencies of the free internal waves are confined to

frequencies between f and N . In the upper ocean at middle and high latitudes, N typically exceeds f by one or two orders of magnitude. At low frequencies approaching f , the Earth's rotational effects are critical and the waves are referred to as near-inertial internal

waves (Garrett, 2001; Puig *et al.*, 2001; van Haren *et al.*, 2013). At higher frequencies approaching N , rotational effects become negligible. In the deep oceans at middle and high latitudes, f and N are comparable. The weak stratification at the abyssal regions prevents the formation of high-frequency internal waves. (e.g., only low frequencies close to remain). In latitudes approaching the equator, f approaches zero. The diminished rotational component affects the internal wave structure and dynamics primarily at very low frequencies.

As mentioned above internal waves occur due to the disruption of horizontal density surfaces within a stratified water column. The most usual perturbing mechanism is the interaction between currents and the bottom topography (Fig. 14) in regions where it changes more or less abruptly, as ridges, banks, slopes, shelf breaks, etc., (Farmer and Armi, 1999; Shanmugan, 2013a, b). Barotropic tidal currents are often behind this type of forcing. Other forces that generate vertical perturbations also produce internal waves by the same mechanism. These types of forces may derive from the wind stress on the sea surface or from currents induced by other types of barotropic waves, such as continental shelf waves or edge waves (Bruno *et al.*, 2006).

The topographic perturbations often start with a single wave or soliton, which disintegrates in rank, ordered internal wave trains (Vlasenko *et al.*, 2009) of lesser wavelengths and shorter periods, relative to the original internal wave that approached the pycnocline (Apel *et al.*, 1995). These secondary perturbations exhibit relatively high amplitudes and have induced currents that reach intensities of 200 cm/s.

Internal waves have been described in coastal areas of California (Emery, 1956), in the Sea of Japan (Navrotsky *et al.*, 2004), the Indian Ocean (Santek and Winguth, 2005), the Bay of Biscay (Baines, 1982) and on other areas along the Iberian Margin (Puig *et al.*, 2004; Hernández-Molina *et al.*, 2011, 2014; Van Haren *et al.*, 2013).

The energy associated with internal waves is particularly important close to the continental margins (maximum horizontal velocities up to 200 cm/s and vertical velocities of 20 cm/s, Shanmugan, 2012a, 2012b, 2013a). Internal waves may act as the primary mechanism in along-slope and across-slope processes, maintenance of intermediate and bottom nepheloid layers (McCave, 1986; Dickson and McCave, 1986; Cacchione *et al.*, 2002; Puig *et al.*, 2004) and in the erosion of contourite terraces (Hernández-Molina *et al.*, 2009; Preu *et al.*, 2013).

High amplitude internal wave generation in the Strait of Gibraltar strongly affects the Iberian margin.

These processes primarily occur around the Camarinal Sill and other minor sills nearby where the tide-topography interaction generates internal bores that evolves into the well-shaped wave trains mentioned above (Armi and Farmer, 1988; Farmer and Armi, 1988; Vlasenko *et al.*, 2009; Sanchez-Garrido *et al.*, 2011, see also Figure 15), with amplitudes of 50 to 100 m and wavelengths of 1 to 4 km (Armi and Farmer, 1988; Farmer and Armi, 1988; Brandt *et al.*, 1996; Jackson, 2004). The wave trains extend at least 200 km into the western Mediterranean and persist for more than 2 days before dissipating (Apel, 2000; Jackson, 2004) (Fig. 15). Solitons and internal waves have been observed in many other areas along the Iberian margin (Fig. 15), including the Gulf of Cadiz, the west coast of Portugal and the Galician and Cantabrian margins (Pingree *et al.*, 1986; Pingree and Newt, 1989, 1991; Correia, 2003; Apel, 2004; Jackson, 2004; Azevedo *et al.*, 2006; Pichon *et al.*, 2013); at the NW flank of Le Danois at the Cantabrian margin (Gonzalez-Pola *et al.* 2012); and the Gulf of Valencia continental slope (van Haren *et al.*, 2013). Solitons also frequently occur along the shelf break of the Iberian margin (Apel, 2004). Although current knowledge about internal waves and solitons is limited, many features along the Iberian slope maybe related to their effect as sedimentary waves on the Galician continental margin (Fig.16, Hanebuth *et al.*, 2012). Internal waves amplify their influence within submarine canyons (e.g., Shanmugam, 2012a, 2013a,b; Puig *et al.*, 2014), contributing to higher velocity bottom currents within the canyon (Quaresma *et al.*, 2007; Sánchez *et al.*, 2014) and reworking sandy deposits, as in the Gaviera Canyon of the Cantabrian margin (Fig. 17, Gómez-Ballesteros *et al.*, 2014). Sedimentary waves are very common at certain depths within submarine canyons, and some of them are reworked sedimentary waves such as those described in the Setubal, Nazaré and Cascais Canyons (Arzola *et al.*, 2008; Lastras *et al.*, 2009, Fig. 18) and interpreted as being due to the action of turbiditic processes. To what extent these sedimentary waves might be related to the action of internal waves on submarine canyons is unknown. The fact is the role of internal waves on submarine canyons, gullies, etc., has been overlooked and should be considered in future multi-disciplinary works.

Tsunami-related traction current

Tsunamis consist of a wave or series of waves with long wavelengths and long periods (Fig. 2), caused by an abrupt vertical displacement of the ocean bottom,

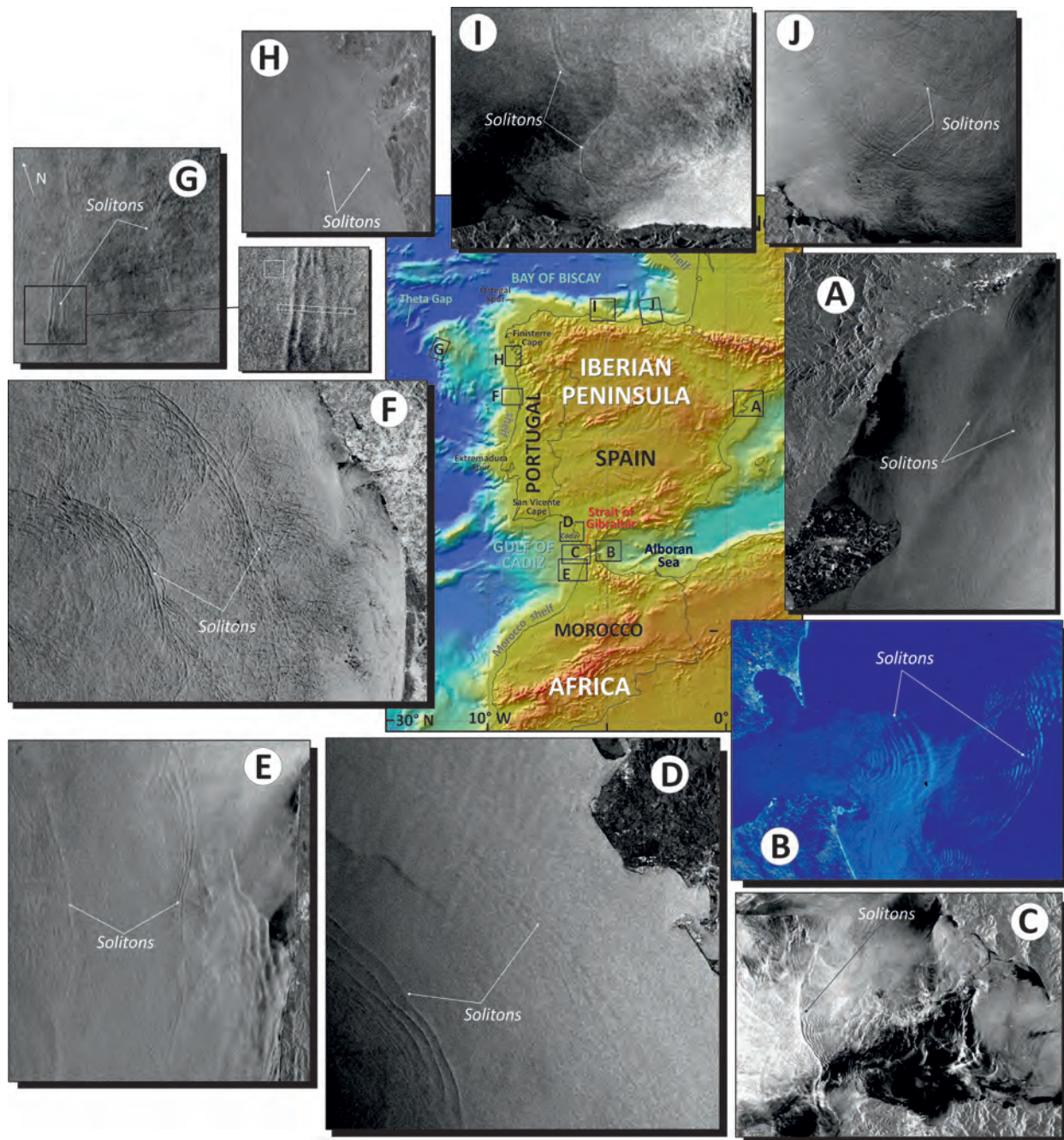


Figure 15. Selected examples of internal solitons propagating toward the continental slope and shelf around the Iberian margin from: A) the Catalanian margin; B) east of the Strait of Gibraltar; C) west of the Strait of Gibraltar; D) Cadiz; E) NW Morocco; F) NW Portugal; G) the Galicia Bank; H) Rías Baixas (Galicia margin); I) Cantabrian margin (off Gijón); J) the Cantabrian margin (off Bilbao). These oceanographic processes are ubiquitous around Iberia as well as in the adjacent continental margins from Morocco, France and Porcupine, related mainly to the shelf break, seamounts and banks. Their real implications in sedimentary processes have not been considered until now, although they represent energetic and constant oceanographic processes. Images are synthetic aperture radar images [from Apel, 2004 and EOLi (Earth Observation Link, European Space Agency, <http://earth.esa.int/EOLi/EOLi.html>)].

Figura 15. Selección de ejemplos de solitones internos que se propagan hacia el talud continental y la plataforma alrededor del margen Ibérico en: A) Cataluña; B) Este del Estrecho de Gibraltar; C) Oeste del Estrecho de Gibraltar; D) Cádiz; E) NO de Marruecos; F) NO de Portugal; G) Banco de Galicia; H) Rías Baixas (margen de Galicia); I) Margen Cantábrico (frente a Gijón); J) Margen Cantábrico (frente a Bilbao). Estos procesos oceanográficos son muy frecuentes alrededor de Iberia, así como en los márgenes continentales adyacentes de Marruecos, Francia y Porcupine, en relación principalmente con el borde de plataforma, montes submarinos y bancos. Hasta la fecha no se han considerado sus implicaciones reales en los procesos sedimentarios, a pesar de representar procesos oceanográficos frecuentes y energéticos. Las imágenes son imágenes de radar de apertura sintética [de Apel, 2004 y EOLi (Earth Observation Link, European Space Agency, <http://earth.esa.int/EOLi/EOLi.html>)].

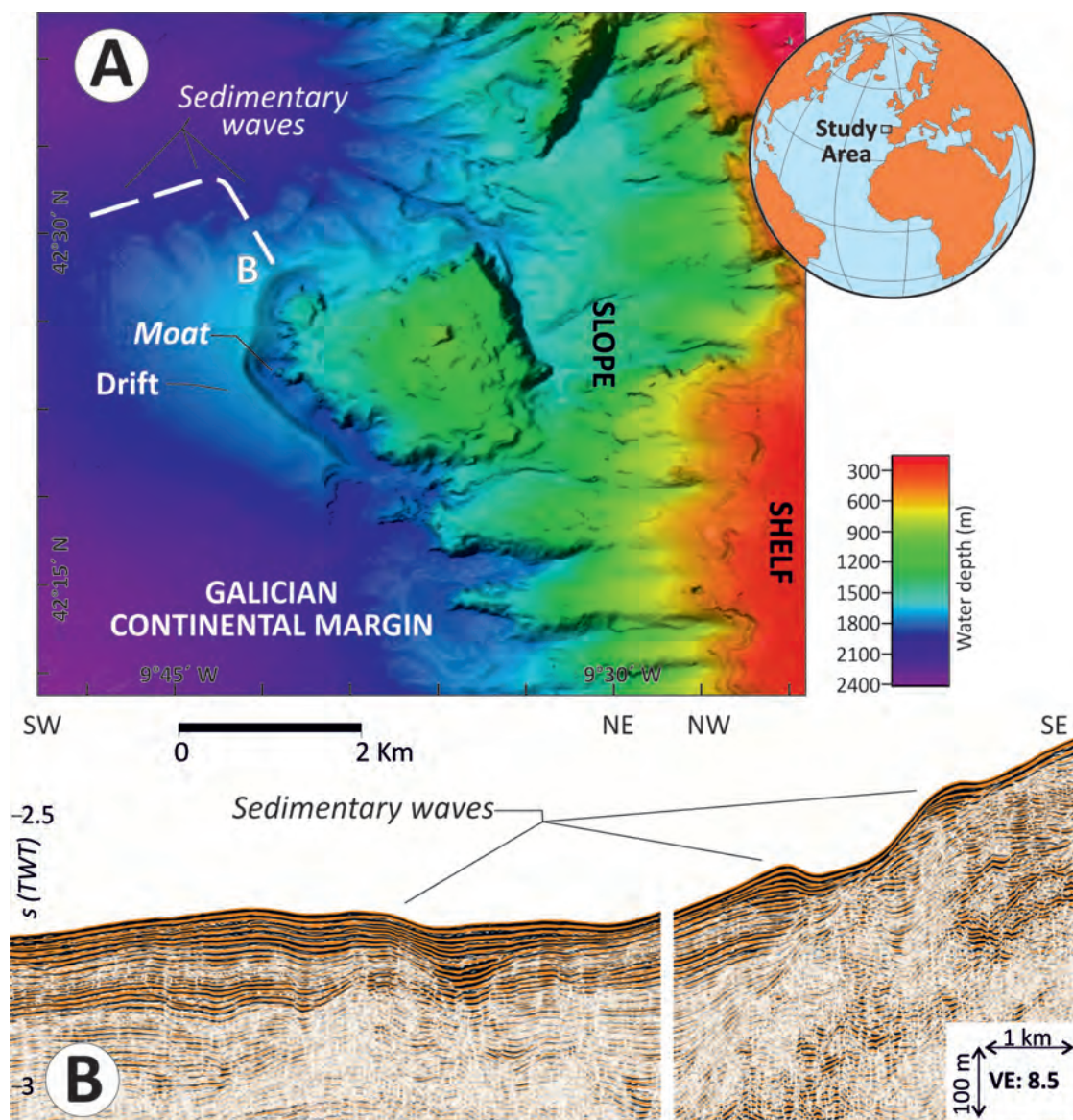


Figure 16. Example of sedimentary waves in the Galician continental margin, which could be attributed to internal waves. A) Swath bathymetric map of the margin indicating the position of the sedimentary waves along the NW flank of a contourite drift in the lower slope; B) seismic profile across the sediment waves (data courtesy from the MARUM project GALIOMAR, from Hanebuth, *et al.*, 2012).

Figura 16. Ejemplo de ondas sedimentarias en el margen continental de Galicia que podrían ser atribuidos a ondas internas. A) Mosaico batimétrico del margen que indica la posición de las ondas sedimentarias a lo largo del flanco NO del drift contourítico en el talud inferior; B) Perfil sísmico transversal a las ondas de sedimento (cortesía de datos del proyecto GALIOMAR MARUM, de Hanebuth, *et al.*, 2012).

usually due to earthquakes, landslides or to other external agents, such as volcanic eruptions or meteorite impacts (Shanmugam, 2006, 2012a). Tsunami waves carry energy through the water, but do not displace the water horizontally, nor do they transport sediment. During the transformation stage, however, tsunami waves erode and incorporate sediment into the incoming wave. Tsunami-related traction currents can thus transport large concentrations of sediment

in suspension (Abrantes *et al.*, 2008; Shanmugam, 2006, 2012a). Tsunamis are also important mechanisms for triggering sediment failures, as the advancing tsunami wave front can generate large hydrodynamic pressures on the seafloor that overwhelm slope stability factors (Wright and Rathje, 2003).

The southern Iberian margin is seismically active due to the convergent plate boundary between Eurasia (Iberian sub-plate) and Africa (Nubian sub-

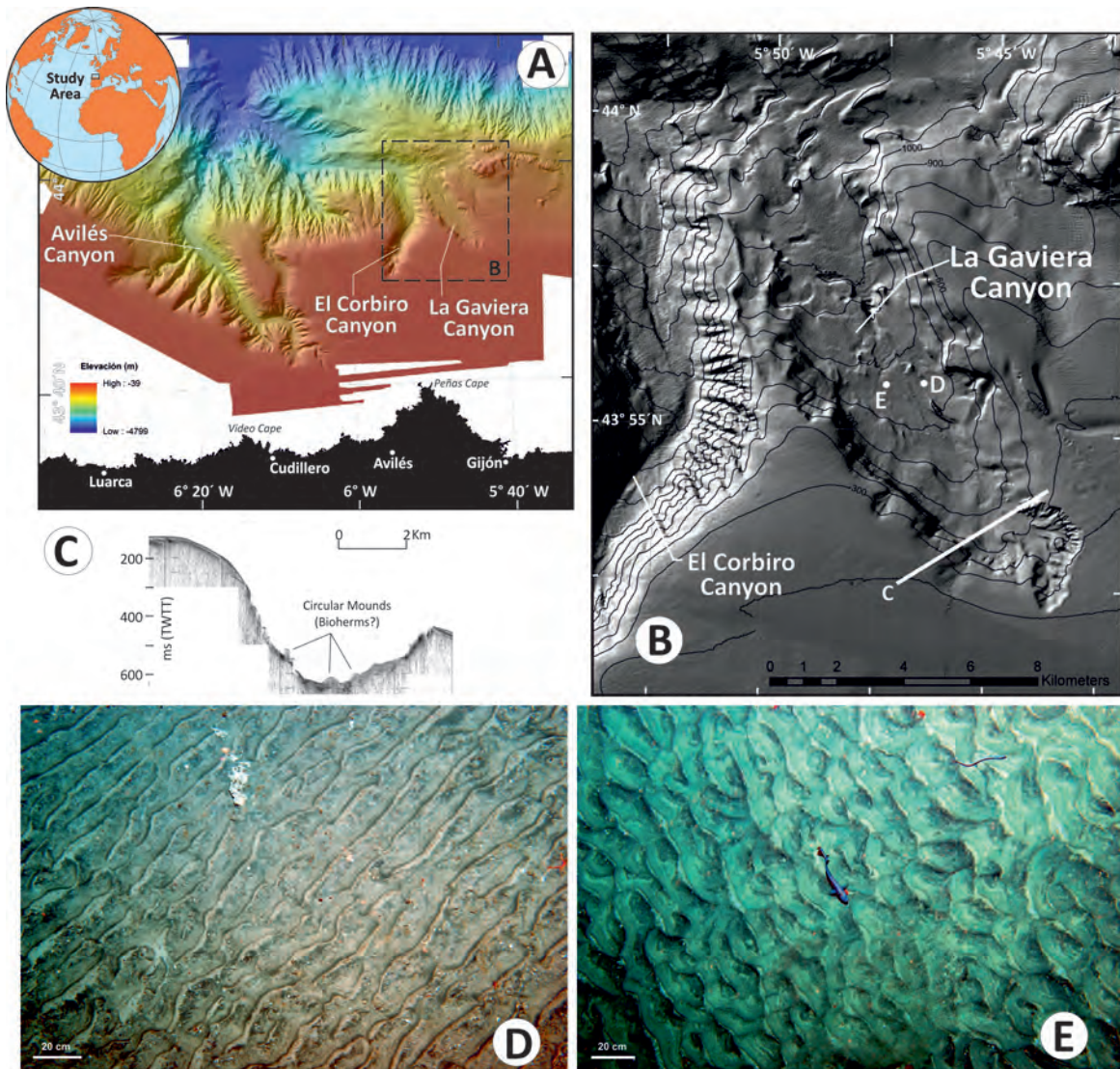
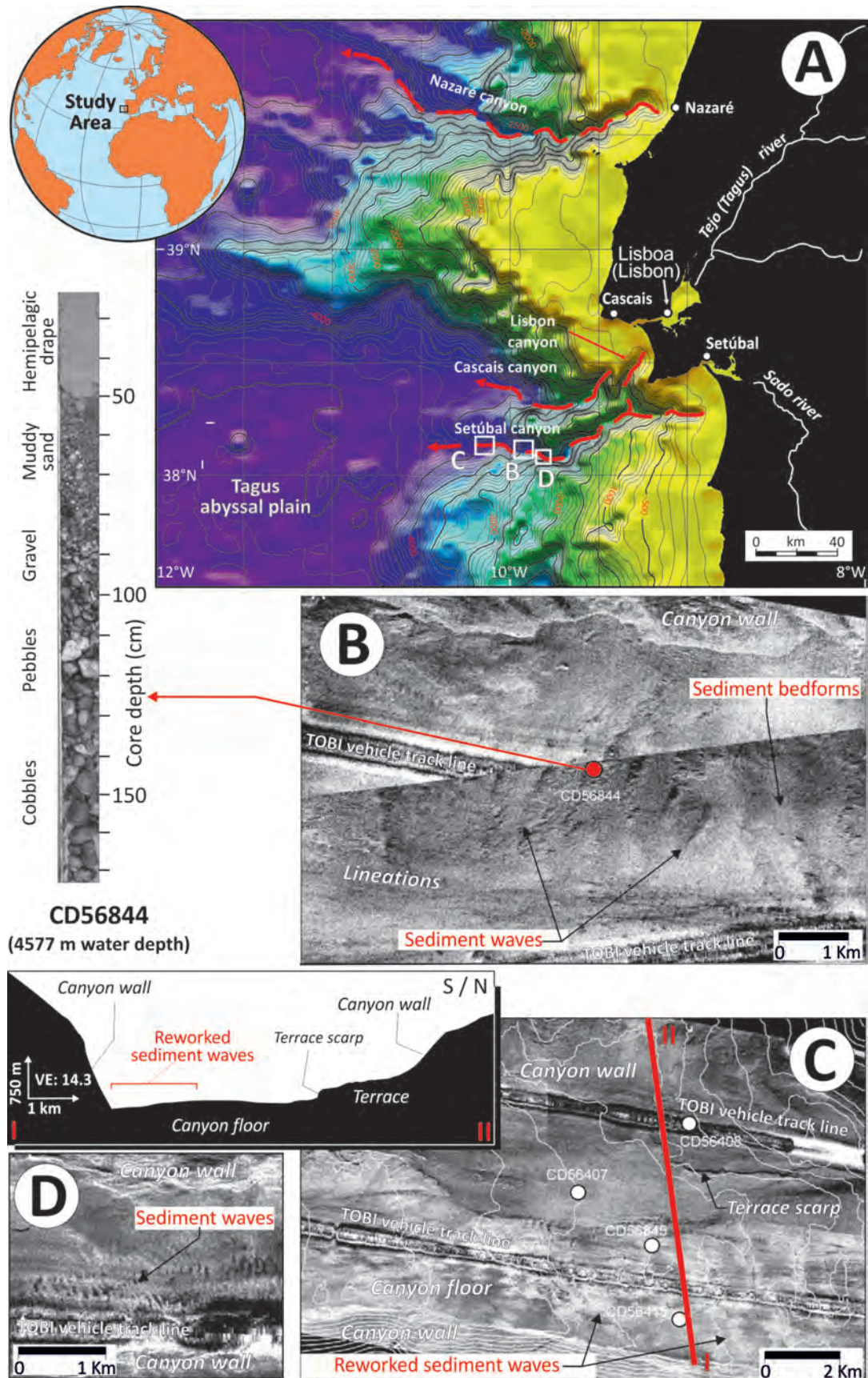


Figure 17. Examples of sandy bedforms related to internal tides and waves within the Gaviera Canyon, in the Cantabrian margin. A) Regional area location; B) shaded bathymetric map of part of the Cantabrian Sea margin (isobaths equidistance 100 m) indicating the position of the major canyons, with illumination from the NW (Gómez-Ballesteros *et al.*, 2013). C) Top as profile crossing NE the head of the Gaviera canyon (Gómez-Ballesteros *et al.*, 2013). Submarine photographs of the Gaviera canyon sea floor; D) at 863 m water depth (-5.78628 / 43.92902) taken 24 April 2010 at 15:05. Water temperature was approximately 9.93°C; salinity 35.76 and potential density 27.54 kg/m³; E) at 837.6 m water depth (-5.77847°E / 43.93003°N) taken 26 April 2010 at 15:41. Water temperature was approximately 9.95°C; salinity 35.75 and potential density 27.53 kg/m³ (Photo taken by F. Sánchez, IEO).

Figura 17. Ejemplos de formas de fondo de arena relacionadas con las mareas y las ondas internas dentro del Cañón de Gaviera, en el margen del Cantábrico. A) Localización regional del área; B) Mosaico batimétrico sombreado de parte del margen Cantábrico (distancia entre isobatas de 100 m) indicándose la localización de los grandes cañones (Gómez-Ballesteros *et al.*, 2013, con iluminación del NO); C) Perfil de Topas que cruza la cabecera del Cañón de Gaviera con dirección NE (Gómez-Ballesteros *et al.*, 2013). Fotografías submarinas del fondo del mar del Cañón de Gaviera; D) a 863 m de profundidad (-5.78628 / 43.92902) tomadas el 24 de abril 2010 a las 15:05. La temperatura del agua era de 9.93°; salinidad de 35.76 y densidad de 27.54; E) a 837,6 m de profundidad (-5.77847/43.93003) tomada el 26 de abril 2010 a las 15:41. La temperatura del agua era de 9.95°; salinidad de 35.75 y la densidad de 27,53 (Foto tomada por F. Sánchez, IEO).

plate) (Zitellini *et al.*, 2009). Earthquakes have triggered a number of tsunamis in the historic past (Rodríguez-Vidal *et al.*, 2011). These include the 1755 Lisbon tsunami (Baptista *et al.*, 2003), the 1856 and 2003 tsunamis in Algeria (Roger and Hébert, 2008;

Sahal *et al.*, 2009) and the 1969 tsunami in the Atlantic (Guesmia *et al.*, 1998). The earthquake-induced Lisbon tsunami appears in the geologic record from Portugal to the Gibraltar Strait (i.e., Dawson *et al.*, 1991, 1995; Hindson *et al.*, 1996; Dabrio *et al.*, 1998,



2000; Hindson and Andrade, 1999; Luque *et al.*, 1999, 2001, 2004; Luque, 2002; Whelan and Kelletal, 2005; Viana-Baptista *et al.*, 2006; Gracia *et al.*, 2006; Cuven *et al.*, 2013) and even in southern England (Banerjee *et al.*, 2001). The geologic record also shows evidence of ancient tsunamis impacting southwestern Spain, Portugal, Morocco (Galbis, 1932; Campos, 1991; Reicherter, 2001; Luque *et al.*, 2001, 2002; Luque, 2002; Ruiz *et al.*, 2004, 2005; Scheffers and Kelletal, 2005), and the Alboran Sea (IGN, 2009; Reicherter and Becker-Heidmann, 2009).

Few studies have considered the deep-sea sedimentary implications of the tsunamis that have impacted the Iberian margin. The 1522 Almeria earthquake ($M > 6.5$) affected a large area of the western Mediterranean, even though its epicentre occurred in the Gulf of Almeria along the Carboneras fault zone. The earthquake triggered submarine slides in the Gulf of Almeria and tsunami waves (Reicherter and Becker-Heidmann, 2009). The IODP Expedition 339 identified sandy deposits along the Gulf of Cadiz and west of the Portuguese slope (Fig. 19) as tsunami deposits (Stow *et al.*, 2013b). Other tsunami-related traction currents and deposits may occur along the Iberian slopes. While evidence of other events may exist in the study region, researchers have not yet established consistent sedimentological criteria for identifying paleo-tsunami deposits (Shanmugan, 2012b). Deeper water tsunami deposits and structures may resemble their shallow water counterparts, or might resemble turbidity and debris (or mud) flow sequences in terms of facies associations (Dawson and Stewart, 2007).

Rogue- and cyclone-related traction currents

Similar to tsunamis, rogue waves and cyclone waves are categorized as intermittent processes. Oceanic rogue waves (also known as freak waves, killer waves, monster waves, extreme events, abnormal waves, etc.) are surface gravity waves whose wave heights are at least twice as large as the significant wave height expected for the sea state (Shanmugan, 2012a, Fig. 2). Tropical cyclones are meteorological phenomena. They can trigger bottom currents and generate large hydrodynamic pressures on the sea floor that produce submarine mudflows and slope instabilities. As such, they accelerate deep-water sedimentation and/or reworking of previous deposits. Structurally, tropical cyclones are large, rotating systems of clouds, winds and thunder storms. In the Northern Hemisphere the rotation of cyclones is counterclockwise, but in the Southern Hemisphere the rotation is clockwise due to the Coriolis force. Rogue and cyclone waves do not appear to have created any known morphologic features along the Iberian Margin, although theoretically these events may have influenced deep-water environments in the past.

Morphologic and sedimentary implications

The descriptions above highlight a number of permanent and intermittent processes that affect bottom currents. These processes maybe very variable and appear as overflows, tides, eddies, deep-sea storms,

Figure 18. Examples of sedimentary waves described in the Setúbal Canyon, west Iberian margin. A) Regional bathymetry map. Contours are every 100 m and outlined in bold every 500 m. Side scan sonar images (A, B and C) showing details of the canyon floor in the lower Setúbal Canyon; B) Transverse linear bedforms illustrating sediment facies in the Core CD56844, interpreted to comprise of coarse-grained sediment wave deposits (from Arzola *et al.*, 2008); C) Reworked sediment waves on the canyon floor and profile show the contrast between the steep canyon walls and edge of the northern margin terrace, and the wide, relatively flat but slightly domed canyon floor (from Arzola *et al.*, 2008); D) Sediment bedforms from the channel-lobe transition zone (from Lastras *et al.* 2009). These sedimentary wave examples (locations in A) are described in the Setubal, Nazaré and Cascais Canyons and interpreted as being due to the actions of turbiditic processes. However, they are very common within submarine canyons worldwide and in many other cases are generated and / or reworked by oceanographic processes, as tidal current or internal waves (e.g., Shanmugan, 2012a, 2013b). The role of these processes on submarine canyons, gullies, etc. have been underestimated but should be considered in future multidisciplinary studies.

Figura 18. Ejemplos de ondas sedimentarias que se describen en el Cañón de Setúbal, en el margen Ibérico occidental. A) Mapa batimétrico regional. Se indican las curvas de nivel cada 100 metros y en negrita cada 500 m. Imágenes de sonar de barrido lateral (A, B y C) que muestran el detalle del fondo del Cañón de Setúbal en su parte distal; B) Formas de fondo transversalmente lineales donde se reflejan sus facies sedimentarias (Testigo CD56844), interpretadas como depósitos de ondas de sedimentos de grano grueso (de Arzola *et al.*, 2008); C) Ondas de sedimento re TRABAJADAS en el fondo del cañón y cuyo perfil muestra el contraste entre las paredes escarpadas del cañón y el borde de la terraza en su margen norte, con el fondo del cañón relativamente plano (de Arzola *et al.*, 2008); D) Formas de fondo sedimentarias de la zona de transición entre el lóbulo y el canal (de Lastras *et al.* 2009). Estos ejemplos de ondas sedimentarias (localización en A) están descritas en los cañones de Setúbal, Nazaré y Cascais e interpretados como depósitos generados por la acción de procesos turbidíticos, que posteriormente pueden ser re TRABAJADAS. Sin embargo, estas ondas sedimentarias son muy comunes en los cañones submarinos de todo el mundo, y en muchos casos se generan y/o re TRABAJAN por procesos oceanográficos, como corrientes de marea u ondas internas (por ejemplo, Shanmugan, 2012a, 2013b). El papel de estos procesos en los cañones submarinos, gullies, etc. ha sido subestimado, pero deberían estar considerados en futuros trabajos multidisciplinarios.

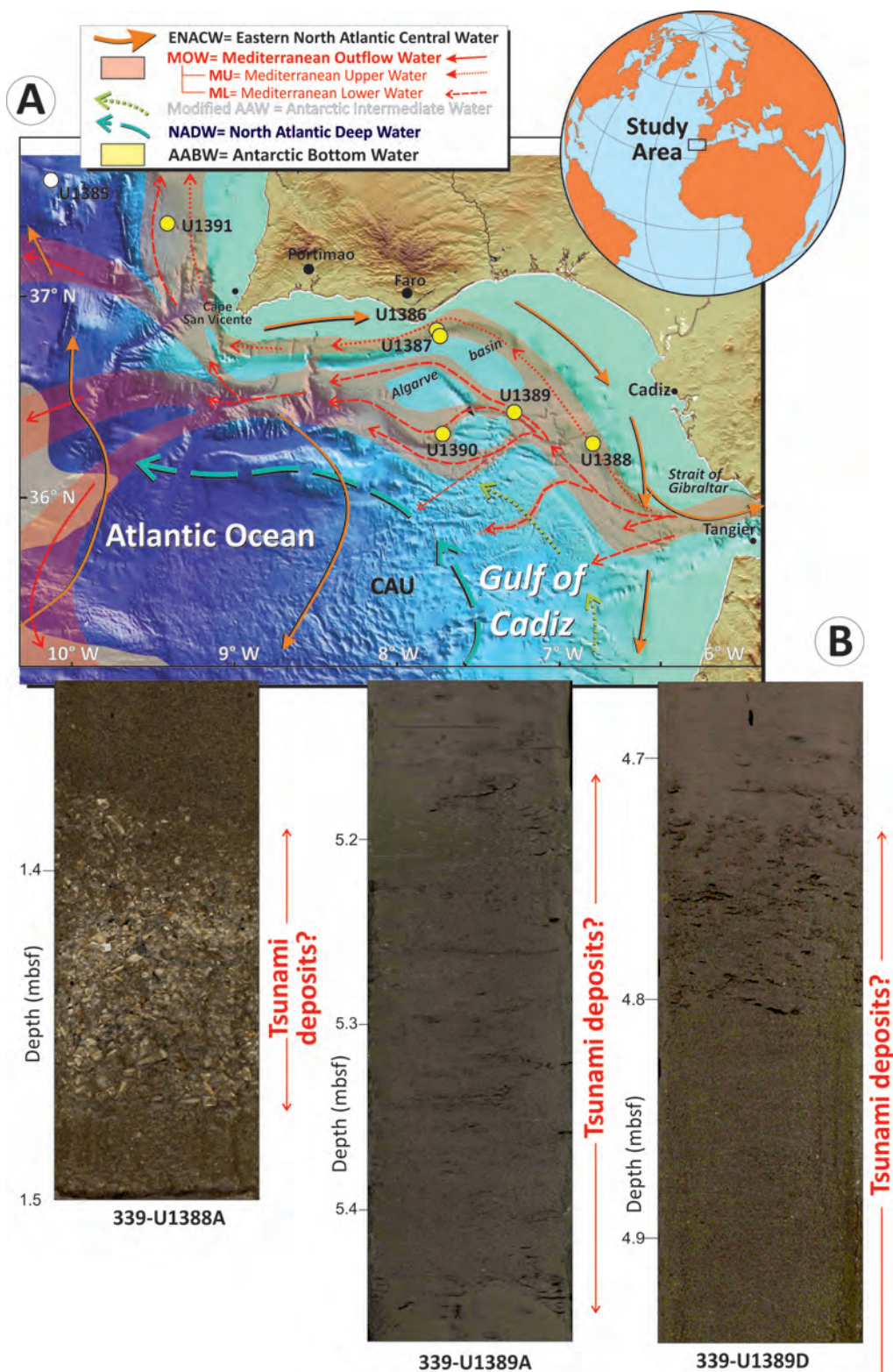


Figure 19. A) Regional water masses and Gulf of Cadiz CDS site locations sampled during IODP Expedition 339; B) Sandy Holocene deposits drilled during IODP Expedition 339 (Sites U1388 and U1389) interpreted as tsunami deposits (Stow *et al.*, 2013b, Pers. Comm., Yasuhiro Takashimizu, Niigata University, Japan).

Figura 19. A) Localización de las masas de agua regionales, y puntos de perforación durante la Expedición IODP 339 en el Golfo de Cádiz y oeste de Portugal; B) Durante la Expedición IODP 339 se perforaron depósitos de arena Holocenos (Sondeos U1388 y U1389) que han sido interpretados como depósitos de tsunami (Stow *et al.*, 2013b, Comm. Pers., Yasuhiro Takashimizu, la Universidad de Niigata, Japón).

secondary circulation, internal waves and tsunamis, rogue waves and cyclone waves. All these processes show some degree of variability and, although one of them may prevail in a particular situation, it is likely that there are several processes acting in combination to determine the local direction and velocity of the bottom current. Many of these processes and their effects on deep-water sedimentation are not well understood. Along the Iberian margin, several of these processes interact with the seafloor to affect its morphology and sediment distribution on a local or regional scale. We cannot however yet discern specific sequences of events or the relative influence of these processes from sedimentary evidence. Discussion and debate continue on how bottom currents form the range of morphologies observed among contourites. To stimulate this discussion, future analyses must include the wider and more complex range of deep-water processes described above. While local oceanographic settings provide first order constraints on contourite morphology, ancient contourite examples from the geologic record can also reveal how they may vary in response to different deep-marine conditions.

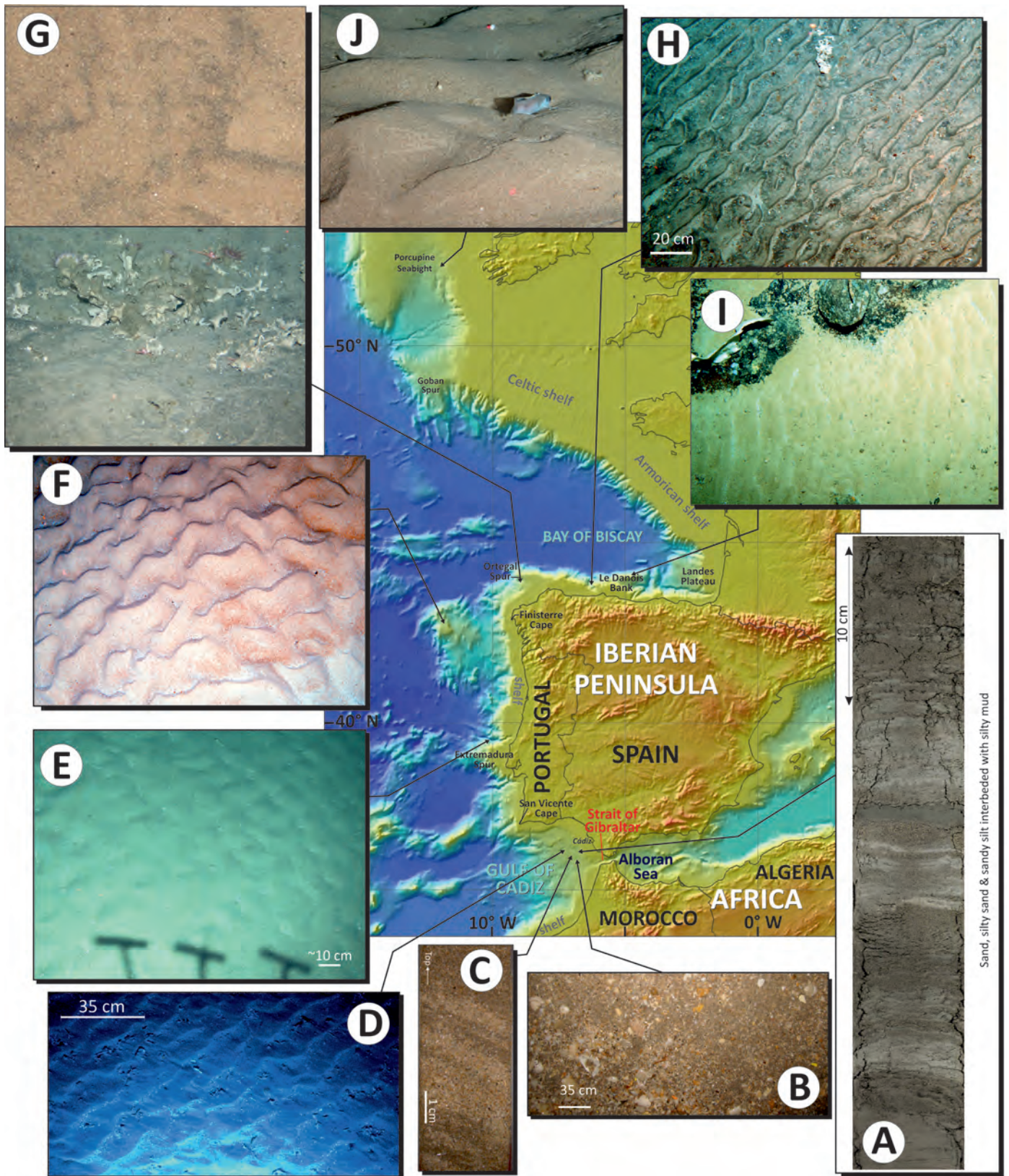
Specific bottom-current facies have been described by many authors (see a recent compilation in Rebesco *et al.*, 2014). The standard contourite facies model sequence was first proposed by Gonthier *et al.* (1984) and Faugères *et al.* (1984), based on the Faro Drift within the middle slope of the Gulf of Cadiz. This model involves a cyclic trend, composed of three main facies: (1) homogeneous mud, (2) mottled silt and mud, and (3) sand and silt. These facies are typically arranged in a coarsening-up to fining-up cycle that defines the standard bi-gradational sequence for contourites. This general model for contourites represents the transition from weaker to stronger bottom-current flow, and then back to weaker conditions (Stow and Holbrook, 1984; Stow *et al.*, 2002a; Huneke and Stow, 2008). The bi-gradational facies sequences are observed among ancient to recent contourite deposits, including the Brazilian margin (Viana and Faugères, 1998), the Irish margin (Øvrebø *et al.*, 2006) and in ancient deposits (e.g., Chinese sedimentary basins, Gao *et al.*, 1988). Authors commonly report partial or incomplete contourite sequences (Howe *et al.*, 1994; Stoker *et al.*, 1998; Shanmugam, 2000; Howe *et al.*, 2002; Stow *et al.*, 2002a, 2013a; Mulder *et al.*, 2013). Further modifications of the contourite model (e.g., Stow *et al.*, 2002a, b; Stow, 2005; Stow and Faugères, 2008) have demonstrated a considerable degree of variation, thus complicating the establishment of a unique and systematic facies designation. Mulder *et al.* (2013)

have recently demonstrated that a particular facies sequence may depend on the supply of coarser terrigenous clastic material provided by increased erosion of indurated mud along the flanks of confined contourite channels (mud clasts), by increased sediment supply from rivers (quartz grains) and/or by downslope mass transport along the continental shelf and upper slope. These results are consistent with the findings of Masson *et al.* (2010), that the classical contourite depositional sequence proposed by Gonthier *et al.* (1984) should be interpreted with special consideration given to the regional sedimentological background.

The Faro Drift deposits do not offer the best example of a contourite facies sequence due to the preponderance of mud within these deposits, and their location along the distal part of a much larger contourite depositional system (CDS). Other facies from different parts of the same depositional system do not fit neatly into the conceptual model suggested by the Faro Drift (e.g., Mulder *et al.*, 2013; Stow *et al.*, 2013a; Hernández-Molina *et al.*, 2013, 2014). Mulder *et al.*, 2013 have in fact shown that most of the contacts between the classical contourite facies (mottled, fine sand, coarse sand) are sharp rather than transitional, an observation that supports the interpretation by Shanmugam (2006, 2012a, 2013b). The proposed facies sequence for the Faro Drift could therefore serve as an appropriate model for fine-grained contourite deposits, for which pervasive bioturbation is a diagnostic feature. This interpretation, however, suggests that the Faro Drift does not offer a representative example of other types of contourite deposits (Martín-Chivelet *et al.*, 2008; Shanmugam, 2012a, 2013b; Mulder *et al.*, 2013). Other authors have described contourite settings with a higher proportion of sand (Shanmugam *et al.*, 1993; Shanmugam, 2000, 2012a, 2013b), indicating that activity of bottom currents prevails over bioturbation.

This controversy in contourite identification demonstrates that contourites exhibit greater variation than the established facies model suggests and commonly include traction sedimentary structures. The contourite facies model would thus benefit from further modification. A consistent facies model, however, faces substantial challenges in terms of the wide range of oceanographic permanent and intermittent processes (and their spatial and temporal variation) that may influence the development of CDSs.

We began an effort to reassess contourite facies during the IODP Expedition 339 along the Iberian margin, in the Gulf of Cádiz and off western Portugal (http://iodp.tamu.edu/scienceops/expeditions/mediterranean_outflow.html), (Expedition 339 Scientists,



2012; Stow *et al.*, 2013b; Hernández-Molina *et al.*, 2013). Contourites were the most prevalent material in sediment cores, constituting up to 95% of the Quaternary section and about 50% of the recovered Pliocene section. The facies included sand-rich, muddy sand, silty-mud and mud-rich contourites, all of which formed at moderate (20-30 cm/ky) to very high (> 100 cm/ky) rates of sedimentation. The contourites recovered during this expedition were remarkably uniform in composition and textural attributes. The muddy and silty contourite deposits displayed an absence of primary sedimentary structures, but exhibited intense continuous bioturbation throughout the section sampled. The cores also showed consistent, bi-gradational sequences with inverse and then normal grading as well as a number of partial sequence types. Expedition 339 also identified thick and extensive contourite sand deposits, as well as turbidite sands apparently reworked by bottom currents (Expedition 339 Scientists, 2012; Stow *et al.*, 2013b; Hernández-Molina *et al.*, 2013). These sands occurred in the proximal part of the CDS close to the Strait of Gibraltar (Fig. 20), where Expedition 339 retrieved a very thick, sandy contourite layer (> 10 m) that showed traction sedimentary structures (Hernández-Molina *et al.*, 2013, 2014; Brackenridge, 2014). Sand-rich contourites also occur in other areas

around Iberia, such as the Galician and Cantabrian margins (Fig. 20) (Alejo *et al.*, 2012). Future work around the Iberian margin will systematically categorize these sedimentary facies and frame them according to bottom-current dynamics and other oceanographic processes.

Sedimentologists have debated the differentiation between contourites and turbidites for almost five decades (Hollister, 1967; Piper, 1972, Hollister and Heezen, 1972; Bouma, 1972, 1973; Bouma and Hollister, 1973) but have not definitively established which structures distinguish contourites. Contourite processes can in fact trigger gravitational collapse that forms submarine lobes as in the Gulf of Cadiz (Habgood *et al.*, 2003; Hanquiez *et al.*, 2010) or rework previous turbiditic deposits (Shanmugam *et al.*, 1993, Shanmugam 2012a, 2013b). Contourite and turbiditic processes can also intermingle in both vertical and lateral dimensions, and thus form mixed deposits. Differentiating contourites from turbidites represents a major challenge for future research along the Iberian margin, especially given the legacy of emphasis on mass-transport and turbiditic processes in interpretations of Iberian margin deposits.

Regional interpretations of the Iberian margin have generally underestimated the role of bottom currents in shaping the seafloor and controlling the

Figure 20. Examples of deep water sandy deposits around the Iberian margin. Some of them are related to the action of contour currents, but others are related to other oceanographic processes such as internal waves, tides, etc. Most of these deposits have not been studied yet and future work should clarify their characteristics and genesis. A) Examples of sandy contourite facies sampled during IODP Expedition 339, in the Gulf of Cadiz close to the exit of the Strait of Gibraltar (modified from Hernández-Molina *et al.*, 2014); B) coarse sands and bioclastic gravel deposits in the slope of the Gulf of Cadiz at the exit of the Strait of Gibraltar collected with the CONTOURIBER Project (2010); C) laminated sandy contourite facies, showing inclined lamination as a result of sand wave migration in the Gulf of Cadiz, sand sheet in proximal sector (Stow and Fauquères, 2008); D) contourite sandy deposits affected by bottom currents and barotropic and internal tides in the slope channels of the middle slope of the Gulf of Cadiz (from Stow *et al.*, 2013a); E) sandy turbiditic (reworked?) facies from ISIS from ca. 4,300m water depth in the Nazaré Canyon (courtesy from V. Huvenne of NOCS, UK); F) sandy deposits on top of the Galicia Bank by bottom current (INDEMARES Project, Photo taken by F. Sánchez, IEO, Spain); G) example of sandy deposits from the middle slope of the Ortegal Spur (From A Selva Cruise, 2008 and R/V Belgica 09/14a cruise, EC FP7 IP HERMIONE project); H) submarine photographs of reworked sandy deposits within the Gaviera Canyon, Cantabrian Sea (Photo taken by F. Sánchez, IEO, Spain); I) sandy deposits along the SE flank of the Le Danois Bank in the slope of the Cantabrian Sea (ECOMARG 3 Project, Photo taken by F. Sánchez, IEO, Spain); and J) sandy deposits in the Porcupine Seabight, Irish continental slope (courtesy of MARUM, Germany).

Figura 20. Ejemplos de depósitos de arena profundos alrededor del margen Ibérico. Algunos de ellos están relacionados con la acción de las corrientes de contorno, pero otros están relacionados con otros procesos oceanográficos (ondas internas, mareas, etc.). La mayor parte de estos depósitos no se han estudiado en todavía y futuros trabajos deberían determinar sus características y su génesis. A) Ejemplos de facies arenosas contorníticas muestreadas durante la Expedición IODP 339 en el Golfo de Cádiz, cerca de la salida del Estrecho de Gibraltar (Modificado de Hernández-Molina *et al.*, 2014); B) Arenas gruesas y depósitos de grava bioclásticos en el talud del Golfo de Cádiz a la salida del Estrecho de Gibraltar que se recogieron en el Proyecto CONTOURIBER (2010); C) Facies laminares de contornitas arenosas mostrando laminación inclinada como resultado de la migración de ondas de arena en el sector proximal del Golfo de Cádiz (Stow and Fauquères, 2008); D) Depósitos contorníticos de arena afectados por la corriente de fondo y de la mareas en los canales del talud medio del Golfo de Cádiz (de Stow *et al.*, 2013a); E) Facies turbidíticas arenosas (retrabajadas?) de ISIS desde aproximadamente 4300 m de profundidad en el cañón de Nazaré (cortesía de V. Huvenne of NOCS, Reino Unido); F) Depósitos de arena en la parte superior del Banco de Galicia generados por corrientes de fondo (Proyecto INDEMARES, Foto tomada por F. Sánchez, IEO, España); G) Ejemplo de depósitos de arena en el talud medio de Cabo Ortegal (de la Campaña A Selva 2008 y R/V Belgica 09/14a, proyecto HERMIONE de la CE FP7 IP); H) Fotografías submarinas de depósitos arenosos retrabajados dentro del cañón de Gaviera, Mar Cantábrico (Foto tomada por F. Sánchez, IEO, España); I) Depósitos de arena a lo largo del flanco SE del Banco Le Danois; en el talud continental del Mar Cantábrico (Proyecto ECOMARG 3, foto tomada por F. Sánchez, IEO, España); y J) Depósitos de arena en Porcupine Seabight, en el talud continental Irlandés (cortesía de MARUM, Alemania).

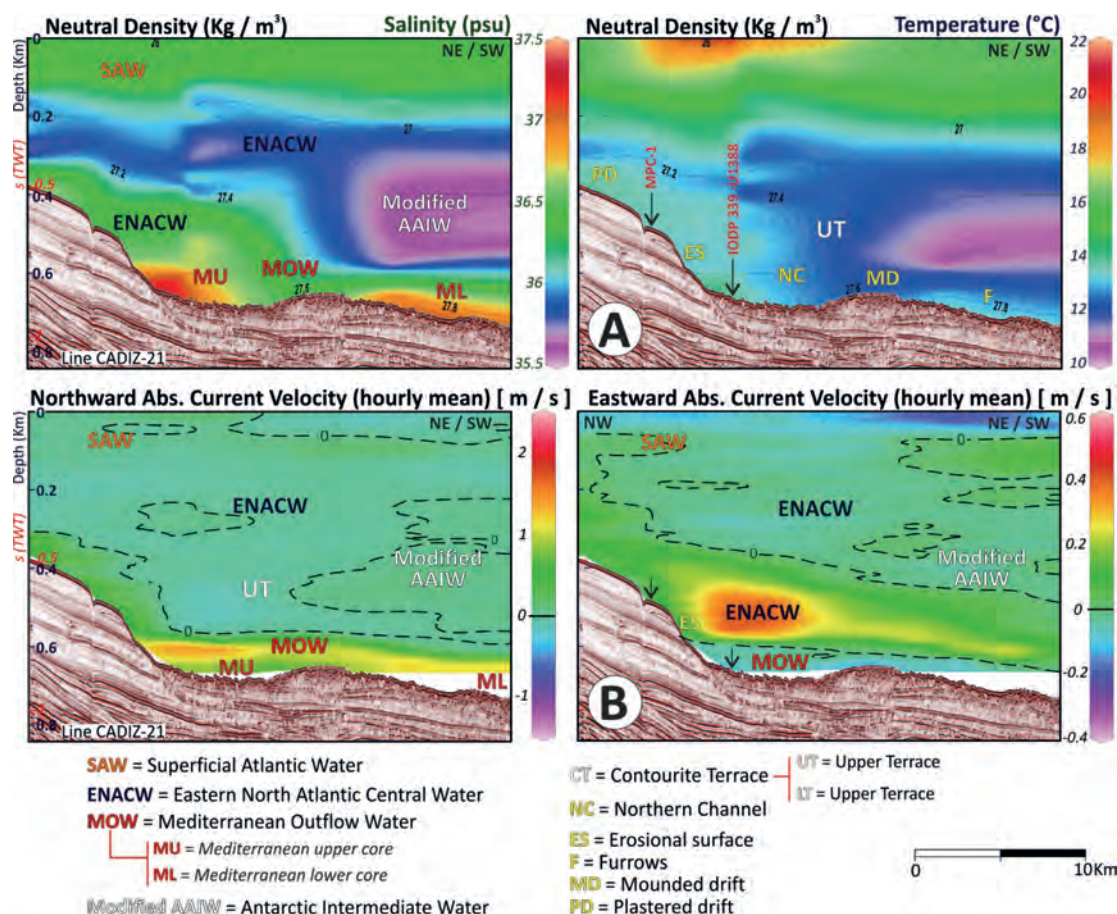


Figure 21. Examples of combination of physical oceanographic and geologic/geophysical data showing the relationship between the long-term current regime, seafloor morphology and sub-bottom sediment geometry in the Gulf of Cadiz, from the exit of the Strait of Gibraltar (Hernández-Molina *et al.*, 2014, with permission from Geological Society of America). A) Salinity and temperature data in the water columns. The black lines refer to isopycnals and neutral density (kg/m^3); B) vertical sections of ocean velocity measured at the eastern area close to the exit of the Strait of Gibraltar. The water colour code displays the Acoustic Doppler Current Profiler (ADCP) velocity components. The panels on the left correspond to the velocity component in the east-west direction (positive values indicate currents towards the east), and the panels on the right correspond to the velocity component in the north-south direction (positive values indicate current towards the north). The dashed black lines indicate where the current velocity is zero. See Fig. 4 for section locations.

Figura 21. Ejemplos de la combinación de datos de oceanografía física y geológicos/geofísicos que muestran la relación entre un régimen de corrientes a largo plazo, la morfología del fondo marino y la geometría actual de sedimentos del fondo en el Golfo de Cádiz, desde la salida del Estrecho de Gibraltar (Hernández-Molina *et al.*, 2014, con permiso de la Sociedad Geológica de América). A) Salinidad y temperatura de las columnas de agua. Las líneas negras se refieren a isopícnas y de densidad neutra (kg/m^3); B) Secciones verticales de velocidad del océano medidas en la zona oriental cerca de la salida del Estrecho de Gibraltar. El código de color de agua muestra las componentes de la velocidad del Perfilador de Corrientes Acústico Doppler (Acoustic Doppler Current Profiler-ADCP). Los paneles de la izquierda corresponden a la componente de la velocidad en la dirección este-oeste (los valores positivos indican las corrientes hacia el este), y los paneles de la derecha corresponden a la componente de la velocidad en la dirección norte-sur (los valores positivos indican la corriente hacia el norte). Las líneas discontinuas negras indican que la velocidad de la corriente es cero. Ver Fig. 4 para la localización de las secciones.

sedimentary stacking pattern. Very large contourite drifts occur along this margin (see Llave *et al.*, this issue) and small to intermediate sized drifts are ubiquitous (e.g., Ercilla *et al.*, submitted). While CDS genetic models are under revision, bottom currents and associated oceanographic processes clearly control the physiography and sedimentation around the Iberian continental margins and adjacent basins. The position of interfaces between major water masses

and their vertical and spatial variation in time specifically appears to exert primary control in determining major morphologic changes (changes along the slope gradient) (Figs.6, 7 and 21). Density contrasts that form boundaries (Hernández-Molina *et al.*, 2011; Ercilla *et al.*, submitted) similar to those reported for other margins (e.g., Hernández-Molina *et al.*, 2009; Preu *et al.*, 2013) are important components of these interfaces due to their responses to internal waves,

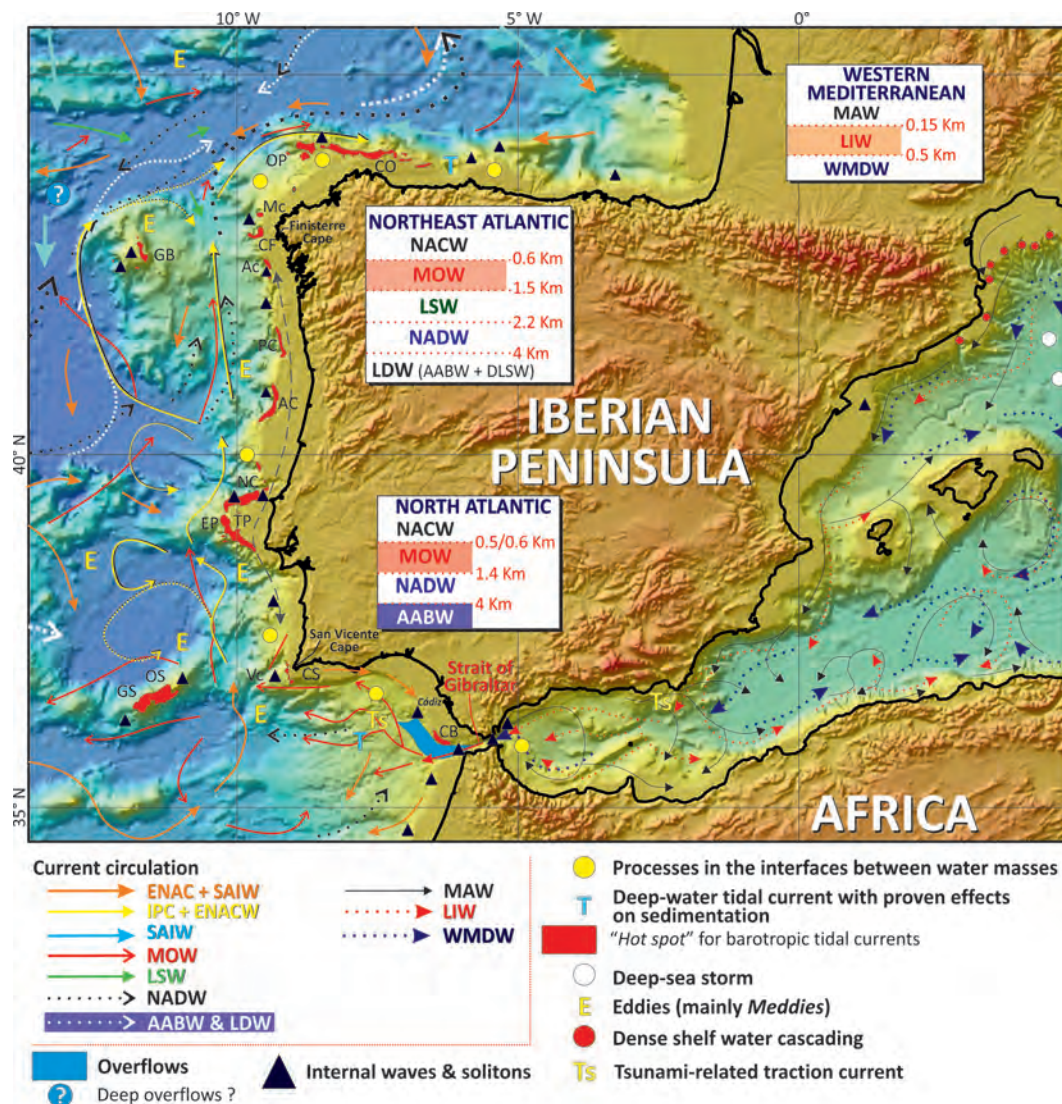


Figure 22. Sketch summarizing the locations of permanent or intermittent oceanographic processes along the Iberian margin and their short- and long-term controls on sedimentary facies and seafloor morphology. These processes include overflows, barotropic currents, tides, eddies, deep-sea storms, horizontal vortices, internal waves, tsunamis, rogue waves and cyclonic waves. In one particular area, one of these processes may be dominant, but usually several processes act in tandem to determine the local direction and velocity of bottom currents. Legend for the internal tide generation "hotspots": AC= Arosa Canyon; AV= Aveiro Canyon; CB= Conil-Barbate; CF= Cape of Finisterre; CS= Cape of Sagres; CO= Cape of Ortegal; EC= Estremadura promontory; GB= Galician Bank; GS= Gettysburg seamount; MC= Murgia Canyon; NC= Nazaré Canyon; OP= Ortegal promontory; OS= Ormonde seamount; PC= Porto Canyon; TP= Tagus Plateau; VC= S. Vicente Canyon. Legend for water masses in alphabetic order: AABW= Antarctic Bottom Water; ENAC= Eastern North Atlantic Current; ENACW= Eastern North Atlantic Central Water; IPC= Iberian Poleward Current; LDW= Lower Deep Water; LIW= Levantine Intermediate Water; LSW= Labrador Sea Water LSW; MAW= Modified Atlantic Water; MOW= Mediterranean Outflow Water; NADW= North Atlantic Deep Water; NASW= North Atlantic Superficial Water; SAIW= Subarctic Intermediate Water; WMDW= Western Mediterranean Deep Water

Figure 22. Esquema que resume la distribución regional de algunos procesos oceanográficos permanentes o intermitentes a lo largo del margen Ibérico y que puedan ejercer un control a corto y largo plazo sobre las facies sedimentarias y la morfología del fondo marino. Estos procesos incluyen overflows, corrientes de mareas, eddies, tormentas profundas, vórtices horizontales, ondas internas, tsunamis, olas aisladas y ciclónicas. En un área en particular, uno de estos procesos puede ser dominante, pero por lo general actúan varios procesos en conjunto, determinando la dirección local y la velocidad de las corrientes de fondo. Leyenda para la generación de "puntos calientes" de mareas internas: Ac = Cañón de Arosa; AV = Cañón de Aveiro; CB = Conil-Barbate; CF = Cabo de Finisterre; CS = Cabo de Sagres; CO = Cabo de Ortegal; EC = Promontorio de Extremadura; GB = Banco de Galicia; GS = Montaña submarina de Gettysburg; MC = Cañón de Murgia; NC = Cañón de Nazaré; OP = Promontorio de Ortegal; OS = Montaña submarina de Ormonde; PC = Cañón de Oporto; TP = Meseta del Tajo; VC = Cañón de S. Vicente. Leyenda de las masas de agua, por orden alfabético y con el nombre original en inglés: AABW= Antarctic Bottom Water; ENAC= Eastern North Atlantic Current; ENACW= Eastern North Atlantic Central Water; IPC= Iberian Poleward Current; LDW= Lower Deep Water; LIW= Levantine Intermediate Water; LSW= Labrador Sea Water LSW; MAW= Modified Atlantic Water; MOW= Mediterranean Outflow Water; NADW= North Atlantic Deep Water; NASW= North Atlantic Superficial Water; SAIW= Subarctic Intermediate Water; WMDW= Western Mediterranean Deep Water.

tidal waves, deep-sea storms, eddies, secondary circulations and other processes. A consistent CDS model thus requires the monitoring of these processes and an accurate cause and effect description of how these processes affect deep-water sedimentation, sedimentary structures and CDS architecture.

Final considerations

A new multidisciplinary approach

Bottom-current controlled depositional, erosional and mixed morphological features commonly occur along the Iberian continental margin at different depths and in various settings. This paper depicts the bottom-current circulation around the Iberian continental margin is affected by a number of permanent and intermittent oceanographic processes (Fig. 22). Previous models for the margin have not fully appreciated the role of these processes and they continue to elude our fullest understanding. Internal waves, tidal waves, deep-sea storms, eddies, secondary circulations and other deep-sea processes generally shape the seafloor over short- and long-term time scales. Future research should seek to interpret these oceanographic processes in sedimentary stacking patterns and the overall architecture of continental margin deposits.

A clearer understanding of oceanographic processes related to bottom currents and their associated sedimentary features requires a multidisciplinary approach, given the complexity of the phenomena under consideration. This approach should integrate the frameworks of Marine geology, Physical Oceanography and Benthic Biology. A combined analysis of sedimentology and fluid dynamics is a priority objective. The approach should specifically include the following topics:

- Detailed studies of deep-water oceanographic processes related to flow phenomena, including internal waves, tides, benthic storms, eddies and vortices with the objective of understanding their importance, interactions and influence on bathymetric features.
- A more systematic understanding of the depositional, erosional and mixed morphological features, as well as their evolution over time and distribution at different points along the margin. Linking these features to specific oceanographic processes will help categorize small and large-scale features and clarify sedimentary facies associations.
- The general physiographic architecture of the mar-

gins and its relationship with the structure of water masses and associated interphases requires more attention.

- Numerical modelling may help to link the variation in genetic processes to the range of observed erosional and depositional features.
- Detection and characterization of past pycnoclines based on proxies from the sedimentary record represents an important objective for future multidisciplinary research. Estimation of the depth range of water-mass interfaces and the study of processes associated with these interfaces (such as baroclinic tides and internal waves) could clarify the interpretation of contourite terraces along the Iberian continental slope. Paleoceanographic models can help to determine potential periods of greater density contrasts within the pycnocline. Contourite terraces suggest relict features along the slope that hint at colder oceanic conditions in the past. These hypothetical conditions require further investigation due to their implications for regional and global climate dynamics.
- Researchers should also seek to detect and characterise intermediate and deep nepheloid layers. These layers often occur at water-mass interfaces. Benthic boundary layers are also critical interfaces that determine seafloor morphology. These interfaces have mostly been studied from a biogeochemical perspective and have not been systematically integrated in the sedimentological and oceanographic models.
- We require a more comprehensive understanding of fluid dynamics around submarine obstacles.
- Oceanographic monitoring should also focus on linking erosional contourite morphological features to specific bottom-current conditions (e.g., velocity, energy).
- Analysis of sedimentary evidence and ROV-assisted visual observations should relate modern erosional, depositional and mixed features to bottom currents and associated processes. This analysis should query local outcrops on the seafloor, including channel flanks, slide scarps, etc., and synthesize observation with facies associations evident from cores (IODP, etc.) and other sedimentary evidence.
- A wide range of small-scale features (cores, outcrops and their lithologic facies), and large-scale features (depositional systems and seismic facies) require more specific linkages to oceanographic processes.
- Researchers should foster the analysis and evaluation of the influence of oceanographic processes on fragile geohabits, relict or active today, which

maybe situated in scenarios of risk due to deep environmental changes derived from water-mass circulation modifications.

- The current facies model must be adapted to include sandy facies. The facies model should also address interactions between bottom-current and turbidite processes, and offer consistent interpretations of both sandy contourites and bottom-current reworked turbidite sands that occur along the Iberian margin.

The differing objectives, frameworks and terminology used in marine geology, physical oceanography and benthic biology make these integrative efforts a formidable task. Some of the challenges can be circumvented by deploying remote sensing technology (e.g., automated underwater vehicles, AUVs, and remotely operated vehicles, ROVs) and capitalizing on advances in data acquisition and processing to build a more complete picture of water column dynamics, seafloor morphology, contourite distribution and benthic community structure. Further development of seismic oceanographic techniques (Buffett *et al.*, 2009; Carniel *et al.*, 2012; Pinheiro *et al.*, 2010) will help to integrate *in-situ* observations with 2D (or 3D) images of the seafloor and water column (Fig.21), while acoustic approaches integrated with oceanographic data such as CTD or (L) ADCP (Preu *et al.*, 2011, 2013; Hernández-Molina *et al.*, 2014) and instrumented moored stations (Rebesco *et al.*, 2013). High-resolution, 3D seismic images (Campbell and Deptuck, 2012), multibeam and backscatter data (Palomino *et al.*, 2011; Sweeney *et al.*, 2012) will also help characterize contourite features and correlate them with specific oceanographic processes.

Applied research

Multidisciplinary approaches to understanding contourite development carry major implications for climate research, resource exploration and basic science. Sandy contourites represent an entirely different deep-water sand deposit to turbidite sands. Given the prominent role of turbidite sands in deep-water oil and gas, understanding how their contourite counterparts form could fundamentally change deep water exploration paradigms (Viana, 2008; Stow *et al.*, 2013b; Hernández-Molina *et al.*, 2013). We will continue to explore the contourite processes and their implications for resource exploration using IODP Expedition 339 data. These data show extensively distributed and well sorted sand deposits (Expedition 339 Scientists, 2012; Stow *et al.*, 2013b; Hernández-Molina *et al.*, 2013) that may potentially serve as

reservoir units, as well as muddy contourites that may function as hydrocarbon sinks or source rocks and/or unconventional reservoirs (Viana, 2008; Shanmugan, 2012a, 2013a, b; Brackenridge *et al.*, 2013; Stow *et al.*, 2013b). The frequent association of both sandy and muddy contourite deposits with cold-water coral mounds (Huvenne *et al.*, 2009; Van Rooij *et al.*, 2011; Somoza *et al.*, 2014; Sánchez *et al.*, 2014), which may function as unconventional reservoirs (Henriet *et al.*, 2014) further demonstrate the potential for exploitation in these settings. As the climate warms due to the usage of these fossil fuels, we must also consider the role of deep-water circulation as a climate modulator. In addition to its effects on global circulation as variability in deep water circulation also affects deep-water ecosystems, such as reefs. Growing interest in seafloor mining of metalliferous resources (Hoffert, 2008; Rona, 2008) will also benefit from a better understanding of bottom current dynamics. These types of deposits have been identified along the Iberian margin (González *et al.*, 2009, 2010a, b) and mapping of these deposits will help to interpret their formation with respect to bottom currents and seafloor morphology parameters.

Acknowledgements

We thank the main Editor for the invitation to write this review for the SI in the BGM related to 'Geological processes in the Iberian Continental Margin: new developments and trends'. This contribution is a product of the IGCP-619 and INQUA-1204 projects, and is partially supported through the CTM 2008-06399-C04/MAR (CONTOURIBER); CTM 2012-39599-C03 (MOWER); CTM 2010-21229/MAR projects and MARUM project GALIOMAR, as well as the Continental Margins Research Group (CMRG) at Royal Holloway University of London (UK). This study interpreted samples and data provided by the Integrated Ocean Drilling Program (IODP). The figures presented in this paper are original, partially adapted from previous research, and partially reproduced from previous papers and permission has been obtained for their reproduction or adaptation. We thank the British Oceanographic Data Center (BODC) and National Oceanographic Centre, Southampton (NOCS) for current meter data for Fig. 10, the EOLi (Earth Observation Link, European Space Agency) for some images included in Fig. 15; Galderic Lastras (Univ. Barcelona, Spain) for providing the original figures included in Fig. 18; Yasuhiro Takashimizu (Niigata University, Japan) for permission to include an example of possible tsunami deposits in the Gulf

of Cadiz in Fig. 19, V. Huvenne (NOCS, UK) for the submarine photo in Fig. 20 E; and Ron Blakey (Colorado Plateau Geosystems, <http://cpgeosystems.com/mollglobe.html>) for permission to use the base map layer in Figs. 1 and 3. We are grateful to A. Piola (SHN, Argetina) and D. G. Borisov (Russian Academy of Sciences, Russia) for their helpful guidance in revising the manuscript. Their input has greatly improved the presentation of this research.

References

- Abrantes, F., Alt-Epping, U., Lebreiro, S., Voelker, A. and Schneider, R. 2008. Sedimentological record of tsunamis on shallow-shelf areas: the case of the 1969 AD and 1755 AD tsunamis on the Portuguese shelf off Lisbon, *Marine Geology*, 249, 283-293.
- Albérola, C., Rousseau, S., Millot, C., Astraldi, M., Font J., Garcia-Lafuente J., Gasparini G.P., Send U. and Annick V. A., 1995. Tidal currents in the western Mediterranean Sea. *Oceanologica Acta*, 18, 2, 273-284.
- Allen, S.E. and Durrieu de Madron, X. 2009. A review of the role of submarine canyons in deep-ocean exchange with the shelf. *Ocean Science*, 5, 607-20.
- Alvarez Fanjul, E., Pérez, B. and Rodríguez, I., 1997. A description of the tides in the eastern North Atlantic. *Progress in Oceanography*, 40, 217-244.
- Ambar, I. and Howe, M.R. 1979a. Observations of the Mediterranean Outflow - I Mixing in the Mediterranean Outflow. *Deep-Sea Research*, 26A, 535-554.
- Ambar, I. and Howe, M.R. 1979b. Observations of the Mediterranean Outflow - II The Deep Circulation in the Vicinity of the Gulf of Cádiz. *Deep-Sea Research*, 26A, 555-568.
- Ambar, I., Serra, N., Brogueira, M. J., Cabeçadas, G., Abrantes, F., Freitas, P., Gonçalves, C. and Gonzalez, N. 2002. Physical, chemical and sedimentological aspects of the Mediterranean outflow off Iberia, *Deep Sea Research II*, 49, 4163- 4177.
- Ambar, I., Serra, N., Neves, F. and Ferraira, T. 2008. Observations of the Mediterranean undercurrent and eddies in the Gulf of Cádiz during 2001. *Journal of Marine Systems*, 71(1-2), 195-220.
- Apel, J.R. 2000. Solitons near Gibraltar: views from the European remote sensing satellites. Report GOA 2000-1, *Global Ocean Association*, Silver Spring, MD.
- Apel, J.R. 2004. Oceanic internal waves and solitons, In: Jackson C.R., Apel J.R. (eds.), *Synthetic aperture radar marine user's manual*. US Department of Commerce, National Oceanic and Atmospheric Administration, Silver Spring, 189-206 pp.
- Apel, J.R., Ostrovsky, L. A. and Stepanyants, Y. A. 1995. Internal solitons in the ocean, *Report MERCJRA0695*, Milton S. Eisenhower Research Center, APL, The John Hopkins University, US, 69 pp.
- Arhan, M., Carton, X., Piola, A. and Zenk, W. 2002. Deep lenses of circumpolar water in the *Argentine Basin*. *Journal of Geophysical Research* 107 (C1), 3007.
- Arhan, M., Mercier, H. and Park, Y.-H. 2003. On the deep water circulation of the Eastern South Atlantic Ocean. *Deep Sea Research Part I: Oceanographic Research Papers*, 50, 880-916.
- Armi, L. and Zenk, W. 1984. Large Lenses of Highly Saline Mediterranean Water. *Journal of Physical Oceanography*, 14, 1560-1576.
- Armi, L. and Farmer, D.M. 1988. The flow of Mediterranean water through the Strait of Gibraltar. *Progress in Oceanography*, 21, 1-105
- Arzola, R.G., Wynn, R.B., Lastras, G., Masson, D.G. and Weaver, P.P.E. 2008. Sedimentary features and processes in the Nazaré and Setúbal submarine canyons, west Iberian margin. *Marine Geology*, 250, 64-88
- Azevedo, A., da Silva, J.C.B. and New, A.L. 2006. On the generation and propagation of internal solitary waves in the southern Bay of Biscay. *Deep-Sea Research I*, 53, 927-941.
- Bache, F. Popescu, S.-M., Rabineau, M., Gorini, C., Suc, J.-P., Clauzon, G., Olivet, J.-L., Rubino, J.-L., Melinte-Dobrinescu, M.C., Estrada, F., Londeix, L., Armijo, R., Meyer, B., Jolivet, L., Jouannic, G., Leroux, E., Aslanian, D., Dos Reis, A.T., Mocochain, L., Dumurdžanov, N., Zagorchev, I., Lesi, V., Tomi, D., Ça atay, M.N., Brun, J.-P., Sokoutis, D., Csato, I., Uçarkus, G. and Çakir, Z. 2012. A two-step process for the reflooding of the Mediterranean after the Messinian Salinity Crisis. *Basin Research*, 24, 125-153.
- Baines, P. G. 1982. On internal tide generation models. *Deep-Sea Research*, 29 (3A), 307-338.
- Banerjee, D., Murray, A.S. and Foster, J.L.D. 2001. Scilly islands UK: optical dating of a possible tsunami deposit from the 1755 Lisbon earthquake. *Quaternary Science Reviews*, 20(5-9), 715-718.
- Baptista, M.A., Miranda, J.M., Chierici, F. and Zitellini, N. 2003. New study of the 1755 earthquake source based on multi-channel seismic survey data and tsunami modeling. *Natural Hazards and Earth Systems Sciences*, 3, 333-340.
- Baringer, M.O. and Price, J.F. 1997. Mixing and Spreading of the Mediterranean Outflow. *Journal of Physical Oceanography*, 27, 1654-1677.
- Baringer, M.O. and Price, J.F. 1999. A review of the physical oceanography of the Mediterranean Outflow. *Marine Geology*, 155(1-2), 63-82.
- Battisti, D.S. and Clarke, A.J. 1982. A simple method for estimating barotropic tidal currents on continental margins with specific applications to the M2 tide off the Atlantic and Pacific coasts of the United States. *Journal of Physical Oceanography*, 12, 8-16.
- Bearmon, G. 1989. *Ocean chemistry and deep-sea sediments*. The Open University, Pergamon, 134 pp.
- Borenäs, K. and Wählin, A. 2000. Limitations of the Streamtube Model, *Deep-Sea Research*, 47, 1333-1350.
- Borenas, K., Wahlin, A., Ambar, I. and Serra, N. 2002. The Mediterranean Outflow Splitting - A Comparison between Theoretical Models and CANIGO Data. *Deep-Sea Research II*, 49, 4195-4205.
- Bouma, A.H. 1972. Recent and ancient turbidites and contourites. *Transactions Gulf Coast Association of Geological Societies*, 22, 205-221.

- Bouma, A.H. 1973. Contourites in Niessensflysch, Switzerland. *Eclogae Geologicae Helvetica*, 66, 315-323.
- Bouma, A.H. and Hollister, C.D. 1973. Deep ocean basin sedimentation, In: Middleton, G.V., Bouma, A.H. (eds.), *Turbidites and Deep-Water Sedimentation*. SEPM, Anaheim, CA, SEPM Pacific section Short Course, pp. 79-118.
- Bower, A.S., Armi, L. and Ambar, I. 1997. Lagrangian Observations of Meddy Formation during a Mediterranean Undercurrent Seeding Experiment. *Journal of Physical Oceanography*, 27, 2545-2575.
- Bower, A.S., Fratantoni, D.M., Johns, W.E. and Peters, H. 2002. Gulf of Aden eddies and their impact on Red Sea Water. *Geophysical Research Letters*, 29, 1-21.
- Brackenridge, R.A., 2014. Contourites in the Gulf of Cadiz: characterisation, controls and wider implications for hydrocarbon exploration. PhD thesis, Heriot-Watt University, unpublished.
- Brackenridge, R.A., Hernández-Molina, F.J., Stow, D.A.V. and Llave, E. 2013. A Pliocene mixed contourite-turbidite system offshore the Algarve Margin, Gulf of Cádiz: Seismic response, margin evolution and reservoir implications. *Marine and Petroleum Geology*, 46, 36-50.
- Brandt, P., Alpers, W. and Backhaus, J.O. 1996. Study of the generation and propagation of internal waves in the Strait of Gibraltar using a numerical model and synthetic aperture radar images of the European ERS 1 satellite. *Journal of Geophysical Research*, 101, 14237-14252.
- Bruno, M., Vázquez, A., Gómez-Enri, J., Vargas, J.M., García-Lafuente, J.M., Ruiz-Cañavate, A., Mariscal, L. and Vidal, J. M., 2006. Observations of internal waves and associated mixing phenomena in the Portimao Canyon area. *Deep Sea Research Part II*, 53 (11-13), 1219-1240.
- Bryden, H.L., Candela, J. and Kinder, T.H. 1994. Exchange through the Strait of Gibraltar. *Progress in Oceanography*, 33, 201- 248.
- Buffett, G.G., Biescas, B., Pelegrí, J.L., Machín, F., Sallar, V., Carbonell, R., Klaeschen, D. and Hobbs, R. 2009. Seismic reflection along the path of the Mediterranean Undercurrent, *Continental Shelf Research*, 29, 1848-1860.
- Cacchione, D.A., Pratson, L.F. and Ogston, A.S. 2002. The shaping of continental slopes by internal tides. *Science* 296(5568), 724-727.
- Campbell, D.C. and Deptuck, M.E. 2012. Alternating Bottom-Current-Dominated and Gravity-Flow-Dominated Deposition in a Lower Slope and Rise Setting—Insights From the Seismic Geomorphology of the Western Scotian Margin, Eastern Canada, In: Prather, B.E., Deptuck, M.E., Mohrig, D., Van Hoorn, B., Wynn, R.B. (eds.), *Application of the Principles of Seismic Geomorphology to Continental-Slope and Base-of-Slope Systems: Case Studies from Seafloor and Near-Seafloor Analogues*. Society for Sedimentary Geology, Tulsa, Special Publication 99, pp. 329-346.
- Campos, M.L. 1991. Tsunami hazard on the Spanish coasts of the Iberian Peninsula. *Science of Tsunami Hazards* 9, 83-90.
- Canals, M., Puig, P., Durrieu de Madron, X., Heussner, S., Palanques, A. and Fabrès, J. 2006. Flushing submarine canyons. *Nature*, 444(7117), 354-357.
- Canals, M., Danovaro, R., Heussner, S., Lykousis, V., Puig, P., Trincardi, F., Calafat, A.M., Durrieu de Madron, X., Palanques, A. and Sanchez-Vidal, A. 2009. Cascades in Mediterranean Submarine Grand Canyons. *Oceanography*, 22, 26-43.
- Candela, J. 2001. Mediterranean water and global circulation, In: G. Siedler, J. Church, and J. Gould (eds.), *Ocean Circulation and Climate*, pp. 419- 429, Academic Press, San Diego, Ca.
- Carniel, S., Bergamasco, A., Book, J.W., Hobbs, R.W., Sclavo, M. and Wood, W.T. 2012. Tracking bottom waters in the Southern Adriatic Sea applying seismic oceanography techniques. *Continental Shelf Research*, 44, 30-38.
- Carton, X., Cherubin, L., Paillet, J., Morel, Y., Serpette, A. and Le Cann, B. 2002. Meddy Coupling with a Deep Cyclone in the Gulf of Cádiz. *Journal of Marine Systems*, 32, 13-42.
- Cartwright, D.E., Edden, A.C., Spencer, R. and Vassie, J.M. (1980). The Tides of the Northeast Atlantic Ocean, *Philosophical Transactions of the Royal Society of London A*, 298 (1436), 87-139. DOI:10.1098/rsta.1980.0241.
- Cheney, R.E., Marsh, J.G. and Beckley, B.D., 1983. Global mesoscale variability from collinear tracks of Seasat altimeter data. *Journal of Geophysical Research* 88, 4343-4354.
- Cherubin, L., Carton, X., Paillet, J., Morel, Y. and Serpette, A. 2000. Instability of the Mediterranean Water Undercurrents Southwest of Portugal: Effects of Baroclinicity and of Topography. *Oceanological Acta*, 23(5), 551-573.
- Correia, S.M.L. 2003. *Observation of internal waves using multisensory satellite data off the Iberian Peninsula*. PhD thesis, University of Lisbon, Institute of Oceanography.
- Cossu, R., Wells, M. and Wählin, A. 2010. Influence of the Coriolis force on the flow structure of turbidity currents in submarine channel systems. *Journal of Geophysical Research - Oceans*, 115(11), C11016.
- Cossu, R. and Wells, M. 2013. The evolution of submarine channels under the influence of Coriolis forces: experimental observations of flow structures. *Terra Nova*, 25, 65-71. doi: 10.1111/ter.12006
- Cuven, S., Paris, R., Falvard, S., Miot-Noirault, E., Benbakkar, M., Schneider, J.-L. and Billy, I. 2013. High-resolution analysis of a tsunami deposit: case-study from the 1755 Lisbon tsunami in southwestern Spain. *Marine Geology*, 337, 98-111.
- Dabrio, C.J., Zazo, C., Lario, J., Goy, J.L., Sierro, F.J., Borja, F., González, J.A. and Flores, J.A. 1998. Holocene incised-valley fills and coastal evolution in the Gulf of Cádiz (southern Spain). *Mediterranean and Black Sea Subcommission Newsletter*, 20, 45-48.
- Dabrio, C. J., Zazo, C., Goy, J. L., Sierro, F. J., Borja, F., Lario, J., González, J. A. and Flores, J.A. 2000. Depositional history of estuarine infill during the Last Postglacial transgression (Gulf of Cádiz, Southern Spain). *Marine Geology*, 162(2-4), 381-404.
- Davies, T.A. and Laughton, A.S. 1972. Sedimentary Processes in the North Atlantic, In: Laughton, A.S.,

- Berggren, W.A. (eds.), *Initial Reports of Deep Sea Drilling Project 12*. U.S. Government Printing Office, Washington D.C., pp. 905-934.
- Dawson, A.G. and Stewart, I. 2007. Tsunami deposits in the geological record. *Sedimentary Geology*, 200, 166-183.
- Dawson, A.G., Foster, I. D., Shi, S., Smith, D. E. and Long, D. 1991. The identification of tsunami deposits in coastal sediment sequences. *Science of Tsunami Hazards*, 9, 73-82.
- Dawson, A.G., Hindson, R., Andrade, C., Freitas, C., Parish, R. and Bateman, M. 1995. Tsunami sedimentation associated with the Lisbon earthquake of 1 November AD 1755: Boca do Rio, Algarve, Portugal. *The Holocene* 5, 209-215.
- Dewar, W.K. and Meng, H. 1995. The Propagation of Submesoscale Coherent Vortices. *Journal of Physical Oceanography*, 25, 1745-1770.
- Dickson, R. and McCave, I.N., 1986. Nepheloid layers on the continental slope west of Porcupine Bank. *Deep-Sea Research Part A: Oceanographic Research Papers*, 33, 791-818.
- Dickson, R. B., Gould, W.J., Muller, T.J. and Maillard, C. 1985. Estimates of the mean circulation in the deep (>2000 m) layer of the eastern North Atlantic. *Progress in Oceanography*, 14, 103-127.
- Duggen, S., Hoernle, K., Van den Bogaard, P., Rüpke, L. and Morgan, J.P. 2003. Deep roots of the Messinian salinity crisis. *Nature*, 422, 602-606.
- Durrieu de Madron, X., Zervakis, V., Theocharis, A. and Georgopoulos, D. 2005. Comments on "Cascades of dense water around the world ocean". *Progress in Oceanography*, 64, 83-90.
- Durrieu de Madron, X., Houpert, L., Puig, P., Sanchez-Vidal, A., Testor, P., Bosse, A., Estournel, C., Somot, S., Bourrin, F., Bouin, M.N., Beauverger, M., Beguery, L., Calafat, A., Canals, M., Cassous, C., Coppola, L., Dausse, D., D'Ortenzio, F., Font, J., Heussner, S., Kunesch, S., Lefevre, D., Le Goff, H., Martín, J., Mortier, L., Palanques, A., Raimbault, P. 2013. Interaction of dense shelf water cascading and open-sea convection in the Northwestern Mediterranean during winter 2012. *Geophysical Research Letters*, 40: 1379-1385.
- Dykstra, M. 2012. Deep-Water Tidal Sedimentology. In: R.A. Davis, Jr. and R.W. Dalrymple (eds.), *Principles of Tidal Sedimentology*, 371-395, DOI 10.1007/978-94-007-0123-6_14.
- Einsele, G. 2000. *Sedimentary Basins. Evolution, Facies, and Sediment Budget* (2nd ed.). Springer-Verlag. Berlin, 792 pp.
- Emery, K.O., 1956. Deep standing waves in California basins. *Limnology and Oceanography*, 1, 35-41.
- Ercilla, G., Baraza, J., Alonso, B., Estrada, F., Casas, D. and Farrán, M. 2002. The Ceuta Drift, Alboran Sea (southwestern Mediterranean). In: Stow, D.A.V., Pudsey, C.J., Howe, J.A., Faugères, J.-C., Viana, A.R. (eds.) *Deep-water contourite systems: modern drifts and ancient series, seismic and sedimentary characteristics*. Geological Society, London, Memoir 22, 155-170.
- Ercilla *et al.*, Submitted. Significance of Bottom Currents in Deep Sea Morphodynamics: The Alboran Sea Example. *Marine Geology*.
- Expedition 339 Scientists, 2012. Mediterranean outflow: environmental significance of the Mediterranean Outflow Water and its global implications. IODP Preliminary Report 339. doi:10.2204/iodp.pr.339.2012
- Farmer, D.M. and Armi, L. 1988. The flow of Atlantic water through the Strait of Gibraltar. *Progress in Oceanography*, 21, 1-105.
- Farmer, D.M. and Armi, L. 1999. The generation and trapping of internal solitary waves over topography. *Science*, 283, 188-190.
- Faugères J.-C. and Mulder, T. 2011. Contour currents and contourite drifts, In: Hüneke H., Mulder, T. (eds.), *Deep-sea sediments*. Elsevier, Amsterdam, Developments in Sedimentology 63, 149-214.
- Faugères, J.-C., Gonthier, E. and Stow, D.A.V. 1984. Contourite drift molded by deep Mediterranean Outflow. *Geology*, 12, 296-300.
- Faugères, J.-C., Mezeraïs, M.L. and Stow, D.A.V. 1993. Contourite drift types and their distribution in the North and South Atlantic Ocean basins. *Sedimentary Geology*, 82, 189-203.
- Faugères, J.-C., Stow, D.A.V., Imbert, P., Viana, A.R. 1999. Seismic features diagnostic of contourite drifts. *Marine Geology*, 162, 1-38.
- Flood, R.D. and Shor, A.N. 1988. Mudwaves in the Argentine Basin and their relationship to regional bottom circulation patterns. *Deep Sea Research*, 35, 943-972.
- Fohrmann, H., Backhaus, J.O., Blaume, F. and Rumohr, J. 1998. Sediments in bottom-arrested gravity plumes: Numerical case studies. *Journal of Physical Oceanography*, 28, 2250-2274.
- Font, J., Puig, P., Salat, J., Palanques, A. and Emelianov, M. 2007. Sequence of hydrographic changes in the NW Mediterranean deep water due to the exceptional winter 2005. *Scientia Marina*, 71, 339-346.
- Galbis, R.J. 1932. *Catálogo sísmico de la zona comprendida entre los meridianos 58 E y 208W de Greenwich y los paralelos 458 y 258N*. Dirección General del Instituto Geográfico, Catastral y de Estadística, Madrid.
- Gasser, M., Pelegrí, J.L., Nash, D., Peters, H. and García-Lafuente, J. (2011) Topographic control on the nascent Mediterranean outflow, *Geo-Marine Letters*, 31, 301-314. DOI 10.1007/s00367-011-0255-x.
- Gao, Z.Z., Eriksson, K.A., He, Y.B., Luo, S.S. and Guo, J.H. 1998. *Deep-Water Traction Current Deposits - A Study of Internal Tides, Internal Waves, Contour Currents and Their Deposits*. Science Press, Beijing, New York, 128 pp.
- García Lafuente, J.M. and Cano Lucana, N. 1994. Tidal dynamics and associated features of the northwestern shelf of the Alboran Sea. *Continental Shelf Research*, 14 (1), 1-21.
- García-Lafuente, J., Delgado, J., Sánchez-Román, A., Soto, J., Carracedo, L. and Díaz del Río, G. 2009. Interannual variability of the Mediterranean outflow observed in Espartel sill, western Strait of Gibraltar, *Journal of Geophysical Research*, 114, C10018.
- García, M., Hernández-Molina, F.J., Llave, E., Stow, D.A.V., León, R., Fernández-Puga, M.C., Díaz del Río, V. and Somoza, L. 2009. Contourite erosive features caused by the Mediterranean Outflow Water in the Gulf of Cádiz:

- Quaternary tectonic and oceanographic implications. *Marine Geology*, 257, 24-40.
- Gardner, W.D. and Sullivan, L.G. 1981. Benthic storms: temporal variability in a deep ocean nepheloid layer. *Science*, 213, 229-331.
- Garrett, C., 2001. What is the "near-inertial" band and why is it different from the rest of the internal wave spectrum? *Journal of Physical Oceanography*, 31, 962-971.
- Garrett, C. 2003. Internal tides and ocean mixing. *Science*, 301, 1858-1859.
- Gaudin, M., Berné, S., Jouanneau, J.-M., Palanques, A., Puig, P., Mulder, T., Cirac, P., Rabineau, M. and Imbert, P. 2006. Massive sand beds attributed to deposition by dense water cascades in the Bourcart canyon head, Gulf of Lions (northwestern Mediterranean Sea). *Marine Geology*, 234, 111-128.
- Gill, A.E. 1982: *Atmosphere-Ocean Dynamics*, Academic Press, 662 pp.
- Gómez-Ballesteros, M., Druet, M., Muñoz, A., Arrese, B., Rivera, J., Sánchez, F., Cristobo, J., Parra, S., García-Alegre, A., González-Pola, C., Gallastegui, J. and Acosta, J. 2014. Geomorphology of the Avilés Canyon System, Cantabrian Sea (Bay of Biscay). *Deep-Sea Research III*, 106, 99-117.
- Gong, C., Wang Y., Zhu, W., Li, W. and Xu, Q. 2013. Upper Miocene to Quaternary unidirectionally migrating deep-water channels in the Pearl River Mouth Basin, northern South China Sea. *AAPG Bulletin*, 97, 285-308.
- Gong, C., Wang, Y., Hernández-Molina, F.J., Li, W., Zhu, W. and Peng, X. 2014 Accepted. Bottom current-reworked sands within unidirectionally migrating deep-water channels: Processes, diagnostic criteria and exploration significance. *Basin Research*.
- Gonthier, E., Faugères, J.-C. and Stow, D.A.V. 1984. Contourite facies of the Faro Drift, Gulf of Cádiz, In: Stow, D.A.V., Piper, D.J.W. (eds.), *Fine Grained Sediments, Deep-Water Processes and Facies*. Geological Society, London, Special Publication 15, pp. 275-291.
- González, F.J., Somoza, L., Lunar, R., Martínez-Frías, J., Martín Rubí, J.A., Torres, T., Ortiz, J.E., Díaz del Río, V., Pinheiro, L. and Magalhaes, V.H. 2009. Hydrocarbon-derived ferromanganese nodules in carbonate-mud mounds from the Gulf of Cádiz: mud-breccia sediments and clasts as nucleation sites. *Marine Geology*, 261(1/4), 64-81.
- González, F.J., Somoza, L., Lunar, R., Martínez-Frías, J., Martín Rubí, J.A., Torres, T., Ortiz, J.E. and Díaz del Río, V. 2010a. Internal features, mineralogy and geochemistry of Fe-Mn nodules from the Gulf of Cádiz: the role of the Mediterranean outflow water undercurrent. *Journal of Marine Systems*, 80(3/4), 203-218. doi:10.1016/j.jmarsys.2009.10.010.
- González, F.J., Somoza, L., León, R. and Medialdea, T. 2010b. Ferromanganese deposits associated to the Cádiz Contourite channel: imprints of the Mediterranean outflow water. *Geo-Temas*, 11, 55-56.
- Gonzalez-Pola, C., Díaz del Río, G., Ruiz-Villarreal, M., Sanchez, R.F. and Mohn, C., 2012. Circulation patterns at Le Danois Bank, an elongated shelf-adjacent seamount in the Bay of Biscay. *Deep-Sea Research Part I*, 60, 7-21.
- Gracia, F.J, Alonso C., Benavente J., Anfuso G. and Del Rio L. 2006. The different coastal records of the 1755 tsunami waves along the South Atlantic Spanish coast. *Zeitschrift für Geomorphologie, Supplementbände*, 146, 195-220.
- Gross, T.F. and Willimans, A.J. III 1991. Characterization of deep-sea storms. *Marine Geology*, 99, 281-301.
- Guesmia, M., Heinrich, Ph. and Mariotti, C. 1998. Numerical Simulation of the 1969 Portuguese Tsunami by a Finite Element Method, *Natural Hazards*, 17(1), 31-46.
- Habgood, E.L., Kenyon, N.H., Masson, D.G., Akhmetzhanov, A., Weaver, P.P.E., Gardner, J. and Mulder, T. 2003. Deep-water sediment wave fields, bottom current sand channels and gravity flow channel-lobe systems: Gulf of Cádiz, NE Atlantic. *Sedimentology*, 50, 483-510.
- Hanebuth, T.J.J., Alekseev, W., Andrade Grand, e A., Baasch, B., Baumann, K.-H., Behrens, P., Bender, V.B., von Döbenek, T., dos S. Marques, A.I., Frederichs, Th., Haberkorn, J., Hangen, J., Hilgenfeldt, Chr., Just, J., Kockisch, B., Lantzsich, H., Lenhart, A., Lipke, A., Lobo Sánchez, F.J., Mena Rodríguez, A., Müller, H., Petrovic, A., Rodríguez Germade, I., Roud, S., Schwab, A., Schwenk, T., Voigt, I. and Wenau, S. 2012. Cruise Report and Preliminary Results RV METEOR Cruise M84 / 4 GALIOMAR III, Vigo – Vigo (Spain), May 1 – 28, 2011. *Berichte, Fachbereich Geowissenschaften, Universität Bremen*, 283, 139 pp.
- Hanquiez, V., Mulder, T., Toucanne, S., Lecroart, P., Bonnel, C., Marchès, E. and Gonthier, E. 2010. The sandy channel-lobe depositional systems in the Gulf of Cádiz: Gravity processes forced by contour current processes. *Sedimentary Geology*, 22, 110-123.
- Henriet, J.P., Hamoumi, N., Da Silva, A.C., Foubert, A., Lauridsen, B.W., Rüggeberg, A. and Van Rooij, D., 2014. Carbonate mounds: from paradox to World heritage. *Marine Geology*, In press. <http://dx.doi.org/10.1016/j.margeo.2014.01.008>.
- Haynes, R. and Barton, E. D. 1990. A poleward flow along the Atlantic coast of the Iberian Peninsula. *Journal of Geophysical Research*, 95 (C7), 11425-11441.
- Heezen B. C., Tharp M. and Cwing M., 1959. The floors of the ocean: 1. The North Atlantic, *Geological Society of America*, Special Paper, 65, 122 pp.
- Hernández-Molina, F.J., Llave, E., Somoza, L., Fernández-Puga, M.C., Maestro, A., León, R., Barnolas, A., Medialdea, T., García, M., Vázquez, J.T., Díaz del Río, V., Fernández-Salas, L.M., Lobo, F., Alveirinho Dias, J.M., Rodero, J. and Gardner, J. 2003. Looking for clues to paleo-oceanographic imprints: A diagnosis of the Gulf of Cádiz contourite depositional systems. *Geology*, 31, 19-22.
- Hernández-Molina, F.J., Maldonado, A. and Stow, D.A.V. 2008a. Abyssal Plain Contourites, In: Rebesco, M., Camerlenghi, A. (eds.), *Contourites*. Elsevier, Amsterdam, Developments in Sedimentology 60, pp. 345-378.
- Hernández-Molina, F.J., Stow, D.A.V. and Llave, E. 2008b. Continental slope contourites, In: Rebesco, M., Camerlenghi, A. (eds.), *Contourites*. Elsevier, Amsterdam, Developments in Sedimentology 60, pp. 379-408.

- Hernández-Molina, F.J., Paterlini, M., Violante, R., Marshall, P., de Isasi, M., Somoza, L. and Rebesco, M., 2009. Contourite depositional system on the Argentine slope: An exceptional record of the influence of Antarctic water masses. *Geology*, 37, 507-510.
- Hernandez-Molina, F.J., Serra, N., Stow, D.A.V., Llave, E., Ercilla, G. and Van Rooij, D. 2011. Along-slope oceanographic processes and sedimentary products around the Iberian margin. *Geo-Marine Letters*, 31, 315-341.
- Hernández-Molina F.J., Stow D.A.V., Alvarez-Zarikian, C. and Expedition IODP 339 Scientists, 2013. IODP Expedition 339 in the Gulf of Cádiz and off West Iberia: decoding the environmental significance of the Mediterranean Outflow Water and its global influence. *Scientific Drilling*, 16, 1-11, doi:10.5194/sd-16-1-2013.
- Hernández-Molina, F.J., Llave, E., Preu, B., Ercilla, G., Fontan, A., Bruno, M., Serra, N., Gomiz, J.J., Brackenridge, R.E., Sierro, F.J., Stow, D.A.V., García, M., Juan, C., Sandoval, N. and Arnaiz, A. 2014. Contourite processes associated with the Mediterranean Outflow Water after its exit from the Strait of Gibraltar: Global and conceptual implications. *Geology*, 42, 227-230.
- Hill, A.E., Souza, A.J., Jones, K., Simpson, J.H., Shapiro, G.I., McCandliss, R., Wilson, H. and Leftley, J. 1998. The Malin cascade in winter 1996. *Journal of Marine Research*, 56, 87-106.
- Hindson, R. A. and Andrade, C. 1999. Sedimentation and hydrodynamic processes associated with the tsunami generated by the 1755 Lisbon earthquake. *Quaternary International*, 56, 27-38.
- Hindson, R.A., Andrade, C. and Dawson, A.G. 1996. Sedimentary processes associated with the tsunami generated by the 1755 Lisbon Earthquake on the Algarve Coast, Portugal. *Physics and Chemistry of the Earth*, 21, 57-63.
- Hoffert, M. 2008. *Les nodules polymétalliques dans les grands fonds océaniques*. Vuibert, Paris.
- Hogg, N.G. and Stommel, H.M. 1990. How Currents in the Upper Thermocline Could AdveCT Meddies Deeper Down. *Deep-Sea Research*, 37, 613-623.
- Holger, K. 1987. Benthic storms, vortices, and particle dispersion in the deep western Europe. *Deutsche Hydrographische Zeitschrift*, 40, 88-12.
- Hollister, C.D., 1967. *Sediment distribution and deep circulation in the western North Atlantic*. PhD thesis, Columbia University, New York.
- Hollister, C.D. 1993. The concept of deep-sea contourites. *Sedimentary Geology*, 82, 5-11.
- Hollister, C.D., Heezen, B.C., 1967. Contour current evidence from abyssal sediments. *Transactions American Geophysical Union*, 48, 142 pp.
- Hollister, C.D. and Heezen, B.C. 1972. Geological effects of ocean bottom currents: Western North Atlantic, In: Gordon, A.L. (eds.), *Studies in Physical Oceanography*. Gordon and Breach, New York, 2, pp. 37-66.
- Hollister, C.D. and McCave, I.N. 1984. Sedimentation under deep-sea storms. *Nature*, 309, 220-225.
- Hollister, C.D., Nowell, A.R.M. and Smith, J.D. 1980. The Third Annual Report of the High Energy Boundary Layer Experiment. *WHOI. Technical Report*, 80, 32-48.
- Howe, J.A., Stoker, M.S. and Stow, D.A.V. 1994. Late Cenozoic sediment drift complex, northeast Rockall Trough, North Atlantic. *Paleoceanography*, 9, 989-999.
- Howe, J.A., Stoker, M.S., Stow, D.A.V. and Akhurst, M.C. 2002. Sediment drifts and contourite sedimentation in the northeastern Rockall Trough and Faeroe-Shetland Channel, North Atlantic Ocean, In: Stow, D.A.V., Pudsey, C.J., Howe, J.A., Faugères, J.-C., Viana, A.R. (eds.), *Deep-Water Contourite Systems: Modern Drifts and Ancient Series, Seismic and Sedimentary characteristics*. Geological Society, London, Memoir 22, 65-72.
- Huneke, N.V. and Stow, D.A.V., 2008. Identification of ancient contourites: problems and palaeoceanographic significance, In: Rebesco, M., Camerlenghi, A. (eds.), *Contourites*. Amsterdam, Elsevier, Developments in Sedimentology 60, 323-344.
- Huvenne, V.A.I., Van Rooij, D., De Mol, B., Thierens, M., O'Donnell, R. and Foubert, A. 2009. Sediment dynamics and palaeo-environmental context at key stages in the Challenger cold-water coral mound formation: Clues from sediment deposits at the mound base. *Deep Sea Research Part I: Oceanographic Research Papers*, 56, 2263-2280.
- IGN (INSTITUTO GEOGRÁFICO NACIONAL). 1991. *El medio marino*. Atlas Nacional de España, Sección III. Madrid.
- Iorga M. and Lozier MS (1999) Signatures of the Mediterranean outflow from a North Atlantic climatology 1. Salinity and density fields. *Journal Geophysical Researchers*, 104:25985-26009.
- Ivanov, V.V., Shapiro, G.I., Huthnance, J.M., Aleynik, D.L. and Golovin, P.N. 2004. Cascades of dense water around the world ocean. *Progress in Oceanography*, 60, 47-98.
- Jackson, C.R. 2004. *An atlas of oceanic internal solitary waves*. Global Ocean Associates, Rockville, MD, prepared for Office of Naval Research.
- Jane, G., Llave, E., Hernández-Molina, F.J., Maestro, A., Ercilla, G., López-Martínez, J., De Andrés, J.R., González-Aller, D. and Catalán-Morollón, M. 2012. Contourite features along the Northwestern Iberian continental margin and abyssal plain: the local influence of regional water masses in a down-slope dominate margin. *34 International Geological Congress*, Volume of Abstracts, Brisbane (Australia).
- Johnson, G.C., Lueck, R.G. and Sanford, T.B. 1994a. Stress on the Mediterranean outflow plume: Part ii. turbulent dissipation and shear measurements. *Journal of Physical Oceanography*, 24, 2084-2092, doi:10.1175/1520-0485(1994)024.
- Johnson, G.C., Sanford, T.B. and Baringer, M. O'Neil. 1994b. Stress on the Mediterranean outflow plume: Part i. velocity and water property measurements. *Journal of Physical Oceanography*, 24, 2072-2083, doi:10.1175/1520-0485(1994)024.
- Johnson, J. and Stevens, I. 2000. A fine resolution model of the eastern North Atlantic between the Azores, the Canary Islands, and the Gibraltar Strait. *Deep-Sea Research, Part I*, 47(5), 875-899.
- Kantha, L.H. and Clayson, C.A. 2000. *Small scale processes in geophysical fluid flows*. Academic 432 Press, San Diego, 940 pp.

- Kase, R.H. and Zenk, W. 1996. Structure of the Mediterranean Water and Meddy Characteristics in the Northeastern Atlantic. In: W. Krauss (ed.), *"The Warmwatersphere of the North Atlantic Ocean"*, Gebruder Borntraeger, 365-395.
- Kase, R.H., Beckmann, A. and Hinrichsen, H.-H. 1989. Observational Evidence of Salt Lens Formation in the Iberian Basin. *Journal of Geophysical Research*, 94(C4), 4905-4912.
- Kennett, J.P. 1982. *Marine Geology*. Prentice-Hall, Englewood.
- Killworth, P.D. 1983. Deep convection in the world ocean. *Reviews of Geophysics and Space Physics*, 21, 1-26.
- Kuhlbrodt, T., Griesel, A., Montoya, M., Levermann, A., Hofmann, M. and Rahmstorf, S. 2007. On the driving processes of the Atlantic meridional overturning circulation. *Reviews of Geophysics*, 45, RG2001
- Kunze, K., Rosenfeld, L.K., Carter, G.S. and Gregg, M.C. 2002. Internal waves in Monterey submarine canyon. *Journal of Physical Oceanography*, 32, 1890-1913.
- Lastras, G., Arzola, R.G., Masson, D.G., Wynn, R.B., Huvenne, V.A.I., Huhnerbach, V. and Canals, M. 2009. Geomorphology and sedimentary features in the Central Portuguese submarine canyons, Western Iberian margin. *Geomorphology*, 103, 310-329.
- Laughton A. S. 1960. An interplain deep-sea channel system. *Deep-Sea Research*, 7, 75-88.
- Laughton A. S. 1968. New evidence of erosion on the deep ocean floor. *Deep-Sea Research*, 15, 21-29.
- Legg, S., Briegleb, B., Chang, Y., Chassignet, E.P., Danabasoglu, G., Ezer, T., Gordon, A.L., Griffies, S., Hallberg, R., Jackson, L., Large, W., Özgökmen, T.M., Peters, H., Price, J., Riemenschneider, U., Wu, W., Xu, X. and Yang, J. 2009. Improving Oceanic overflow representation in climate models. The Gravity Current Entrainment Climate Process Team. *Bulletin of the American Meteorological Society*, 657-670.
- Llave, E., Hernández-Molina, F.J., Somoza, L., Stow, D.A.V. and Díaz del Río, V. 2007. Quaternary evolution of the contourite depositional system in the Gulf of Cádiz. In: Viana, A.R., Rebesco, M. (eds.), *Economic and Palaeoceanographic Significance of Contourite Deposits*. Geological Society, London, Special Publication 276, 49-79.
- Llave, E., Hernández-Molina, F.J., Ercilla, G., Roque, C., Van Rooij, D., García, M., Juan, C., Mena, A., Brackenridge, R.E., Jané, G., Stow, D.A.V. and Gómez-Ballesteros, M. (this issue). Bottom current processes along the Iberian continental margin. *Boletín Geológico y Minero*, 126 (2-3), 219-256.
- Lobo, F.J., Hernández-Molina, F.J., Bohoyo, F., Galindo-Zaldívar, J., Maldonado, A., Martos, Y.M., Rodríguez-Fernández, J., Somoza, L. and Vázquez, J.T. 2011. Furrows in the southeastern Scan Basin, Antarctica: Interplay between tectonic and oceanographic influences. *Geo Marine Letters*, 31(5-6), 451-464.
- Luque, L. 2002. *Cambios en los paleoambientes costeros del sur de la Península Ibérica (España) durante el Holoceno*. Tesis Doctoral. Universidad Complutense de Madrid.
- Luque, L., Lario, J., Zazo, C., Goy, J.L., Dabrio, C.J. and Silva, P.G. 2001. Tsunami deposits as palaeoseismic indicators: examples from the Spanish coast. *Acta Geologica Hispanica* 36 (3-4), 197-211.
- Luque, L., Zazo, C., Goy, J.L., Dabrio, C.J., Civis, J., Lario, J. and Gómez-Ponce, C. 1999. Los depósitos del tsunami de Lisboa de 1755. Su registro en la Bahía de Cádiz: Flecha de Valdelagrana (Spain). En *Actas de la X Reunión Nacional del 152 Luis de Luque, RAMPAS*, 10, 2008 Revista Atlántica-Mediterránea de Prehistoria y Arqueología Social, 10, 2008, 131-153. Universidad de Cádiz *Cuaternario*, 63-66. Girona.
- Luque, L., Zazo, C., Lario, J., Goy, J.L., Civis, J., González-Hernández, F.M., Silva, P. G. and Dabrio, C.J. 2004. El efecto del tsunami del año 1755 en el litoral de Conil de la Frontera (Cádiz). In: Baquedano, E., Rubio, S., (Coords.): *Miscelanea en homenaje a Emiliano Aguirre* 1. *Geología*, pp. 72-82. Madrid.
- Maestro, A., López-Martínez, J., Llave, E., Bohoyo, F., Acosta, J., Hernández-Molina, F.J., Muñoz, A. and Jané, G. 2013. Geomorphology of the Iberian Continental Margin. *Geomorphology*, 196, 13-35.
- Marta-Almeida, M. and Dubert, J. 2006. The structure of tides in the western Iberian region. *Continental Shelf Research*, 26, 385-400.
- Martín-Chivelet, J., Fregenal Martínez, M.A. and Chacón, B. 2008. Traction structures in Contourites, In: Rebesco, M. and Camerlenghi, A. (eds.), *Contourites*. Elsevier, Amsterdam, Developments in Sedimentology 60, 159-181.
- Martín, J., Durrieu de Madron, X., Puig, P., Bourrin, F., Palanques, A., Houpert, L., Higuera, M., Sanchez-Vidal, A., Calafat, A.M., Canals, M. and Heussner, S. 2013. Sediment transport along the Cap de Creus Canyon flank during a mild, wet winter. *Biogeosciences*, 10, 3221-3239.
- Masson, D.G., Plets, R.M.K., Huvenne, V.A.I., Wynn, R.B. and Bett, B.J. 2010. Sedimentology and depositional history of Holocene sandy contourites on the lower slope of the Faroe-Shetland Channel, northwest of the UK. *Marine Geology*, 268, 85-96
- McCartney, M.S. 1992. Recirculating components to the deep boundary current of the northern North Atlantic. *Progress in Oceanography*, 29, 283-383.
- McCave, I.N. 1986. Local and global aspects of the bottom nepheloid layers in the world ocean. *Netherlands Journal of Sea Research*, 20, 167-181.
- McCave, I.N. and Carter, L. 1997. Recent sedimentation beneath the deep Western Boundary Current off northern New Zealand. *Deep-Sea Research Part I: Oceanographic Research Papers* 44, 1203-1237.
- McCave, I.N. and Tucholke, B.E. 1986. Deep current-controlled sedimentation in the western North Atlantic, In: Vogt, P.R., Tucholke, B.E. (eds.), *The Geology of North America, The Western North Atlantic Region, Decade of North American Geology*. Geological Society of America, Boulder, 451-468.
- Millot, C.A. 1990. The Gulf of Lions' hydrodynamic. *Continental Shelf Research*, 10, 885-894.
- Millot, C. 1999. Circulation in the Western Mediterranean Sea. *Journal of Marine Systems*, 20, 423-442

- Millot, C. 2009. Another description of the Mediterranean Sea outflow. *Progress in Oceanography*, 101-124, doi: 10.1016/j.pocean.2009.04.016.
- Millot, C. 2014. Heterogeneities of in- and out-flows in the Mediterranean Sea. *Progress in Oceanography*, 120, 254-278.
- Millot, C., Candela, J., Fuda, J. L. and Tber, Y., 2006. Large warming and salinification of the Mediterranean outflow due to changes in its composition. *Deep-Sea Research*, I, 53, 423-442.
- Muench, R.D., Wåhlin, A.K., Özgökmen, T.M., Hallberg, R. and Padman, L. 2009. Impacts of bottom corrugations on a dense Antarctic outflow: NW Ross Sea. *Geophysical Research Letters*, 36, L23607.
- Mulder, T., Hassan, R., Ducassou, E., Zaragosi, S., Gonthier, E., Hanquiez, V., Marchès, E. and Toucanne, S. 2013. Contourites in the Gulf of Cádiz: a cautionary note on potentially ambiguous indicators of bottom current velocity. *Geo-Marine Letters*, 33, 357-367.
- Navrotsky, V.V., Lozovatsky, J.D., Pavlova, E.P. and Fernando, H.J.S. 2004. Observations of internal waves and thermocline splitting near a shelf break of the Sea of Japan (East Sea). *Continental Shelf Research*, 24, 1375-1395.
- Nelson, C.H., Baraza, J. and Maldonado, A. 1993. Mediterranean undercurrent sandy contourites, Gulf of Cádiz, Spain. *Sedimentary Geology*, 82(1-4), 103-131.
- Nof, D. 1982. On the beta-induced Movement of Isolated Baroclinic Eddies. *Journal of Physical Oceanography*, 11, 1662-1672.
- Nof, D. 1991. Lenses Generated by Intermittent Currents. *Deep-Sea Research*, 38(3), 325-345.
- Nowell, A.R.M. and Hollister, C.D. 1985. Deep Ocean Sediment Transport - Preliminary Results of the High Energy Benthic Boundary Layer Experiment. *Marine Geology*, 66, 420 pp.
- Ochoa, J. and Bray, N.A. 1991. Water mass exchange in the Gulf of Cádiz. *Deep-Sea Research, Part A*, 38(S1), S465-S503.
- Orsi, A.H., Whitworth, T. Illand Nowlin, W.D., Jr. 1995. On the meridional extent and fronts of the Antarctic Circumpolar Current. *Deep-Sea Research*, I 42, 641-673.
- Øvrebø, L.K., Houghton, P.D.W. and Shannon, P.M. 2006. A record of fluctuating bottom currents on the slopes west of the Porcupine Bank, offshore Ireland - implications for Late Quaternary climate forcing. *Marine Geology*, 225, 279-309.
- Paillet, J. and Mercier, H. 1997. An inverse model of the eastern North Atlantic general circulation and thermocline ventilation. *Deep Sea Research*, I, 44(8), 1293-1328.
- Paillet, J., Le Cann, B., Carton, X., Morel, Y. and Serpette, A. 2002. Dynamics and Evolution of a Northern Meddy. *Journal of Physical Oceanography*, 32, 55-79.
- Palanques, A., Durrieu de Madron, X., Puig, P., Fabrès, J., Guillén, J., Calafat, A., Canals, M., Heussner, S. and Bonnin, J. 2006. Suspended sediment fluxes and transport processes in the Gulf of Lions submarine canyons. The role of storms and dense water cascading. *Marine Geology*, 234, 43-61.
- Palanques, A., Guillén, J., Puig, P. and Durrieu de Madron, X. 2008. Storm-driven shelf-to-canyon suspended sediment transport at the southwestern end of the Gulf of Lions. *Continental Shelf Research*, 28, 1947-1956.
- Palanques, A., Puig, P., Latasa, M. and Scharek, R. 2009. Deep sediment transport induced by storms and dense shelf water cascading in the northwestern Mediterranean basin. *Deep Sea Research I*, 56, 425-434.
- Palanques, A., Puig, P., Durrieu de Madron, X., Sanchez-Vidal, A., Pasqual, C., Martín, J. and Calafat, A., Heussner, S., Canals, M. 2012. Sediment transport to the deep canyons and open-slope of the western Gulf of Lions during the 2006 intense cascading and open-sea convection period. *Progress in Oceanography*, 106, 1-15.
- Palomino, D., Vazquez, J.T., Ercilla, G., Alonso, B., Lopez-Gonzalez, N. and Diaz-del-Rio, V. 2011. Interaction between seabed morphology and water masses around the seamounts on the Motril Marginal Plateau (Alboran Sea, Western Mediterranean). *Geo-Marine Letters*, 31, 465-479.
- Pedlosky, J. 1996. *Ocean circulation theory*. Heidelberg, Springer-Verlag, 453 pp.
- Pickering, K.T., Hiscott, R.N. and Hein, F.J. 1989. *Deep marine environments: clastic sedimentation and tectonics*. Unwin Hyman, London, 416 pp.
- Pichevin, T., and Nof, D., 1996. The Eddy Cannon. *Deep-Sea Research*, 43 (9), 1475-1507.
- Pichon, A., Morel, Y., Baraille, R. and Quaresma, L.S. 2013. Internal tide interactions in the Bay of Biscay: Observations and modeling. *Journal of Marine Systems*, 109-110: S26-S44.
- Pingree, R.D. and Newt, A.L. 1989. Downward propagation of internal tidal energy into the Bay of Biscay. *Deep-Sea Research*, 36(5), 735-758.
- Pingree, R.D. and Newt, A.L. 1991. Abyssal Penetration and Bottom Reflection of Internal Tidal Energy in the Bay of Biscay. *Journal of Physical Oceanography*, 21, 28-39.
- Pingree, R.D. and Le Cann, B. 1993. Structure of a Meddy (Bobby 92) Southeast of the Azores. *Deep-Sea Research*, 40, 2077-2103.
- Pingree, R.D., Mardell, G.T. and Newt, A.L. 1986. Propagation of internal tides from the upper slopes of the Bay of Biscay. *Nature*, 321, 154-158.
- Pinheiro, L.M., Song, H., Ruddick, B., Dubert, J., Ambar, I., Mustafa, K. and Bezerra, R. 2010. Detailed 2-D imaging of the Mediterranean outflow and meddies off W Iberia from multichannel seismic data. *Journal of Marine Systems*, 79, 89-100.
- Piola, A.R. and Matano, R.P. 2001. *Brazil and Falklands (Malvinas) currents*. Academic Press, London.
- Piper, D.J.W. 1972. Sediments of the Middle Cambrian Burgess Shale, Canada. *Lethaia*, 5, 169-175.
- Prater, M.D. and Sanford, T.B. 1994. A Meddy Off Cape St. Vincent. Part I: Description. *Journal of Physical Oceanography*, 24, 1572-1586.
- Preu, B., Spieß, V., Schwenk, T. and Schneider, R., 2011. Evidence for current-controlled sedimentation along the southern Mozambique continental margin since Early Miocene times. *Geo-Marine Letters*, 31, 427-435.
- Preu, B., Hernández-Molina, F.J., Violante, R., Piola, A.R., Paterlini, C.M., Schwenk, T., Voigt, I., Krastel, S. and Spiess, V. 2013. Morphosedimentary and hydrographic

- features of the northern Argentine margin: The interplay between erosive, depositional and gravitational processes and its conceptual implications. *Deep-Sea Research Part I: Oceanographic Research Papers* 75, 157-174.
- Price, J.F. and Baringer, M.O. 1994: Outflows and deep water production by marginal seas. *Progress in Oceanography*, 33, 161-200.
- Puig, P., Palanques, A. and Guillén, J. 2001. Near-bottom suspended sediment variability caused by storms and near-inertial internal waves in the Ebro mid-continental shelf (NW Mediterranean). *Marine Geology*, 178, 81-93.
- Puig, P., Palanques, A., Guillén, J. and El Khatib, M. 2004. Role of internal waves in the generation of nepheloid layers on the northwestern Alboran slope: implications for continental margin shaping. *Journal of Geophysical Research*, 109, C09011.
- Puig, P., Palanques, A., Orange, D.L., Lastras, G. and Canals, M. 2008. Dense shelf water cascading and furrows formation in the Cap de Creus Canyon, northwestern Mediterranean Sea. *Continental Shelf Research*, 28, 2017-2030.
- Puig, P., Palanques, A., Martín, J., Ribó, M. and Font, J. 2012. Eventos de resuspensión de sedimento en el ascenso continental del margen Mediterráneo noroccidental. *Geotemas*, 1840-1843.
- Puig, P., Durrieu de Madron, X., Salat, J., Schroeder, K., Martín, J., Karageorgis, A.P., Palanques, A., Roullier, F., Lopez-Jurado, J.L., Emelianov, M., Moutin, T. and Houpert, L. 2013. Thick bottom nepheloid layers in the western Mediterranean generated by deep dense shelf water cascading. *Progress in Oceanography*, 111, 1-23.
- Puig, P., Palanques, A. and Martín, J. 2014. Contemporary Sediment-Transport Processes in Submarine Canyons. *Annual Review of Marine Science*, 6, 53-77.
- Quaresma, L.S. and Pichon, A. 2013. Modelling the barotropic tide along the West-Iberian margin. *Journal of Marine Systems*, 109-110, S3-S25.
- Quaresma, L.S., Vitorino, J., Oliveira, A. and DaSilva, J. 2007. Evidence of sediment resuspension by nonlinear internal waves on the western Portuguese mid-shelf. *Marine Geology*, 246, 123-143.
- Rahmstorf, S. 2006. Thermohaline ocean circulation, In: Elias, S.A. (ed.), *Encyclopedia of Quaternary Science*. Elsevier, Amsterdam, pp. 739 - 750.
- Rebesco M, 2005. Contourites. In: Richard C, Selley RC, Cocks LRM, Plimer IR (eds) *Encyclopedia of geology*, 4. Elsevier, London, 513-527.
- Rebesco, M. and Stow, D.A.V. 2001. Seismic Expression of Contourites and Related Deposits: A Preface. *Marine Geophysical Research*, 22, 303-308.
- Rebesco, M. and Camerlenghi, A. (eds.) 2008. *Contourites*. Elsevier, Amsterdam, Developments in Sedimentology 60.
- Rebesco, M., Wåhlin, A., Laberg, J.S., Schauer, A., Brezczynska-Möller, A., Lucchi, R.G., Noormets, R., Accettella, D., Zarayskaya, Y. and Diviacco, P. 2013. Quaternary contourite drifts of the Western Spitsbergen margin. *Deep-Sea Research Part I: Oceanographic Research Papers*, 79, 156-168.
- Rebesco, M.; Hernández-Molina, F.J.; Van Rooij, D. and Wåhlin, A. 2014. Contourites and associated sediments controlled by deep-water circulation processes: state of the art and future considerations. *Marine Geology*, 352, 111-154. Doi:10.1016/j.margeo.2014.03.011
- Reicherter K. 2001. Paleoseismologic advances in the Granada basin (Betic Cordilleras, Southern Spain). *Acta geologica hispanica*, 36(3-4), 267 - 281.
- Reicherter, K. and Becker-Heidmann, P. 2009. Tsunami deposits in the western Mediterranean: remains of the 1522 Almería earthquake?. *The Geological Society of London*, 316, 217-235.
- Reid, J.L., Nowlin, W.D. and Patzert, W.C. 1977. On the characteristics and circulation of the southwestern Atlantic Ocean. *Journal of Physical Oceanography*, 7, 62-91.
- Ribó, M., Puig, P., Palanques, A. and Lo Iacono, C. 2011. Dense shelf water cascades in the Cap de Creus and Palamós submarine canyons during winters 2007 and 2008. *Marine Geology*, 284, 175-188.
- Richardson, M.J., Weatherly, G.L. and Gardner, W.D. 1993. Benthic storms in the Argentine Basin. *Deep-Sea Research*, 40, 989-999.
- Richardson, P.L., Bower, A.S. and Zenk, W. 2000. A Census of Meddies Tracked by Floats. *Progress in Oceanography*, 45, 209-250.
- Richardson, P.L., Walsh, D., Armi, L., Schroder, M. and Price, J.F. 1989. Tracking Three Meddies with SOFAR Floats. *Journal of Physical Oceanography*, 19, 371-383.
- Roberts, D.G., Hogg, N.G., Derek, G., Bishop, G. and Flewellen, C.G. 1974. Sediment distribution around moated seamounts in the Rockall Trough. *Deep-Sea Research Part A: Oceanographic Research Papers* 21, 175-184.
- Roden, G.I. 1987. Effects of seamount chains on ocean circulation and thermohaline structure, In: Keating B.H. *et al.*, (eds.), *Seamounts, Islands and Atolls*. AGU Geophysics Monograph 96, 335-354.
- Rodríguez-Vidal, J., Ruiz, F., Cáceres, L. M., Abad, M., González-Regalado, M. L., Pozo, M., Carretero, M. I., Monge, A. M. and Gómez, F. 2011. Geomarkers of the 218-209 BC Atlantic tsunami in the Roman Lacus Ligustinus (SW Spain): A palaeogeographical approach. *Quaternary International*, 242, 201-212.
- Roger, J. and Hébert, H. 2008. The 1856 Djijelli (Algeria) earthquake and tsunami: source parameters and implications for tsunami hazard in the Balearic Islands. *National Hazards and Earth SystEms Science*, 8, 721-731.
- Rogers, A.D. 1994. The Biology of Seamounts. *Advances in Marine Biology*, 30, 305-340.
- Rogerson, M., Rohling, E.J., Bigg, G.R. and Ramirez, J. 2012. Paleooceanography of the Atlantic-Mediterranean exchange: Overview and first quantitative assessment of climatic forcing. *Reviews of Geophysics*, 50, RG2003.
- Rona, P.A. 2008. The changing vision of marine minerals. *Ore Geology Reviews*, 33, 618-666.
- Roveri, M., Flecker, R., Krijgsman, W., Lofi, J., Lugli, S., Manzi, V., Sierro, F.J., Bertini, S., Camerlenghi, A., De Lange, G., Govers, R., Hilgen, F.J. Hubscher, C., Meijer, P. Th. and Stoica, M. 2014. The Messinian Salinity Crisis: Past and future of a great challenge for marine sciences.

- Marine Geology*, 352, 25-58, doi:10.1016/j.mar-geo.2014.02.002.
- Ruiz, F., Rodríguez-Ramírez, A., Cáceres, L.M., Rodríguez Vidal, J.R., Carretero, M.I., Clemente, L., Muñoz, J. M., Yañez, C. and Abad, M. 2004. Late Holocene evolution of the southwestern Doñana National Park (Guadalquivir Estuary, SW Spain): a multivariate approach. *Palaeogeography, Palaeoclimatology, Palaeoecology*, 204, 47-65.
- Ruiz, F., Rodríguez-Ramírez, A., Cáceres, L.M., Rodríguez Vidal, J.R., Carretero, M.I., Abad, M., Olias, M. and Pozo, M. 2005. Evidence of high-energy events in the geological record: mid-holocene evolution of the southwestern Doñana National Park (SW Spain). *Palaeogeography, Palaeoclimatology, Palaeoecology*, 229, 212-229.
- Rumín-Caparrós, A., Sánchez-Vidal, A., Calafat, A., Canals, M., Martín, J., Puig, P. and Pedrosa-Pàmies, R. 2013. External forcings, oceanographic processes and particle flux dynamics in Cap de Creus submarine canyon, NW Mediterranean Sea. *Biogeosciences*, 10, 3493-505.
- Sadoux, S., Baey, J.-M., Fincham, A. and Renouard, D., 2000. Experimental Study of the Stability of an Intermediate Current and Its Interaction with a Cape. *Dynamics of Atmospheres and Oceans*, 31, 165-192.
- Sánchez, F., González-Pola, C., Druet, M., García-Alegre, A., Acosta, J., Cristobo, J., Parra, S., Ríos, P., Altuna, A., Gómez-Ballesteros, M., Muñoz-Recio, A., Rivera, J. and Díaz del Río, G. 2014. Habitat characterization of deep-water coral reefs in LaGaviera canyon (Avilés Canyon System, Cantabrian Sea). *Deep-Sea Research II*, 106, 118-140.
- Sahal, A., Roger, J., Allgeyer, S., Lemaire, B., Hebert, H., Schindelé, F. and Lavigne, F. 2009. The tsunami triggered by the 21 May 2003 Boumerdes-Zmmouri (Algeria) earthquake: field investigations on the French Mediterranean coast and tsunami modelling. *National HazardS and Earth System Sciemces*, 9, 1823-1834.
- Salat, J., Puig, P. and Latasa, M. 2010. Violent storms within the Sea: dense water formation episodes in the NW Mediterranean. *Advances in Geosciences*, 26, 53-59.
- Sánchez González, J.M. 2013. *Oceanographic and morphosedimentary features in the northwestern sector of the Galicia margin: implications*. MSc work. University of Vigo (Spain).
- Sánchez-Garrido, J. C., Sannino, G., Liberti, L., García Lafuente, J. and Pratt, L., 2011. Numerical modeling of three-dimensional stratified tidal flow over Camarinal Sill, Strait of Gibraltar, J. Geophys. Res., 116, C12026, doi:10.1029/2011JC007093.
- Sánchez-Román, A., Sannino, G., García-Lafuente, J., Carillo, A. and Criado-Aldeanueva, F., 2009. Transport estimates at the western section of the Strait of Gibraltar: A combined experimental and numerical modeling study, J. Geophys. Res., 114, C06002, doi:10.1029/2008JC005023.
- Santek, D.A. and Winguth, A. 2005. A satellite view of internal waves induced by the Indian Ocean tsunami. *International Journal of Remote Sensing*, 26, 2927-2936.
- Scheffers, A. and Kelletat, D. 2005. Tsunami relics in the coastal landscape west of Lisbon, Portugal. *Science of Tsunami Hazards*, 23, 3-16.
- Schönfeld, J., Zahn, R., and Abreu, L., 2003. Surface and deep water response to rapid climate changes at the Western Iberian Margin. *Global and Planetary Change*, 36, 237-264.
- Schultz-Tokos, K. and Rossby, T. 1991. Kinematics and Dynamics of a Mediterranean Salt Lens. *Journal of Physical Oceanography*, 21, 879-892.
- Schultz-Tokos, K., Hinrichsen, H.-H. and Zenk, W. 1994. Merging and Migration of Two Meddies. *Journal of Physical Oceanography*, 24(10), 2129-2141.
- Serra, N. 2004. *Observations and Numerical Modelling of the Mediterranean Outflow*. PhD Thesis, University of Lisbon.
- Serra, N. and Ambar, I. 2002. Eddy Generation in the Mediterranean Undercurrent. *Deep-Sea Research II*, 49(19), 4225-4243.
- Serra, N., Ambar, I. and Käse, R.H. 2005. Observations and numerical modelling of the Mediterranean outflow splitting and eddy generation. *Deep-Sea Research II*, 52, 383-408.
- Serra, N., Ambar, I. and Boutov, D. 2010a. Surface expression of Mediterranean Water dipoles and their contribution to the shelf/slope - open ocean exchange. *Ocean Science*, 6, 191-209.
- Serra, N., Köhl, R. K. A. and Stammer D. 2010b. On the low-frequency phase relation between the Danmark Strait and the Faroe-Bank Channel overflows. *Tellus, Series a Dynamic Meteorology and Oceanography*, 62, 530-550.
- Serra, N., Sadoux, S., Ambar, I. and Renouard, D. 2002. Observations and Laboratory Modelling of Meddy Generation at Cape St. Vincent. *Jouranl of Physical Oceanography*, 32, 3-25.
- Shanmugam, G. 2000. 50 years of the turbidite paradigm (1950s-1990s): deep-water processes and facies models - a critical perspective. *Marine and Petroleum Geology*, 17, 285-342.
- Shanmugam, G. 2006. The tsunamite problem. *Journal of Sedimentary Research*, 76, 718-730.
- Shanmugam, G. 2012a. New perspectives on deep-water sandstones: origin, recognition, initiation, and reservoir quality. *Handbook of Petroleum Exploration and Production*, 9, Elsevier, Amsterdam, 524 pp.
- Shanmugam, G. 2012b. Process-sedimentological challenges in distinguishing paleo-tsunami deposits, In: A. Kumar and I. Nister, (eds.), *Paleo-tsunamis: Natural Hazards*, 63, 5-30.
- Shanmugam, G. 2013a. Modern internal waves and internal tides along oceanic pycnoclines: Challenges and implications for ancient deep-marine baroclinic sands. *AAPG Bulletin* 97, 767- 811.
- Shanmugam, G., 2013b. New perspectives on deep-water sandstones: Implications. *Petroleum Exploration and Development*, 40, 316-324.
- Shanmugam, G. 2014. Modern internal waves and internal tides along oceanic pycnoclines: Challenges and implications for ancient deep-marine baroclinic sands: Reply. *AAPG Bulletin*, 98(4), 858-879.
- Shanmugam, G., Spalding, T.D. and Rofheart, D.H. 1993.

- Process sedimentology and reservoir quality of deep-marine bottom-current reworked sands (sandy contourites): an example from the Gulf of Mexico. *AAPG Bulletin*, 77, 1241-1259.
- Shapiro, G.I. and Hill, A.E. 1997. Dynamics of Dense Water Cascades at the Shelf Edge. *Journal of Physical Oceanography*, 27, 2381-2394.
- Shapiro, G.I., Huthnance, J.M. and Ivanov, V.V. 2003. Dense Water Cascading off the Continental Shelf. *Journal of Geophysical Research*, 108.C12, 3390.doi:10.1029/2002JC001610.
- Shepard, F.P. 1976. Tidal components of currents in submarine canyons. *Journal of Geology*, 84, 343-350.
- Shepard, F.P., Marshall, N.F., McLoughlin, P.A. and Sullivan, G.G. 1979. Currents in submarine canyons and other sea valleys. *AAPG, Tulsa, Studies in Geology*, 8.
- Simpson, J.E. 1982. Gravity currents in the laboratory, atmosphere and ocean. *Annual Review of Fluid Mechanics*, 14, 213-234.
- Somoza, L., Ercilla, G., Urgorri, V., León, R., Medialdea, T., Paredes, M., Gonzalez, F.J. and Nombela, M.A. 2014. Detection and mapping of cold-water coral mounds and living *Lophelia* reefs in the Galicia Bank, Atlantic NW Iberia margin. *Marine Geology*, 349, 73-90.
- Stabholz, M., Durrieu de Madron, X., Canals, M., Khipounoff, A., Taupier-Letage, I., Testor, P., Heussner, S., Kerherv e, P., Delsaut, N., Houpert, L., Lastras, G. and Dennielou, B. 2013. Impact of open-ocean convection on particle fluxes and sediment dynamics in the deep margin of the Gulf of Lions. *Biogeosciences*, 10, 1097-1116.
- Stoker, M.S., Akhurst, M.C., Howe, J.A. and Stow, D.A.V. 1998. Sediment drifts and contourites on the continental margin off northwest Britain. *Sedimentary Geology*, 115, 33-51.
- Stow, D.A.V., 2005, *Sedimentary rocks in the field: A colour guide*. Manson Publishing, London.
- Stow, D.A.V. and Holbrook, J.A. 1984. North Atlantic contourites: an overview, In: Stow, D.A.V., Piper, D.J.W. (eds.), *Fine Grained Sediments, Deep-Water Processes and Facies*. Geological Society, London, Special Publication 15, 245-256.
- Stow, D.A.V., Pudsey, C.J., Howe, J.A., Faugères, J.-C. and Viana, A.R., 2002a. *Deep-Water Contourite Systems: Modern Drifts and Ancient Series, Seismic and Sedimentary characteristics*. Geological Society, London, Memoirs 22.
- Stow, D.A.V. and Faugères, J.C., 2008. Contourite facies and the facies model, in: Rebescó, M., Camerlenghi, A. (Eds.), *Contourites*. Elsevier, Amsterdam, Developments in Sedimentology 60, 223-256.
- Stow, D.A.V., Hernández-Molina, F.J., Llave, E., Sayago-Gil, M., Díaz-del Río, V. and Branson, A. 2009. Bedform-velocity matrix: The estimation of bottom current velocity from bedform observations. *Geology*, 37, 327-330.
- Stow, D.A.V., Faugères, J.-C., Howe, J.A., Pudsey, C.J. and Viana, A.R. 2002b. Bottom currents, contourites and deep-sea sediment drifts: current state-of-the-art. In: Stow, D.A.V., Pudsey, C.J., Howe, J.A., Faugères, J.-C., Viana, A.R. (eds.), *Deep-Water Contourite Systems: Modern Drifts and Ancient Series, Seismic and Sedimentary Characteristics*. Geological Society, London, Memoirs 22, 7-20.
- Stow, D.A.V., Hernández-Molina, F.J., Llave, E., Bruno, M., García, M., Díaz del Río, V., Somoza, L. and Brackenridge, R.E. 2013a. The Cádiz Contourite Channel: Sandy contourites, bedforms and dynamic current interaction. *Marine Geology*, 343, 99-114.
- Stow, D.A.V., Hernández-Molina, F.J., Alvarez Zarikian, C.A., and the Expedition 339 Scientists, 2013b. Proceedings IODP, 339. *Integrated Ocean Drilling Program Management International*, Tokyo.doi:10.2204/iodp.proc.339.2013.
- Sweeney, E.M., Gardner, J.V., Johnson, J.E. and Mayer, L.A. 2012. Geological interpretations of a low-backscatter anomaly found on the New Jersey continental margin. *Marine Geology*, 326-328, 46-54.
- Tucholke, B.E. 2002. The Greater Antilles Outer Ridge: development of a distal sedimentary drift by deposition of fine-grained contourites, In: Stow, D.A.V., Pudsey, C.J., Howe, J.A., Faugères, J.-C., Viana, A.R. (eds.), *Deep-Water Contourite Systems: Modern Drifts and Ancient Series, Seismic and Sedimentary Characteristics*. Geological Society, London, Memoirs 22, 39-55.
- Toucanne, S., Mulder, T., Schönfeld, J., Hanquiez, V., Gonthier, E., Duprat, J., Cremer, M., and Zaragosi, S., 200.) Contourites of the Gulf of Cadiz: a high-resolution record of the paleocirculation of the Mediterranean outflow water during the last 50,000 years. *Palaeogeography, Palaeoclimatology and Palaeoecology*, 246, 354-366.
- van Aken, H.M. 2000. The hydrography of the mid-latitude Northeast Atlantic Ocean, II. The intermediate water masses. *Deep-Sea Research, Part I*, 47(5), 789-824.
- van Haren, H., Ribó, M. and Puig P. 2013. (Sub-) inertial wave boundary turbulence in the Gulf of Valencia. *Journal of Geophysical Research*, 118, 1-7.
- Van Rooij, D., Blamart, D., De Mol, L., Mienis, F., Pirlet, H., Wehrmann, L.M., Barbieri, R., Maignien, L., Templer, S.P., de Haas, H., Hebbeln, D., Frank, N., Larmagnat, S., Stadnitskaia, A., Stivaletta, N., van Weering, T., Zhang, Y., Hamoumi, N., Cnudde, V., Duyck, P. and Henriët, J.P. 2011. Cold-water coral mounds on the Pen Duick Escarpment, Gulf of Cádiz: The MiCROSYSTEMS project approach. *Marine Geology*, 282, 102-117.
- Viana-Baptista, M., A., Soares, P., M., Miranda, J., M. and Luis, J., F. 2006. Tsunami propagation along Tagus estuary (Lisbon, Portugal) preliminary results. *Science of Tsunami Hazards*, 24(5), 329-338.
- Viana, A.R. 2008. Economic relevance of contourites, In: Rebescó, M., Camerlenghi, A. (eds.), *Contourites*. Elsevier, Amsterdam, Developments in Sedimentology 60, 493-510.
- Viana, A.R. and Faugères, J.-C. 1998. Upper slope sand deposits: The example of Campos Basin, a latest Pleistocene/Holocene record of the interaction between along and across slope currents, In: Stoker, M.S., Evans, D., Cramp, A. (eds.), *Geological Processes on Continental Margins – Sedimentation, Mass-Wasting and Stability*. Geological Society, London, Special Publication 129, 287-316.

- Viana, A.R., Faugères, J.-C. and Stow, D.A.V. 1998. Bottom-current controlled sand deposits: A review from modern shallow to deep water environments. *Sedimentary Geology*, 115, 53-80.
- Vlasenko, V., J. C. Sánchez Garrido, N. Stashchuk, J. García Lafuente, and M. Losada (2009), Three-dimensional evolution of large-amplitude internal waves in the Strait of Gibraltar, *Journal of Physical Oceanography*, 39, 2230–2246.
- Voelker, A.H.L., Lebreiro, S.M., Schönfeld, J., Cacho, I., Erlenkeuser, H., and Abrantes, F., 2006. Mediterranean Outflow strengthening during Northern Hemisphere coolings: a salt source for the glacial Atlantic? *Earth and Planetary Science Letter*, 245 (1–2), 39–55.
- Von Lom-Keil, H., Speiss, V. and Hopfau, V. 2002. Fine-grained sediment waves on the western flank of the Zapiola Drift, Argentine Basin -Evidence for variations in Late Quaternary bottom flow activity. *Marine Geology*, 192, 239-258.
- Wählin, A.K. and Walin, G. 2001. Downward migration of dense bottom currents. *Environmental Fluid Mechanics*, 1, 257-279.
- Wählin, A. 2004. Topographic advection of dense bottom water. *Journal of Fluid Mechanics*, 210, 95-104.
- Whelan, F. and Kelletat, D. 2005. Boulder deposits on the southern Spanish Atlantic coast: possible evidence for the 1755 AD Lisbon tsunami?. *Science of Tsunami Hazards*, 23(3), 25-38.
- Wright, S.G. and Rathje, E.M. 2003. Triggering Mechanisms of Slope Instability and their Relationship to Earthquakes and Tsunamis. *Pure and Applied Geophysics*, 160(10-11), 1865-1877.
- Wunsch, C. 2002. What is the thermohaline circulation?. *Science*, 298(5596), 1179-1181. 10.1126/science.1079329, PMID 12424356.
- Zenk, W. 2008. Abyssal and Contour Currents, In: Rebesco, M., Camerlenghi, A. (eds.), *Contourites*. Elsevier, Amsterdam, Developments in Sedimentology 60, pp. 37–57.
- Zenk, W. and Armi, L. 1990. The Complex Spreading Pattern of Mediterranean Water Off the Portuguese Continental Slope. *Deep-Sea Research*, 37, 1805-1823.
- Zitellini, N., Gràcia, E., Matias, L., Terrinha, P., Abreu, M.A., DeAlteriis, G., Henriët, J.P., Dañobeitia, J.J., Masson, D.G.; Mulder, T., Ramella, R., Somoza, L. and Diez, S. 2009. The quest for the Africa-Eurasia plate boundary west of the Strait of Gibraltar. *Earth and Planetary Science Letters*, 280(1-4), 13-50.

Recibido: mayo 2014

Revisado: noviembre 2014

Aceptado: diciembre 2014

Publicado: junio 2015